Ridong Zhang · Anke Xue · Furong Gao

Model Predictive Control

Approaches Based on the Extended State Space Model and Extended Non-minimal State Space Model

Springer

Model Predictive Control

Ridong Zhang · Anke Xue
Furong Gao

Model Predictive Control

Approaches Based on the Extended State Space Model and Extended Non-minimal State Space Model

Springer

Ridong Zhang
Institute of Information and Control
Hangzhou Dianzi University
Hangzhou, Zhejiang, China

Anke Xue
Key Lab for IOT and Information Fusion Technology of Zhejiang, Institute of Information and Control
Hangzhou Dianzi University
Hangzhou, Zhejiang, China

Furong Gao
Department of Chemical and Biomolecular Engineering
Hong Kong University of Science and Technology
Hong Kong, China

ISBN 978-981-13-0082-0 ISBN 978-981-13-0083-7 (eBook)
https://doi.org/10.1007/978-981-13-0083-7

Library of Congress Control Number: 2018949340

This Springer imprint is published by the registered company Springer Nature Singapore Pte Ltd.
The registered company address is: 152 Beach Road, #21-01/04 Gateway East, Singapore 189721, Singapore

Preface

Aims of the Book

The aim of this book is (1) to present the novel extended state space model and extended non-minimal state space model-based model predictive control (MPC), predictive functional control (PFC), PID control optimization, and the relevant system performance analysis; (2) to introduce the constraint handling in MPC and the relaxed constrained optimization approach; (3) to address the improved genetic algorithm (GA) based MPC; and (4) to illustrate the corresponding industrial applications.

As a promising control algorithm, MPC plays a vital role in the control of industrial processes. During the past decades, great progress in both theory and application has been obtained. Driven by the rapid development of economy and stricter requirements, the improvement of MPC performance is still an open topic. It is known that the process dynamics are useful for the controller design. However, only limited dynamic information is considered in the design of conventional state space model based MPC; thus, the relevant control performance may be restricted. How to improve MPC performance employing more process dynamics or combining other optimization algorithms is the issue we need to investigate. Meanwhile, the constraint treatment in MPC is significant in practice, and research on effective constraint dealing methods is meaningful.

Based on such backgrounds, this book aims at proposing several approaches for the improvement of MPC performance and its constraint handling. Besides, the proposed extended state space model used to improve MPC performance is also employed to optimize PID control with relevant industrial applications. Therefore, this book may provide some insight for readers who prepare to make improvements to MPC approaches and other relevant aspects.

Novel State Space Model, Constraint Handling, and Further Optimization for MPC

(1) New state space model
It is clear that conventional state space models representing the process dynamics are employed in conventional MPC designs, which serve as obtaining the set point tracking or regulation together with limiting the control action. However, under complex situations, such design may encounter difficulty to achieve satisfactory closed-loop performance. This is due to the fact that the degree of freedom for the controller design may be limited; thus, the relevant control performance may be restricted. How to use the process dynamics in the controller design as much as possible to improve the ensemble control performance is what we need to consider. In view of this, an improved extended state space model in which additional aspects of the process dynamics are taken into account for the MPC strategy is presented in this book. By employing the new state space model, more degrees of freedom are provided for the subsequent MPC design.

(2) Constraint handling for MPC
Constraints handling is an essential step in MPC design. Proper treatment of the constraints in industrial process brings significant advantages, such as operation safety, higher profit, smaller pollution, etc. In this book, a basic constraint dealing method is introduced first. However, the preset constraints for the plants in industry in practice may become rigorous because the working conditions are continuously changing. Under such background, there may be trouble for the primary constrained optimization method, i.e., there is no feasible solution and a wrong result may be given. In order to handle this issue, a relaxed constrained optimization approach is put forward in this book. Based on the new constrained optimization scheme, the probability of unsuccessful solution for constrained MPC algorithms is avoided.

(3) Further optimization for MPC
In order to meet the stricter requirements on the operation of industrial processes, MPC strategies need to be improved continuously. As to the control parameters of MPC schemes, they influence the control performance greatly. How to select the optimal control parameters is also the problem we need to pay attention to. In this book, the example of adopting genetic algorithm (GA) is employed to optimize MPC parameters for improved control performance.

Outline of the Book

The structure of this book is organized as follows:

Chapter 1 presents the entire introduction and the motivation of the work proposed in this book.

The following contents are divided into two parts. Part I is the Basic Algorithms, and it includes Chaps. 2–7. Part II is the System Performance Analysis, Optimization, and Application that contains Chaps. 8–11.

Chapter 2 describes the construction of extended state space models from conventional state space models. Meanwhile, the relevant model-based MPC strategy is presented.

Chapter 3 gives the extended state space model-based PFC scheme.

Chapter 4 illustrates the conversion of input–output models to extended non-minimal state space (ENMSS) models. Besides, the MPC approach based on the ENMSS model is described.

Chapter 5 introduces the corresponding PFC method that uses the ENMSS model.

Chapter 6 discusses the basic constraints dealing in the ENMSS model-based MPC.

Chapter 7 explores the optimization of PID control parameters using the ENMSS model-based MPC strategies.

Chapter 8 gives the relevant closed-loop system performance analysis.

Chapter 9 describes the improved ENMSS model-based MPC approaches in which GA is used to optimize the choice of the control parameters.

Chapter 10 presents the industrial application of the novel ENMSS model-based MPC.

Chapter 11 introduces the relaxed constrained optimization scheme for ENMSS model-based MPC and PFC.

Hangzhou, China — Ridong Zhang
Hangzhou, China — Anke Xue
Hong Kong, China — Furong Gao

Acknowledgements

The material proposed in this book is the outcome of several years of research work dated back to 2007 by the authors. We start to prepare the book in 2016 when the first author was visiting the Hong Kong University of Science and Technology with the third author Prof. Furong Gao. Many parts of the book have been modified after significant discussion with colleagues and graduate students. We would like to take this opportunity to appreciate the support of these people. We would like to thank Profs. Shuqing Wang and Hongye Su (Zhejiang University), Prof. Ping Li (Liaoning Shihua University), Prof. Steven Ding (University of Duisburg), Prof. Rolf Findeison (Otto-von-Guericke University Magdeburg), Prof. Babatunde A. Ogunnaike (University of Delaware), and Profs. Biao Huang and Jinfeng Liu (University of Alberta, Canada). A former graduate student Sheng Wu helped me in editing the contents. Moreover, my research work has been supported by National Natural Science Foundation of China (60804010, 61273101, 61673147) and projects supported by Ministry of Science and Technology of China (2013DFH10120) and Zhejiang Province (LR16F030004).

Contents

About the Authors

Ridong Zhang received the Ph.D. degree in control science and engineering from Zhejiang University, Hangzhou, China, in 2007. From 2007 to 2015, he was a Full Professor with the Institute of Information and Control, Hangzhou Dianzi University, Hangzhou. From 2015 to now, he was a Visiting Professor at the Chemical and Biomolecular Engineering Department, The Hong Kong University of Science and Technology, Hong Kong. His research interests include process modeling, model predictive control and nonlinear systems.

Anke Xue received the Ph.D. degree in control science and engineering from Zhejiang University, Hangzhou, China, in 1997. He is currently a Full Professor with the Institute of Information and Control, Hangzhou Dianzi University, Hangzhou. His research interest covers robust control theory and applications.

Furong Gao received B.Eng. degree in automation from China University of Petroleum, China, in 1985 and M.Eng. and Ph.D. degrees in chemical engineering from McGill University, Montreal, Canada, in 1989 and 1993, respectively. He was employed as a Senior Research Engineer by Moldflow International Company Ltd. Since 1995, he has been with Hong Kong University of Science and Technology, where he is currently a Chair Professor in the Department of Chemical and Biomolecular Engineering. His research interests include process monitoring and control and polymer processing.

Chapter 1
Introduction

1.1 An Overview of This Book

As to the control problem of industrial processes with various constraints, the desired control performance may not be obtained by the employment of conventional control strategies, such as PID control [1–4]. In order to cope with the control of these processes that exist widely in practice, MPC was proposed as an effective advanced control strategy and has gained lots of industrial applications [5–11]. Driven by the rapid development of economy and stricter requirement, there are challenges on both control performance and applications for the earlier basic MPC algorithms, i.e., dynamic matrix control (DMC), model algorithmic control (MAC) and generalized predictive control (GPC). Therefore, how to improve their control performance, extend their applications, simplify their computation, etc., are important open issues we need to focus on.

The introduction of state space models that contain more system information facilitates the development of MPC approaches, due to the fact that the relevant controller design is more straightforward and the system analysis is more convenient. There were numerous fruits on the theory and applications of state space model based MPC strategies during the past decades [12–17].

It is known that complex high-order and multivariable processes exist widely in industry, meanwhile, dozens or even hundreds of constraints may need to be handled, such that the requirements for the servers on computational performance may be stricter in order to solve the corresponding on-line optimization [18–20]. Based on such backgrounds, distributed MPC schemes are presented [21–24]. By employing the distributed MPC methods, the large-scale on-line optimization problem can be decomposed into many small-scale distributed optimization of intelligent agents, hence the demands on the computational performance for servers can be reduced. Note that the effect on the performance caused by the information loss in the traditional decentralized MPC can be compensated for in the distributed MPC methods, because there are information communications between these intelligent

R. Zhang et al., *Model Predictive Control*,
https://doi.org/10.1007/978-981-13-0083-7_1

agents. Many researchers contribute to the development of distributed MPC schemes [25–32]. In order to handle the control of a group of nonlinear agents under input constraints and disturbance, a robust distributed MPC scheme was investigated by Li et al. [33]. In [34], an improved distributed controller in which the performance index is enhanced and feasibility is guaranteed was presented for nonlinear systems. For a class of large-scale systems that consists of discrete-time linear coupled subsystems, a cooperative distributed MPC strategy was developed [35]. To cope with the coupled and constrained linear discrete systems, the limited-communication distributed MPC approach was proposed by Jalal et al. [36]. Based on the accelerated gradient methods using dual decomposition, a distributed MPC scheme was presented for the mixed L-1/L-2-norm optimization problem [37]. It is the fact that the control performance of distributed MPC approaches is affected by the condition of the information communications between the intelligent agents greatly. Unfortunately, the inevitable disturbance and other uncertainty in practice imply that the ideal information exchanges between these agents can hardly be ensured.

Consider the above mentioned situations, how to reduce the computational burden of MPC is also investigated, and many significant results on the development of fast computation of MPC have been put forward [38–43]. In [44], a fast nonlinear MPC scheme in which the particle swarm optimization algorithm is employed to handle the nonlinear optimization problem was described. In order to reduce the computational burden of finite control set MPC strategy for multilevel cascade H-bridge STATCOM, a fast MPC method was developed by Zhang et al. [45]. Nguyen et al. [46] presented the fast MPC method for the linear periodic systems with state and control constraints. By solving a parametric optimization problem that can be pre-computed offline, an MPC scheme in which an explicit map from the state to the control input is provided was given in [47]. In [48], an improved MPC strategy in which the complexity of the relevant optimization problem is reduced was presented for the urban traffic networks. Among these important fruits, it is an important fact that the introduction of explicit MPC strategies in which the multi-parameter quadratic programming is adopted and the repetitive computation can be finished offline is promising because the amount of on-line calculation is decreased largely. There are also many representative results on the development of explicit MPC schemes [49–55]. In [56], an explicit MPC approach for the attitude of a satellite was presented. A sensorless explicit MPC method was developed for the dc–dc boost converter [57]. In order to handle the control of hybrid systems, the explicit MPC strategies in which the control inputs serving as a set of functions of the state variables were proposed by Charitopoulos et al. [58]. In [59], the explicit MPC schemes were developed for nonlinear systems with state constraints and fast dynamics. Nascu et al. [60] put forward a hybrid explicit MPC approach in which a piece-wise affine model is employed for intravenous anaesthesia. It is known that the explicit MPC approaches can only be employed under the small-scale optimization situation, and the requirement on high speed and real-time application may not be satisfactory for complex large-scale control systems.

In conclusion, there is still room for the development of simplifying the computation of MPC algorithms for complex systems. In order to ensure more benefits, the product quality, the operation safety, etc., maintaining the desired control per-

formance of MPC strategies for industrial processes under various disturbances and uncertainty is also important [61–63]. To achieve this goal, the robust MPC scheme is viewed as a significant research goal, and a lot of results are developed by combing with Lyapunov functions [64, 65], linear matrix inequality (LMI) [66–70], state feedback control laws [71–73], min–max problems [74–76], and so on. In [77], a robust MPC scheme for nonlinear systems under constraints, uncertainty and actuator faults was discussed. To cope with the control of continuous time nonlinear systems under bounded disturbance, the event-triggered robust MPC strategy was studied by Li et al. [78]. Calafiore et al. [79] presented a robust MPC method in which a novel probabilistic approach is used for linear systems under parametric uncertainty and disturbance. In [80], the robust fuzzy MPC strategy for nonlinear systems subjected to time delays and disturbances was investigated. In order to deal with the control of nonlinear systems with state-dependent uncertainty, a new design of robust MPC scheme was described by Ojaghi et al. [81]. Besides, the study on tube-based robust MPC schemes and stochastic robust MPC strategies are also hot issues [82–85]. For nonlinear systems under bounded uncertainty, a robust MPC method in which a collective neurodynamic approach is employed was proposed by Yan et al. [86]. In [87], the robust tube based MPC scheme was applied to constrained linear switched systems subjected to bounded additive disturbance. In order to achieve robust control of nonlinear systems with additive disturbance, the tube-based MPC strategy was presented [88]. The development of stochastic MPC algorithms for systems under stochastic disturbances and model uncertainty was reviewed by Farina et al. [89]. In [90], a Gaussian process based stochastic MPC method was developed for the drinking water networks. Great progress has been made in the theory for robust MPC algorithms, however, its implementations in practice are restricted due to the huge amount of on-line computation. The efforts on how to develop more effective and feasible MPC algorithms for industrial processes still need to be explored.

In addition to the above issues, the extension of the applications of MPC approaches also attracts a lot of attention, and many studies on the adoption of MPC strategies on hybrid systems, such as piecewise affine systems [91–93], switch systems [94–97], and so on, have been presented. In order to reduce the energy cost in a hybrid heating system, an effective MPC method was designed by Khanmirza et al. [98]. In [99], a novel MPC strategy that uses the slope information to improve fuel economy was developed for the hybrid electric vehicle platooning. Based on the uncontrollable divergence metric, the hybrid MPC schemes that switch between two predictor functions were described [100]. In order to optimize the fuel economy and reduce tailpipe emissions simultaneously for hybrid electric vehicles, a MPC method was investigated by Zhao et al. [101]. In [102], a nonlinear MPC strategy was proposed for the thermal management of plug-in hybrid electric vehicles. During the running process of the hybrid systems that have several models, it is hard to prevent the appearance of oscillations and the deterioration of the system performance when the models or dynamics are switched. Hence, MPC schemes with stronger robustness and better ensemble control performance are needed.

In addition to the conventional applications of MPC algorithms in many chemical processes regarded as slow processes, the extension of MPC strategies to the

fast processes, such as the embedded systems, are also hot topics. In [103], the state-of-the-art in the emerging field of dependable embedded MPC strategy was surveyed. The computational complexity for solving the linearly constrained convex problems in MPC scheme using the dual gradient method for embedded systems was discussed by Necoara et al. [104]. The arithmetic operation necessaries for solving the MPC optimization problems of embedded systems were exploited in [105]. In order to achieve accurate control and high computational performance of embedded MPC, the efficient step response model implementation methods were put forward by Kufoalor et al. [106]. In [107], a real-time explicit MPC strategy that is implemented on a microcontroller unit was developed for a vibration suppression system. To meet the applications of MPC on embedded systems, the MPC approaches need to be simplified because the computational power and the memory capacity of these small processors are limited. Meanwhile, improved control performance of the MPC methods is necessary to cope with the uncertainty in practice.

To gain more profits is a principal target for industrial processes. In order to increase the profits by considering more factors in the actual processes, economic MPC schemes are investigated. To cope with the actuator faults in an economics-based feedback controller, a data-driven method was described in [108]. In [109], the robust economic MPC strategy was developed for the control of diesel generators. Wang et al. [110] exploited a nonlinear economic MPC approach for the water distribution networks. In [111], an economic MPC algorithm was employed for linear systems with indefinite quadratic costs. Maestre et al. [112] applied the economic MPC scheme to the inventory management in a real hospital. Although more benefits are acquired by employing the economic objective function, the complexity for the relevant solution process is increased simultaneously, so that the enhanced MPC strategies with lower complexity are required.

As to the complex constrained control systems, there may be no feasible solutions due to the abominable working conditions, rigorous parameters, etc. Under such situations, the control law for the control system cannot be updated timely, thus the acceptable control performance may not be guaranteed. How to handle the constraints in the control system properly and effectively is a vital topic needed to be focused on, and there are many important viewpoints [113–118]. In [119], a constrained MPC method was employed for the mobile manipulation tracking problems. In order to guarantee the feasibility of on-line optimization, a novel soft constrained MPC strategy was presented by Zeilinger et al. [120]. Through introducing additional points, improved constraint handling performance was obtained [121]. In [122], the constrained state feedback speed control was exploited for a permanent-magnet synchronous motor. Based on a newly developed coupled thermoelectric model, the constrained GPC approach was proposed to charge the battery by Liu et al. [123]. Limited by the power of the processor, the cycle of the controller, etc., some existing constrained MPC methods may not be implemented in the industrial process at present, thus the development of more effective and practical constrained MPC strategies is still necessary.

Besides the above topics, there are also many other research directions of MPC schemes. In a word, how to develop an effective MPC approach with ideal con-

trol performance, acceptable amount of computation and lower complexity is the direction we still need to explore.

As to the issues mentioned above, several relevant ideas are proposed in this book. In order to enhance the ensemble control performance of MPC strategies, the improved extended state space model [124–128] in which the state variables and the tracking error are combined and regulated separately is employed. Compared with conventional state space models, more process information is considered in the new state space model, and the degrees of freedom for the relevant controller design are increased due to the fact that the choice of the corresponding weighting matrices is more flexible. Further, the improved MPC schemes are also used to optimize the parameters of PID control [129–132]. By introducing the control law of PID control into the framework of MPC approaches, the improved PID controller that inherits the simple structure of traditional PID controllers and the excellent control performance MPC algorithms is obtained. In this book, GA is also combined to improve the ensemble control performance of MPC algorithms [133] and more suitable control parameters are obtained. Moreover, some corresponding real applications in the industry [134, 135] are also presented in this book, and the typical PID and MPC approaches in the literature [136, 137] are introduced as the comparison to test the effectiveness of the improved state space model based MPC schemes. For the constraint handling problem in MPC strategies, a relaxed constrained optimization method in which many relaxations are united in the performance index is presented in this book. By adopting this improved relaxed method, the probability of no feasible solutions for the online optimization of constrained MPC strategies under rigorous parameters and bad working conditions is avoided.

1.2 Main Features of This Book

In this book, both the theory and applications of MPC strategies are discussed, and the contents contain four main aspects: the improved state space model for MPC schemes, the constraint handling method for MPC algorithms, further parameter optimization for MPC approaches and the relevant industrial applications. The corresponding features contain:

1. An overview of MPC strategies, including the distributed MPC, the explicit MPC, the robust MPC, the economic MPC, the constrained MPC, etc.
2. An improved extended state space model in which the state variables and the tracking error dynamics are combined and regulated separately for MPC and PFC schemes.
3. The extended non-minimal state space models that are converted from the input–output models for MPC and PFC approaches.
4. The optimization of PID control parameters by introducing the control law of PID control into the framework of MPC methods.

5. The basic constraint handling method and the improved relaxed constrained optimization approach for MPC algorithms.
6. The closed-loop system performance analysis for the proposed MPC schemes.
7. GA is introduced to optimize the choice of the control parameters of MPC approaches.
8. The real-time applications of the corresponding MPC algorithms to the control of temperature and air supply in the industrial coke furnace.

1.3 Organization of This Book

In order to make this book readily comprehensible, the contents are divided into two parts. In Part I, the basic algorithms are described. The system performance analysis, parameter optimization and application of the MPC strategies are shown in Part II.

Part I includes Chaps. 2–7. In Chap. 2, the conventional state space model is converted into the extended form and the corresponding improved MPC strategy is presented. The extended state space model is also employed to enhance the control performance of PFC, and the details are shown in Chap. 3. Chapter 4 describes the extended non-minimal state space model that is transformed from the input–output model and the relevant MPC design. In Chap. 5, the extended non-minimal state space model based PFC approach is discussed. The basic constrained MPC method is discussed in Chaps. 6 and 7 investigates the application of the MPC algorithms to optimize the parameters of PID control. Chapters 8–11 constitute Part II of this book. In Chap. 8, the closed-loop system performance of the relevant control system is analyzed. Chapter 9 describes the improved MPC method in which the GA is employed to optimize the choice of the control parameters. The applications of the corresponding MPC schemes to the industrial coke furnace are presented in Chap. 10. In Chap. 11, the relaxed constrained optimization approach is introduced for the constraint handling in the MPC algorithms.

A large portion of the material in this book was published in relevant journals by the authors several years ago, and included here for relevance and completeness. This includes:

Parts of Chaps. 2–8, reprinted with permission from Industrial & Engineering Chemistry Research, volume 56, Ridong Zhang, Sheng Wu, Furong Gao, “State space model predictive control for advanced process operation: A review of recent development, new results and insight”, 5360–5394, ©2017 American Chemical Society.

Chapter 9, reprinted from Chemometrics and Intelligent Laboratory Systems, volume 137, Ridong Zhang, Hongbo Zou, Anke Xue, Furong Gao, "GA based predictive functional control for batch processes under actuator faults", 67–73, ©2014 Elsevier Ltd., with permission from Elsevier.

Section 10.2 of Chap. 10, ©2014 IEEE. Reprinted, with permission from IEEE Transactions on Industrial Informatics, volume 10, Ridong Zhang, Anke Xue, Furong Gao, "Temperature control of industrial coke furnace using novel state space model predictive control", 2084–2092 and IEEE Transactions on Industrial Electronics, volume 61, Ridong Zhang, Anke Xue, Renquan Lu, Ping Li, Furong Gao, "Real-time implementation of improved state space MPC for air-supply in a coke furnace", 3532–3539.

References

1. Tyreus, B. D., & Luyben, W. L. (1992). Tuning PI controllers for integrator/dead time processes. *Industrial & Engineering Chemistry Research, 31*(11), 2625–2628.
2. Skogestad, S. (2003). Simple analytic rules for model reduction and PID controller tuning. *Journal of Process Control, 13*(4), 291–309.
3. Padula, F., & Visioli, A. (2011). Tuning rules for optimal PID and fractional-order PID controllers. *Journal of Process Control, 21*(1), 69–81.
4. Lee, Y., Park, S., Lee, M., & Brosilow, C. (1998). PID controller tuning for desired closed-loop responses for SI/SO systems. *AIChE Journal, 44*(1), 106–115.
5. Qin, S. J., & Badgwell, T. A. (2003). A survey of industrial model predictive control technology. *Control Engineering Practice, 11*(7), 733–764.
6. Lawrynczuk, M. (2017). Nonlinear predictive control of a boiler-turbine unit: A state-space approach with successive on-line model linearisation and quadratic optimisation. *ISA Transactions, 67,* 476–495.
7. Lee, J. H. (2011). Model predictive control: Review of the three decades of development. *International Journal of Control, Automation and Systems, 9*(3), 415–424.
8. Lu, X. L., Kiumarsi, B., Chai, T. Y., & Lewis, F. L. (2016). Data-driven optimal control of operational indices for a class of industrial processes. *IET Control Theory and Applications, 10*(12), 1348–1356.
9. Wang, T., Gao, H. J., & Qiu, J. B. (2016). A combined fault-tolerant and predictive control for network-based industrial processes. *IEEE Transactions on Industrial Electronics, 63*(4), 2529–2536.
10. Bindlish, R. (2015). Nonlinear model predictive control of an industrial polymerization process. *Computers & Chemical Engineering, 73,* 43–48.
11. Huyck, B., Brabanter, J., Moor, B., Van Impe, J. F., & Logist, F. (2014). Online model predictive control of industrial processes using low level control hardware: A pilot-scale distillation column case study. *Control Engineering Practice, 28,* 34–48.
12. Mayne, D. Q. (2014). Model predictive control: Recent developments and future promise. *Automatica, 50*(12), 2967–2986.
13. Gallego, A. J., & Camacho, E. F. (2012). Adaptative state-space model predictive control of a parabolic-trough field. *Control Engineering Practice, 20*(9), 904–911.
14. Falugi, P., Olaru, S., & Dumur, D. (2010). Multi-model predictive control based on LMI: from the adaptation of the state-space model to the analytic description of the control law. *International Journal of Control, 83*(8), 1548–1563.

15. Miranda, H., Cortes, P., Yuz, J. I., & Rodriguez, J. (2009). Predictive torque control of induction machines based on state-space models. *IEEE Transactions on Industrial Electronics, 56*(6), 1916–1924.
16. Simkoff, J. M., Wang, S. Y., Baldea, M., Chiang, L. H., Castillo, I., Bindlish, R., et al. (2018). Plant-model mismatch estimation from closed-loop data for state-space model predictive control. *Industrial & Engineering Chemistry Research, 57*(10), 3732–3741.
17. Zou, T., Wu, S., & Zhang, R. D. (2018). Improved state space model predictive fault-tolerant control for injection molding batch processes with partial actuator faults using GA optimization. *ISA Transactions, 73,* 147–153.
18. Wang, Y., & Boyd, S. (2010). Fast model predictive control using online optimization. *IEEE Transactions on Control Systems Technology, 18*(2), 267–278.
19. Kim, I., Chan, R., & Kwak, S. (2017). Model predictive control method for CHB multilevel inverter with reduced calculation complexity and fast dynamics. *IET Electric Power Applications, 11*(5), 784–792.
20. Huang, R., Biegler, L. T., & Patwardhan, S. C. (2010). Fast offset-free nonlinear model predictive control based on moving horizon estimation. *Industrial & Engineering Chemistry Research, 49*(17), 7882–7890.
21. Zheng, Y., Li, S. Y., & Tan, R. M. (2018). Distributed model predictive control for onconnected microgrid power management. *IEEE Transactions on Control Systems Technology, 26*(3), 1028–1039.
22. Velarde, P., Maestre, J. M., Ishii, H., & Negenborn, R. R. (2018). Vulnerabilities in Lagrange-based distributed model predictive control. *Optimal Control Applications & Methods, 39*(2), 601–621.
23. Long, Y. S., Liu, S., Xie, L. H., & Johansson, K. H. (2018). Distributed nonlinear model predictive control based on contraction theory. *International Journal of Robust and Nonlinear Control, 28*(2), 492–503.
24. Franze, G., Lucia, W., & Tedesco, F. (2018). A distributed model predictive control scheme for leader-follower multi-agent systems. *International Journal of Control, 91*(2), 369–382.
25. Pourkargar, D. B., Almansoori, A., & Daoutidis, P. (2017). Impact of decomposition on distributed model predictive control: A process network case study. *Industrial & Engineering Chemistry Research, 56*(34), 9606–9616.
26. Tarisciotti, L., Lo Calzo, G., Gaeta, A., Zanchetta, P., Valencia, F., & Saez, D. (2016). A distributed model predictive control strategy for back-to-back converters. *IEEE Transactions on Industrial Electronics, 63*(9), 5867–5878.
27. Kersbergen, B., van den Boom, T., & Schutter, B. (2016). Distributed model predictive control for railway traffic management. *Transportation Research Part C-Emerging Technologies, 68,* 462–489.
28. Farina, M., Ferrari, G. P., Manenti, F., & Pizzi, E. (2016). Assessment and comparison of distributed model predictive control schemes: Application to a natural gas refrigeration plant. *Computers & Chemical Engineering, 89,* 192–203.
29. Esfahani, N. R., & Khorasani, K. (2016). A distributed model predictive control (MPC) fault reconfiguration strategy for formation flying satellites. *International Journal of Control, 89*(5), 960–983.
30. Halvgaard, R., Vandenberghe, L., Poulsen, N. K., Madsen, H., & Jorgensen, J. B. (2016). Distributed model predictive control for smart energy systems. *IEEE Transactions on Smart Grid, 7*(3), 1675–1682.
31. Farhadi, A., & Khodabandehlou, A. (2016). Distributed model predictive control with hierarchical architecture for communication: Application in automated irrigation channels. *International Journal of Control, 89*(8), 1725–1741.
32. Gao, Y. L., Xia, Y. Q., & Dai, L. (2015). Cooperative distributed model predictive control of multiple coupled linear systems. *IET Control Theory and Applications, 9*(17), 2561–2567.

33. Li, H. P., & Shi, Y. (2014). Robust distributed model predictive control of constrained continuous-time nonlinear systems: A robustness constraint approach. *IEEE Transactions on Automatic Control, 59*(6), 1673–1678.
34. Stewart, B. T., Wright, S. J., & Rawlings, J. B. (2011). Cooperative distributed model predictive control for nonlinear systems. *Journal of Process Control, 21*(5), 698–704.
35. Razavinasab, Z., Farsangi, M. M., & Barkhordari, M. (2017). State estimation-based distributed model predictive control of large-scale networked systems with communication delays. *IET Control Theory and Applications, 11*(15), 2497–2505.
36. Jalal, R. E., & Rasmussen, B. P. (2017). Limited-communication distributed model predictive control for coupled and constrained subsystems. *IEEE Transactions on Control Systems Technology, 25*(5), 1807–1815.
37. Giselsson, P., Doan, M. D., Keviczky, T., Schutter, B., & Rantzer, A. (2013). Accelerated gradient methods and dual decomposition in distributed model predictive control. *Automatica, 49*(3), 829–833.
38. Zhuge, J. J., & Ierapetritou, M. G. (2015). An integrated framework for scheduling and control using fast model predictive control. *AIChE Journal, 61*(10), 3304–3319.
39. Li, S. E., Jia, Z. H., Li, K. Q., & Cheng, B. (2015). Fast online computation of a model predictive controller and its application to fuel economy-oriented adaptive cruise control. *IEEE Transactions on Intelligent Transportation Systems, 16*(3), 1199–1209.
40. Richards, A. (2015). Fast model predictive control with soft constraints. *European Journal of Control, 25,* 51–59.
41. Ahmed, H. (2015). Reactive power and voltage control in grid-connected wind farms: An online optimization based fast model predictive control approach. *Electrical Engineering, 97*(1), 35–44.
42. Jaschke, J., Yang, X., & Biegler, L. T. (2014). Fast economic model predictive control based on NLP-sensitivities. *Journal of Process Control, 24*(8), 1260–1272.
43. Lopez-Negrete, R., D'Amato, F. J., Biegler, L. T., & Kumar, A. (2013). Fast nonlinear model predictive control: Formulation and industrial process applications. *Computers & Chemical Engineering, 51,* 55–64.
44. Xu, F., Chen, H., Gong, X., & Mei, Q. (2016). Fast nonlinear model predictive control on FPGA using particle swarm optimization. *IEEE Transactions on Industrial Electronics, 63*(1), 310–321.
45. Zhang, Y. L., Wu, X. J., Yuan, X. B., Wang, Y. J., & Dai, P. (2016). Fast model predictive control for multilevel cascaded H-bridge STATCOM with polynomial computation time. *IEEE Transactions on Industrial Electronics, 63*(8), 5231–5243.
46. Nguyen, H. N., Bourdais, R., & Gutman, P. O. (2017). Fast model predictive control for linear periodic systems with state and control constraints. *International Journal of Robust and Nonlinear Control, 27*(17), 3703–3726.
47. Summers, S., Jones, C. N., Lygeros, J., & Morari, M. (2011). A multiresolution approximation method for fast explicit model predictive control. *IEEE Transactions on Automatic Control, 56*(11), 2530–2541.
48. Lin, S., Schutter, B., Xi, Y. G., & Hellendoorn, H. (2011). Fast model predictive control for urban road networks via MILP. *IEEE Transactions on Intelligent Transportation Systems, 12*(3), 846–856.
49. Wei, C. S., Luo, J. J., Dai, H. H., Yin, Z. Y., Ma, W. H., & Yuan, J. P. (2017). Globally robust explicit model predictive control of constrained systems exploiting SVM-based approximation. *International Journal of Robust and Nonlinear Control, 27*(16), 3000–3027.
50. Oberdieck, R., Diangelakis, N. A., & Pistikopoulos, E. N. (2017). Explicit model predictive control: A connected-graph approach. *Automatica, 76,* 103–112.
51. Chakrabarty, A., Dinh, V., Corless, M. J., Rundell, A. E., Zak, S. H., & Buzzard, G. T. (2017). Support vector machine informed explicit nonlinear model predictive control using low-discrepancy sequences. *IEEE Transactions on Automatic Control, 62*(1), 135–148.
52. Gao, Y., & Sun, L. N. (2016). Explicit solution of min-max model predictive control for uncertain systems. *IET Control Theory and Applications, 10*(4), 461–468.

53. Wallace, M., Kumar, S. S. P., & Mhaskar, P. (2016). Offset-free model predictive control with explicit performance specification. *Industrial & Engineering Chemistry Research, 55*(4), 995–1003.
54. Oberdieck, R., & Pistikopoulos, E. N. (2015). Explicit hybrid model-predictive control: The exact solution. *Automatica, 58,* 152–159.
55. Rivotti, P., & Pistikopoulos, E. N. (2015). A dynamic programming based approach for explicit model predictive control of hybrid systems. *Computers & Chemical Engineering, 72,* 126–144.
56. Hegrenaes, O., Gravdahl, J. T., & Tondel, P. (2005). Spacecraft attitude control using explicit model predictive control. *Automatica, 41*(12), 2107–2114.
57. Beccuti, A. G., Mariethoz, S., Cliquennois, S., Wang, S., & Morari, M. (2009). Explicit model predictive control of dc-dc switched-mode power supplies with extended Kalman filtering. *IEEE Transactions on Industrial Electronics, 56*(6), 1864–1874.
58. Charitopoulos, V. M., & Dua, V. (2016). Explicit model predictive control of hybrid systems and multiparametric mixed integer polynomial programming. *AIChE Journal, 62*(9), 3441–3460.
59. Chakrabarty, A., Buzzard, G. T., & Zak, S. H. (2017). Output-tracking quantized explicit nonlinear model predictive control using multiclass support vector machines. *IEEE Transactions on Industrial Electronics, 64*(5), 4130–4138.
60. Nascu, L., Oberdieck, R., & Pistikopoulos, E. N. (2017). Explicit hybrid model predictive control strategies for intravenous anaesthesia. *Computers & Chemical Engineering, 106*, 814–825.
61. Wang, F. X., Li, S. H., Mei, X. Z., Xie, W., Rodriguez, J., & Kennel, R. M. (2015). Model-based predictive direct control strategies for electrical drives: An experimental evaluation of PTC and PCC methods. *IEEE Transactions on Industrial Informatics, 11*(3), 671–681.
62. Muller, M. A., Angeli, D., & Allgower, F. (2015). On Necessity and robustness of dissipativity in economic model predictive control. *IEEE Transactions on Automatic Control, 60*(6), 1671–1676.
63. Zhang, Y. C., & Qu, C. Q. (2015). Model predictive direct power control of PWM rectifiers under unbalanced network conditions. *IEEE Transactions on Industrial Electronics, 62*(7), 4011–4022.
64. Ma, Y., & Cai, Y. L. (2018). A fuzzy model predictive control based upon adaptive neural network disturbance observer for a constrained hypersonic vehicle. *IEEE Access, 6,* 5927–5938.
65. Du, G. P., Liu, Z. F., Du, F., & Li, J. J. (2017). Performance improvement of model predictive control using control error compensation for power electronic converters based on the Lyapunov function. *Journal of Power Electronics, 17*(4), 983–990.
66. Nodozi, I., & Rahmani, M. (2017). LMI-based model predictive control for switched nonlinear systems. *Journal of Process Control, 59,* 49–58.
67. Ghaffari, V. (2017). A robust control system scheme based on model predictive controller (MPC) for continuous-time systems. *Optimal Control Applications & Methods, 38*(6), 1032–1041.
68. Song, Y., Fang, X. S., & Diao, Q. D. (2016). Mixed H_2/H_∞ distributed robust model predictive control for polytopic uncertain systems subject to actuator saturation and missing measurements. *International Journal of Systems Science, 47*(4), 777–790.
69. Tahir, F., & Jaimoukha, I. M. (2013). Causal state-feedback parameterizations in robust model predictive control. *Automatica, 49*(9), 2675–2682.
70. Ghaffari, V., Naghavi, S. V., & Safavi, A. A. (2013). Robust model predictive control of a class of uncertain nonlinear systems with application to typical CSTR problems. *Journal of Process Control, 23*(4), 493–499.
71. Mohammadkhani, M., Bayat, F., & Jalali, A. A. (2017). Robust output feedback model predictive control: A stochastic approach. *Asian Journal of Control, 19*(6), 2085–2096.
72. Ding, B. C., Xi, Y. G., & Li, S. S. (2004). A synthesis approach of on-line constrained robust model predictive control. *Automatica, 40*(1), 163–167.
73. Zhang, L. W., Xie, W., & Wang, J. C. (2017). Robust distributed model predictive control of linear systems with structured time-varying uncertainties. *International Journal of Control, 90*(11), 2449–2460.

74. Villanueva, M. E., Quirynen, R., Diehl, M., Chachuat, B., & Houska, B. (2017). Robust MPC via min-max differential inequalities. *Automatica, 77,* 311–321.
75. Liu, X. J., Jiang, D., & Lee, K. Y. (2015). Quasi-min-max fuzzy MPC of UTSG water level based on off-line invariant set. *IEEE Transactions on Nuclear Science, 62*(5), 2266–2272.
76. Ramirez, D. R., Alamo, T., & Camacho, E. F. (2011). Computational burden reduction in min-max MPC. *Journal of The Franklin Institute-Engineering and Applied Mathematics, 348*(9), 2430–2447.
77. Mhaskar, P. (2006). Robust model predictive control design for fault-tolerant control of process systems. *Industrial & Engineering Chemistry Research, 45*(25), 8565–8574.
78. Li, H. P., & Shi, Y. (2014). Event-triggered robust model predictive control of continuous-time nonlinear systems. *Automatica, 50*(5), 1507–1513.
79. Calafiore, G. C., & Fagiano, L. (2013). Robust model predictive control via scenario optimization. *IEEE Transactions on Automatic Control, 58*(1), 219–224.
80. Teng, L., Wang, Y. Y., Cai, W. J., & Li, H. (2017). Robust model predictive control of discrete nonlinear systems with time delays and disturbances via T-S fuzzy approach. *Journal of Process Control, 53,* 70–79.
81. Ojaghi, P., Bigdeli, N., & Rahmani, M. (2016). An LMI approach to robust model predictive control of nonlinear systems with state-dependent uncertainties. *Journal of Process Control, 47,* 1–10.
82. Brunner, F. D., Heemels, M., & Allgower, F. (2016). Robust self-triggered MPC for constrained linear systems: A tube-based approach. *Automatica, 72,* 73–83.
83. Ghasemi, M. S., & Afzalian, A. A. (2017). Robust tube-based MPC of constrained piecewise affine systems with bounded additive disturbances. *Nonlinear Analysis-Hybrid Systems, 26,* 86–100.
84. Bumroongsri, P., & Kheawhom, S. (2016). An off-line formulation of tube-based robust MPC using polyhedral invariant sets. *Chemical Engineering Communications, 203*(6), 736–745.
85. Bumroongsri, P. (2015). Tube-based robust MPC for linear time-varying systems with bounded disturbances. *International Journal of Control, Automation and Systems, 13*(3), 620–625.
86. Yan, Z., Le, X. Y., & Wang, J. (2016). Tube-based robust model predictive control of nonlineat systems via collective neurodynamic optimization. *IEEE Transactions on Industrial Electronics, 63*(7), 4377–4386.
87. Hariprasad, K., & Bhartiya, S. (2016). A computationally efficient robust tube based MPC for linear switched systems. *Nonlinear Analysis-Hybrid Systems, 19,* 60–76.
88. Mayne, D. Q., Kerrigan, E. C., van Wyk, E. J., & Falugi, P. (2011). Tube-based robust nonlinear model predictive control. *International Journal of Robust and Nonlinear Control, 21*(11), 1341–1353.
89. Farina, M., Giulioni, L., & Scattolini, R. (2016). Stochastic linear model predictive control with chance constraints—A review. *Journal of Process Control, 44,* 53–67.
90. Wang, Y., Ocampo-Martinez, C., & Puig, V. (2016). Stochastic model predictive control based on Gaussian processes applied to drinking water networks. *IET Control Theory and Applications, 10*(8), 947–955.
91. Putz, E., & Cipriano, A. (2015). Hybrid model predictive control for flotation plants. *Minerals Engineering, 70,* 26–35.
92. Sarailoo, M., Rahmani, Z., & Rezaie, B. (2014). Fuzzy predictive control of a boiler-turbine system based on a hybrid model system. *Industrial & Engineering Chemistry Research, 53*(6), 2362–2381.
93. Rubagotti, M., Barcelli, D., & Bemporad, A. (2014). Robust explicit model predictive control via regular piecewise-affine approximation. *International Journal of Control, 87*(12), 2583–2593.
94. Ong, C. J., Wang, Z. M., & Dehghan, M. (2016). Model predictive control for switching systems with dwell-time restriction. *IEEE Transactions on Automatic Control, 61*(12), 4189–4195.

95. Xu, W. D., Zhang, J. F., & Zhang, R. D. (2017). Application of multi-model switching predictive functional control on the temperature system of an electric heating furnace. *ISA Transactions, 68,* 287–292.
96. Hariprasad, K., & Bhartiya, S. (2017). An efficient and stabilizing model predictive control of switched system. *IEEE Transactions on Automatic Control, 62*(7), 3401–3407.
97. Zhang, L. X., Zhuang, S. L., & Braatz, R. D. (2016). Switched model predictive control of switched linear systems: Feasibility, stability and robustness. *Automatica, 67,* 8–21.
98. Khanmirza, E., Esmaeilzadeh, A., & Markazi, A. H. D. (2016). Predictive control of a building hybrid heating system for energy cost reduction. *Applied Soft Computing, 46,* 407–423.
99. Yu, K. J., Yang, H. Z., Tan, X. G., Kawabe, T., Guo, Y. N., Liang, Q., et al. (2016). Model predictive control for hybrid electric vehicle platooning using slope information. *IEEE Transactions on Intelligent Transportation Systems, 17*(7), 1894–1909.
100. Zhang, K., Sprinkle, J., & Sanfelice, R. G. (2016). Computationally aware switching criteria for hybrid model predictive control of cyber-physical systems. *IEEE Transactions on Automation Science and Engineering, 13*(2), 479–490.
101. Zhao, J. F., & Wang, J. M. (2016). Integrated model predictive control of hybrid electric vehicles coupled with aftertreatment systems. *IEEE Transactions on Vehicular Technology, 65*(3), 1199–1211.
102. Lopez-Sanz, J., Ocampo-Martinez, C., Alvarez-Florez, J., Moreno-Eguilaz, M., Ruiz-Mansilla, R., Kalmus, J., et al. (2017). Nonlinear model predictive control for thermal management in plug-in hybrid electric vehicles. *IEEE Transactions on Vehicular Technology, 66*(5), 3632–3644.
103. Johansen, T. A. (2017). Toward dependable embedded model predictive control. *IEEE Systems Journal, 11*(2), 1208–1219.
104. Necoara, I. (2015). Computational complexity certification for dual gradient method: Application to embedded MPC. *Systems & Control Letters, 81,* 49–56.
105. Lucia, S., Navarro, D., Lucia, O., Zometa, P., & Findeisen, R. (2018). Optimized FPGA implementation of model predictive control for embedded systems using high-level synthesis tool. *IEEE Transactions on Industrial Informatics, 14*(1), 137–145.
106. Kufoalor, D. K. M., Imsland, L., & Johansen, T. A. (2016). Efficient implementation of step response models for embedded model predictive control. *Computers & Chemical Engineering, 90,* 121–135.
107. Takacs, G., Batista, G., Gulan, M., & Rohal'-llkiv, B. (2016). Embedded explicit model predictive vibration control. *Mechatronics, 36,* 54–62.
108. Alanqar, A., Durand, H., & Christofides, P. D. (2017). Fault-tolerant economic model predictive control using error-triggered online model identification. *Industrial & Engineering Chemistry Research, 56*(19), 5652–5667.
109. Broomhead, T., Manzie, C., Hield, P., Shekhar, R., & Brear, M. (2017). Economic model predictive control and applications for diesel generators. *IEEE Transactions on Control Systems Technology, 25*(2), 388–400.
110. Wang, Y., Puig, V., & Cembrano, G. (2017). Non-linear economic model predictive control of water distribution networks. *Journal of Process Control, 56,* 23–34.
111. Olanrewaju, O. I., & Maciejowski, J. M. (2017). Implications of dissipativity on stability of economic model predictive control the indefinite linear quadratic case. *Systems & Control Letters, 100,* 43–50.
112. Maestre, J. M., Fernandez, M. I., & Jurado, T. (2018). An application of economic model predictive control to inventory management in hospitals. *Control Engineering Practice, 71,* 120–128.
113. Deng, K., Sun, Y., Li, S. S., Lu, Y., Brouwer, J., Mehta, P. G., et al. (2015). Model predictive control of central chiller plant with thermal energy storage via dynamic programming and mixed-integer linear programming. *IEEE Transactions on Automation Science and Engineering, 12*(2), 565–579.
114. Vichik, S., & Borrelli, F. (2014). Solving linear and quadratic programs with an analog circuit. *Computers & Chemical Engineering, 70,* 160–171.

115. Jones, C. N., Grieder, P., & Rakovic, S. V. (2006). A logarithmic-time solution to the point location problem for parametric linear programming. *Automatica, 42*(12), 2215–2218.
116. Ke, F., Li, Z. J., Xiao, H. Z., & Zhang, X. B. (2017). Visual servoing of constrained mobile robots based on model predictive control. *IEEE Transactions on Systems Man Cybernetics:Systems, 47*(7), 1428–1438.
117. Harrison, C. A., & Qin, S. J. (2009). Minimum variance performance map for constrained model predictive control. *Journal of Process Control, 19*(7), 1199–1204.
118. Baker, R., & Swartz, C. L. E. (2008). Interior point solution of multilevel quadratic programming problems in constrained model predictive control applications. *Industrial & Engineering Chemistry Research, 47*(1), 81–91.
119. Avanzini, G. B., Zanchettin, A. M., & Rocco, P. (2018). Constrained model predictive control for mobile robotic manipulators. *Robotica, 36*(1), 19–38.
120. Zeilinger, M. N., Morari, M., & Jones, C. N. (2014). Soft constrained model predictive control with robust stability guarantees. *IEEE Transactions on Automatic Control, 59*(5), 1190–1202.
121. Lamburn, D. J., Gibbens, P. W., & Dumble, S. J. (2014). Efficient constrained model predictive control. *European Journal of Control, 20*(6), 301–311.
122. Tarczewski, T., & Grzesiak, L. M. (2016). Constrained state feedback speed control of PMSM based on model predictive approach. *IEEE Transactions on Industrial Electronics, 63*(6), 3867–3875.
123. Liu, K. L., Li, K., & Zhang, C. (2017). Constrained generalized predictive control of battery charging process based on a coupled thermoelectric model. *Journal of Power Sources, 347,* 145–158.
124. Zhang, R. D., Zou, Q., Cao, Z. X., & Gao, F. R. (2017). Design of fractional order modeling based extended non-minimal state space MPC for temperature in an industrial electric heating furnace. *Journal of Process Control, 56,* 13–22.
125. Zhang, R. D., Lu, R. Q., & Xue, A. K. (2014). Predictive functional control for linear systems under partial actuator faults and application on an injection molding batch process. *Industrial & Engineering Chemistry Research, 53*(2), 723–731.
126. Zhang, R. D., Xue, A. K., Wang, S. Q., & Ren, Z. Y. (2011). An improved model predictive control approach based on extended non-minimal state space formulation. *Journal of Process Control, 21*(8), 1183–1192.
127. Zhang, R. D., Gao, F. R., & Christofides, P. D. (2017). An improved approach for H_∞ design of linear quadratic tracking control for chemical processes with partial actuator failure. *Journal of Process Control, 58,* 63–72.
128. Zhang, R. D., Xue, A. K., Wang, S. Q., & Zhang, J. M. (2012). An improved state space model structure and a corresponding predictive functional control design with improved control performance. *International Journal of Control, 85*(8), 1146–1161.
129. Zhang, R. D., Wu, S., Lu, R. Q., & Gao, F. R. (2014). Predictive control optimization based PID control for temperature in an industrial surfactant reactor. *Chemometrics and Intelligent Laboratory Systems, 135*(15), 48–62.
130. Zhang, R. D., Cao, Z. X., Bo, C. M., Li, P., & Gao, F. R. (2014). New PID controller design using extended non-minimal state space model based predictive functional control structure. *Industrial & Engineering Chemistry Research, 53*(8), 3283–3292.
131. Wu, S. (2015). State space predictive functional control optimization based new PID design for multivariable processes. *Chemometrics and Intelligent Laboratory Systems, 143*(15), 16–27.
132. Wu, S. (2015). Multivariable PID control using improved state space model predictive control optimization. *Industrial & Engineering Chemistry Research, 54*(20), 5505–5513.
133. Zhang, R. D., Zou, H. B., Xue, A. K., & Gao, F. R. (2014). GA based predictive functional control for batch processes under actuator faults. *Chemometrics and Intelligent Laboratory Systems, 137*(15), 67–73.
134. Zhang, R. D., Xue, A. K., & Gao, F. R. (2014). Temperature control of industrial coke furnace using novel state space model predictive control. *IEEE Transactions on Industrial Informatics, 10*(4), 2084–2092.

135. Zhang, R. D., Xue, A. K., Lu, R. Q., Li, P., & Gao, F. R. (2014). Real-time implementation of improved state-space MPC for air supply in a coke furnace. *IEEE Transactions on Industrial Electronics, 61*(7), 3532–3539.
136. Wang, L. P., & Young, P. C. (2006). An improved structure for model predictive control using non-minimal state space realisation. *Journal of Process Control, 16*(4), 355–371.
137. Rivera, D., Morari, M., & Skogestad, S. (1986). Internal model control: PID controller design. *Industrial & engineering chemistry process design and development, 25,* 252–265.

Part I
Basic Algorithms

Chapter 2
Model Predictive Control Based on Extended State Space Model

2.1 Introduction

As a promising advanced control strategy, MPC schemes have obtained significant progress in both theory and applications [1–3]. During the development history of MPC, many kinds of models have been adopted, such as step-response models [4–6], input–output models [7–9], state space models [10–12], etc. Among these models, state space models promote the progress of theoretical research of MPC greatly because the corresponding controller design and system analysis are straightforward.

Compared with other models, state space models have their unique feature and can describe the process dynamics in a different way [13]. How to use the model information fully to achieve the desired control performance of MPC strategies is a meaningful issue. In the conventional state space model based MPC approaches, only the tracking errors are focused on for the tracking problem, while limited process dynamics are considered [14, 15]. In some sense, the relevant controller design freedom may be limited. In view of this problem, the extended state space model [16–18] is introduced to improve the control performance of MPC schemes in this book. By employing the extended state space model, both the tracking errors and the state variables are considered in the controller design and more degrees of freedom are provided.

In order to make the contents more consistent and easier to understand, the conventional state space model based MPC method is expressed briefly in this chapter, and the difference between the conventional state space model and extended state space model will be clear for readers.

R. Zhang et al., *Model Predictive Control*,
https://doi.org/10.1007/978-981-13-0083-7_2

2.2 State Space Model Predictive Control

The conventional state space model based MPC strategy will be presented first in this section, then the extended state space (ESS) model based MPC scheme will be described. Finally, a case study on an inverse-response process demonstrates the effectiveness of the ESS model based MPC method.

2.2.1 Conventional State Space Model Predictive Control

In this section, the set-point tracking problem using the conventional state space model based MPC will be discussed. For simplicity, we consider the following single-input single-output (SISO) process, and the relevant state space model is

$$\begin{aligned} x_m(k+1) &= A_m x_m(k) + B_m u(k-d) \\ y_m(k+1) &= C_m x_m(k+1) \end{aligned} \tag{2.1}$$

where $x_m(k)$, $u(k)$, $y_m(k)$ are the state variable, the control input, and the output of the model at time instant k, respectively. A_m, B_m and C_m are the system matrices with appropriate dimensions, and d is the dead time.

Based on Eq. (2.1), the following model can be obtained easily by adding the difference operator Δ.

$$\begin{aligned} \Delta x_m(k+1) &= A_m \Delta x_m(k) + B_m \Delta u(k-d) \\ \Delta y_m(k+1) &= C_m \Delta x_m(k+1) \end{aligned} \tag{2.2}$$

Construct a new state vector as $x(k) = [\Delta x_m(k)^{\mathrm{T}}, y_m(k)]^{\mathrm{T}}$, then the model in Eq. (2.2) can be rewritten as

$$\begin{aligned} x(k+1) &= Ax(k) + B\Delta u(k-d) \\ y_m(k+1) &= Cx(k+1) \end{aligned} \tag{2.3}$$

where

$$A = \begin{bmatrix} A_m & 0 \\ C_m A_m & 1 \end{bmatrix}; \quad B = \begin{bmatrix} B_m \\ C_m B_m \end{bmatrix}; \quad C = \begin{bmatrix} 0 & 1 \end{bmatrix}$$

and 0 in A, C are zero matrices with appropriate dimensions.

Define y_s as the set-point, and the following reference trajectory is introduced.

$$s(k) = y(k)$$

$$s(k+i) = \alpha^i y(k) + (1-\alpha^i) y_s \quad i = 1, 2, \ldots, P, \ldots, P+d \tag{2.4}$$

where α is the smoothing factor of the reference trajectory. $y(k)$ is the process output, and P is the prediction horizon.

Here, the control horizon is selected as M. Based on the model shown in Eq. (2.3), the future prediction from time instant k can be derived easily.

$$\begin{aligned} X &= Fx(k+d) + \Phi \Delta U \\ Y &= Tx(k+d) + G\Delta U \end{aligned} \tag{2.5}$$

where

$$X = \begin{bmatrix} x(k+d+1) \\ x(k+d+2) \\ \vdots \\ x(k+d+P) \end{bmatrix}; \quad \Delta U = \begin{bmatrix} \Delta u(k) \\ \Delta u(k+1) \\ \vdots \\ \Delta u(k+M-1) \end{bmatrix}$$

$$Y = \begin{bmatrix} y_m(k+d+1) \\ y_m(k+d+2) \\ \vdots \\ y_m(k+d+P) \end{bmatrix}; \quad S = \begin{bmatrix} s(k+1+d) \\ s(k+2+d) \\ \vdots \\ s(k+P+d) \end{bmatrix}$$

$$F = \begin{bmatrix} A \\ A^2 \\ \vdots \\ A^P \end{bmatrix}; \quad \Phi = \begin{bmatrix} B & 0 & 0 & \cdots & 0 \\ AB & B & 0 & \cdots & 0 \\ A^2B & AB & B & \cdots & 0 \\ \vdots & \vdots & \vdots & \ddots & \vdots \\ A^{P-1}B & A^{P-2}B & A^{P-3}B & \cdots & A^{P-M}B \end{bmatrix}$$

$$T = \begin{bmatrix} CA \\ CA^2 \\ \vdots \\ CA^P \end{bmatrix}; \quad G = \begin{bmatrix} CB & 0 & 0 & \cdots & 0 \\ CAB & CB & 0 & \cdots & 0 \\ CA^2B & CAB & CB & \cdots & 0 \\ \vdots & \vdots & \vdots & \ddots & \vdots \\ CA^{P-1}B & CA^{P-2}B & CA^{P-3}B & \cdots & CA^{P-M}B \end{bmatrix}$$

Considering the disturbance and various uncertainty in practice, the original output prediction in Eq. (2.5) needs to be corrected to realize more accurate prediction, and the details are as follows.

$$Y_c = Y + E_{\text{pre}} \tag{2.6}$$

where

$$Y_c = \begin{bmatrix} y_{\text{mc}}(k+d+1) \\ y_{\text{mc}}(k+d+2) \\ \vdots \\ y_{\text{mc}}(k+d+P) \end{bmatrix}; \quad E_{\text{pre}} = \begin{bmatrix} e_{\text{pre}}(k)\ e_{\text{pre}}(k)\ \ldots\ e_{\text{pre}}(k) \end{bmatrix}^{\text{T}}$$

$$e_{\text{pre}}(k) = y(k) - y_m(k)$$

The following objective function is employed for the set-point tracking

$$J = (S - Y_c)^{\text{T}} Q (S - Y_c) + \Delta U^{\text{T}} L \Delta U \tag{2.7}$$

where Q, L are the relevant weighting matrices with appropriate dimensions.

Finally, the optimal control law can be obtained by taking a derivative of the cost function J

$$\Delta U = -(G^{\text{T}} Q G + L)^{-1} G^{\text{T}} Q (T x(k+d) + E_{\text{pre}} - S) \tag{2.8}$$

Denote

$$\begin{aligned} K_F &= (G^{\text{T}} Q G + L)^{-1} G^{\text{T}} Q T \\ K_S &= (G^{\text{T}} Q G + L)^{-1} G^{\text{T}} Q \end{aligned} \tag{2.9}$$

then, the control law at time instant k can be expressed as

$$\Delta u(k) = -k_F x(k+d) + k_S (S - E_{\text{pre}}) \tag{2.10}$$

where k_F and k_S are the first rows of K_F and K_S, respectively.

Remark 2.1 Note that the calculation of the past inputs $\Delta u(k-d), \ldots, \Delta u(k-1)$ is meaningless, and $\Delta u(k-d), \ldots, \Delta u(k-1)$ can also be constructed as the elements of the new state vector to simplify the computation process. Under such situation, Eq. (2.3) will be presented in another form in which $\Delta u(k)$ remains as the control input, and the details will be discussed in the next section.

2.2.2 Extended State Space Model Predictive Control [19]

Here, we consider the same SISO state space model in Eq. (2.1), and the following state space model can be obtained by constructing a new state vector as $x_1(k) = [x_m(k)^{\mathrm{T}}, u(k-1), \ldots, u(k-d)]^{\mathrm{T}}$.

$$\begin{aligned} x_1(k+1) &= A_1 x_1(k) + B_1 u(k) \\ y_m(k+1) &= C_1 x_1(k+1) \end{aligned} \tag{2.11}$$

where

$$A_1 = \begin{bmatrix} A_m & 0 & \cdots & 0 & B_m \\ 0 & 0 & \cdots & 0 & 0 \\ 0 & 1 & 0 & \cdots & 0 \\ \vdots & \vdots & \ddots & \vdots & \vdots \\ 0 & 0 & \cdots & 1 & 0 \end{bmatrix}; \quad B_1 = \begin{bmatrix} 0 \\ 1 \\ 0 \\ \vdots \\ 0 \end{bmatrix}; \quad C_1 = \begin{bmatrix} C_m^{\mathrm{T}} \\ 0 \\ \vdots \\ 0 \\ 0 \end{bmatrix}^{\mathrm{T}}$$

Similarly, the following state space model can be obtained by adding the difference operator Δ to Eq. (2.11).

$$\begin{aligned} \Delta x_1(k+1) &= A_1 \Delta x_1(k) + B_1 \Delta u(k) \\ \Delta y_m(k+1) &= C_1 \Delta x_1(k+1) \end{aligned} \tag{2.12}$$

Here, we define the set-point as y_s and choose the reference trajectory as

$$r(k) = y(k)$$

$$r(k+i) = \alpha^i y(k) + (1-\alpha^i) y_s \quad i = 1, 2, \ldots, P \tag{2.13}$$

where $y(k)$ is the process output, α is the smoothing factor of the reference trajectory, and P is the prediction horizon.

Then, we can calculate the output tracking error at time instant k as

$$e(k) = y(k) - r(k) \tag{2.14}$$

Based on Eqs. (2.12)–(2.14), the output tracking error prediction $e(k+1)$ can be derived further as

$$e(k+1) = e(k) + C_1 A_1 \Delta x_1(k) + C_1 B_1 \Delta u(k) - \Delta r(k+1) \tag{2.15}$$

By including the output tracking error $e(k)$ into the extended state vector, the following ESS model is obtained

$$z(k+1) = Az(k) + B\Delta u(k) + C\Delta r(k+1) \tag{2.16}$$

where

$$z(k) = \left[\Delta x_1(k)^{\mathrm{T}} \; e(k) \right]^{\mathrm{T}}$$

$$A = \begin{bmatrix} A_1 & 0 \\ C_1 A_1 & 1 \end{bmatrix}; \quad B = \begin{bmatrix} B_1 \\ C_1 B_1 \end{bmatrix}; \quad C = \begin{bmatrix} 0 \\ -1 \end{bmatrix} \tag{2.17}$$

Here, the 0 in A, C are zero matrices with appropriate dimensions.
Select the control horizon as M, and denote

$$Z = \begin{bmatrix} z(k+1) \\ z(k+2) \\ \vdots \\ z(k+P) \end{bmatrix}; \quad \Delta U = \begin{bmatrix} \Delta u(k) \\ \Delta u(k+1) \\ \vdots \\ \Delta u(k+M-1) \end{bmatrix}; \quad \Delta R = \begin{bmatrix} \Delta r(k+1) \\ \Delta r(k+2) \\ \vdots \\ \Delta r(k+P) \end{bmatrix} \tag{2.18}$$

then, we can obtain the state prediction from time instant k on the basis of Eq. (2.16).

$$Z = Sz(k) + F\Delta U + \theta \Delta R \tag{2.19}$$

where

$$S = \begin{bmatrix} A \\ A^2 \\ \vdots \\ A^P \end{bmatrix}; \quad F = \begin{bmatrix} B & 0 & 0 & \cdots & 0 \\ AB & B & 0 & \cdots & 0 \\ A^2B & AB & B & \cdots & 0 \\ \vdots & \vdots & \vdots & \ddots & \vdots \\ A^{P-1}B & A^{P-2}B & A^{P-3}B & \cdots & A^{P-M}B \end{bmatrix}$$

$$\theta = \begin{bmatrix} C & 0 & 0 & 0 & 0 \\ AC & C & 0 & 0 & 0 \\ A^2C & AC & C & 0 & 0 \\ \vdots & \vdots & \vdots & \ddots & \vdots \\ A^{P-1}C & A^{P-2}C & A^{P-3}C & \cdots & C \end{bmatrix}$$

Here, the prediction error caused by uncertainty and disturbance are taken into account and we employ the following objective function

$$J(k) = (Z + E_{\text{pre}})^{\text{T}} Q(Z + E_{\text{pre}}) + \Delta U^{\text{T}} L \Delta U \tag{2.20}$$

where

$$E_{\text{pre}} = [E, E, \ldots, E]^{\text{T}}; \quad E = [0 \; e_{\text{pre}}(k)]$$
$$e_{\text{pre}}(k) = y(k) - y_m(k)$$

Here, 0 in E is a zero vector with appropriate dimensions. Q, L are the corresponding weighting matrices for the state variables and the control input increments, respectively.

Remark 2.2 From Eq. (2.20), it is obvious that more degrees of freedom are provided in the ESS model based MPC strategies because the state variables and the tracking error can be regulated separately. Based on such merits, improved control performance may be expected.

The optimal control law can be obtained by minimizing the cost function in Eq. (2.20).

$$\Delta U = -(F^{\text{T}} Q F + L)^{-1} F^{\text{T}} Q (Sz(k) + \theta \Delta R + E_{\text{pre}}) \tag{2.21}$$

Define

$$K_F = (F^{\text{T}} Q F + L)^{-1} F^{\text{T}} Q S$$
$$K_S = (F^{\text{T}} Q F + L)^{-1} F^{\text{T}} Q \tag{2.22}$$

then, the control law of the ESS model based MPC at time instant k is

$$\Delta u(k) = -k_F z(k) - k_S(\theta \Delta R + E_{\text{pre}}) \tag{2.23}$$

where k_F and k_S are the first rows of K_F and K_S, respectively.

2.3 Case Study

In this section, the following inverse-response process with unstable open-loop dynamics and time delay is introduced to test the control performance of the ESS model based MPC.

$$x(k+1) = Ax(k) + Bu(k-2)$$
$$y(k+1) = Cx(k+1) \tag{2.24}$$

where

Table 2.1 The control parameters for both methods

Parameters	Proposed	Conventional
P	21	21
M	1	1
L	0.001	0.001
α	0.65	0.65
$Q = \text{diag}(Q_1, Q_2, \ldots, Q_{21})$	$Q_j = \text{diag}(0.02, 0, 0, 0, 1)$ $(j = 1, 2, \ldots, 21)$	$Q_j = 1$ $(j = 1, 2, \ldots, 21)$

$$A = \begin{bmatrix} 1.1053 & 0 \\ -0.01 & 0.8186 \end{bmatrix}; \quad B = \begin{bmatrix} 1 \\ 0.0858 \end{bmatrix}; \quad C = \begin{bmatrix} 0 & 1 \end{bmatrix}$$

In order to verify the control performance of the ESS model based MPC further, the conventional MPC method in Sect. 2.2.1 is employed as the comparison, and the control parameters for the two approaches are listed in Table 2.1.

Note that in the conventional MPC method, the model is not expanded as the ESS model, which shows that there is only one element in Q_j, as is also implied in Eq. (2.7).

For both strategies, the set-point is chosen as 1 and the load disturbance with amplitude -0.2 is added to the process output at time instant $k = 150$. Consider the fact that disturbance and uncertainty exist in practice inevitably, which may cause model/plant mismatches; here the following model/plant mismatched cases are generated to evaluate the ensemble control performance of both methods.

Case 1:

$$A = \begin{bmatrix} 1.2107 & 0 \\ -0.011 & 0.8245 \end{bmatrix}; \quad B = \begin{bmatrix} 0.93 \\ 0.0836 \end{bmatrix} \tag{2.25}$$

Case 2:

$$A = \begin{bmatrix} 1.2104 & 0 \\ -0.009 & 0.8303 \end{bmatrix}; \quad B = \begin{bmatrix} 0.91 \\ 0.0872 \end{bmatrix} \tag{2.26}$$

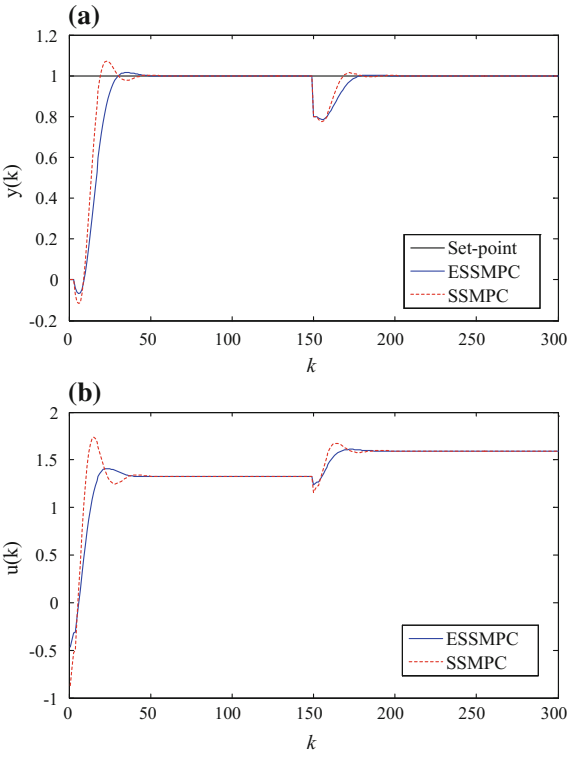

Fig. 2.1 **a** Closed-loop output responses under case 1. **b** Closed-loop input responses under case 1

The responses of both strategies under cases 1, 2 are shown in Figs. 2.1 and 2.2. From an overall perspective, the ESS model based MPC provides better ensemble control performance. In Fig. 2.1a, it is obvious that both approaches achieve the set-point tracking and disturbance rejection successfully. However, the overshoot and oscillations in the responses of conventional MPC are bigger. In Fig. 2.2, the situations are similar to those in Fig. 2.1. The ESS model based MPC shows smaller overshoot and oscillations. In a word, improved control performance is obtained in the ESS model based MPC.

2.4 Summary

The MPC strategies based on conventional state space model and extended state space model are discussed in this chapter. Based on the extended state space model, the state variables and the tracking error are combined and regulated separately, thus more degrees of freedom are provided for the relevant controller design. The case

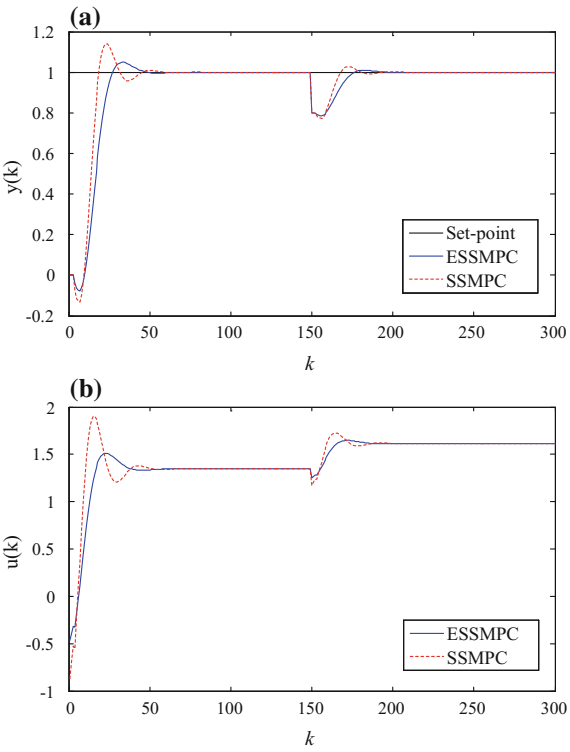

Fig. 2.2 **a** Closed-loop output responses under case 2. **b** Closed-loop input responses under case 2

study on an inverse-response process verifies the effectiveness of the ESS model based MPC. The ESS model also can be applied to the PFC strategy, which will be presented in the next chapter.

References

1. Lee, J. H. (2011). Model predictive control: Review of the three decades of development. *International Journal of Control, Automation and Systems, 9*(3), 415–424.
2. Ellis, M., Durand, H., & Christofides, P. D. (2014). A tutorial review of economic model predictive control methods. *Journal of Process Control, 24*(8), 1156–1178.
3. Garriga, J. L., & Soroush, M. (2010). Model predictive control tuning methods: A review. *Industrial & Engineering Chemistry Research, 49*(8), 3505–3515.
4. Kufoalor, D. K. M., Frison, G., Imsland, L., Johansen, T. A., & Jorgensen, J. B. (2017). Block factorization of step response model predictive control problems. *Journal of Process Control, 53,* 1–14.
5. Esmaili, A., Li, J. Y., Xie, J. Y., & Isom, J. D. (2018). Closed-loop identification for plants under model predictive control. *Control Engineering Practice, 72,* 206–218.
6. Kozlik, C., Geringer, B., Schirrer, A., & Jakubek, S. (2016). Dynamic matrix control applied to emission control of a diesel engine. *International Journal of Engine Research, 17*(5), 556–575.

7. Abbas, H. S., Hanema, J., Toth, R., Mohammadpour, J., & Meskin, N. (2018). An improved robust model predictive control for linear parameter-varying input-output models. *International Journal of Robust and Nonlinear Control, 28*(3), 859–880.
8. Ding, B. C., & Zou, T. (2014). A synthesis approach for output feedback robust model predictive control based-on input-output model. *Journal of Process Control, 24*(3), 60–72.
9. Pang, Z. H., Liu, G. P., Zhou, D. H., & Sun, D. H. (2017). Design and performance analysis of networked predictive control systems based on input-output difference equation model. *International Journal of Control, Automation and Systems, 15*(1), 416–426.
10. Gallego, A. J., & Camacho, E. F. (2012). Adaptive state-space model predictive control of a parabolic-trough field. *Control Engineering Practice, 20*(9), 904–911.
11. Tao, J. L., Zhu, Y., & Fan, Q. R. (2014). Improved state space model predictive control design for linear systems with partial actuator failure. *Industrial & Engineering Chemistry Research, 53*(9), 3578–3586.
12. Simkoff, J. M., Wang, S., Baldea, M., Chiang, L. H., Castillo, I., Bindlish, R., et al. (2018). Plant-model mismatch estimation from closed-loop data from state-space model predictive control. *Industrial & Engineering Chemistry Research, 57*(10), 3732–3741.
13. Wang, L. P., & Young, P. C. (2006). An improved structure for model predictive control using non-minimal state space realisation. *Journal of Process Control, 16*(4), 355–371.
14. Zhang, R. D., Xue, A. K., Lu, R. Q., Li, P., & Gao, F. R. (2014). Real-time implementation of improved state-space MPC for air supply in a coke furnace. *IEEE Transactions on Industrial Electronics, 61*(7), 3532–3539.
15. Zhang, R. D., & Gao, F. R. (2015). An improved decoupling structure based state space MPC design with improved performance. *System Control Letters, 75,* 77–83.
16. Zhang, R. D., Xue, A. K., Wang, S. D., Zhang, J. M., & Gao, F. R. (2012). Partially decoupled approach of extended non-minimal state space predictive functional control for MIMO processes. *Journal of Process Control, 22*(5), 837–851.
17. Wu, S., Jin, Q. B., Zhang, R. D., Zhang, J. F., & Gao, F. R. (2017). Improved design of constrained model predictive tracking control for batch processes against unknown uncertainties. *ISA Transactions, 69,* 273–280.
18. Zhang, R. D., Wu, S., & Gao, F. R. (2017). State space model predictive control for advanced process operation: A review of recent developments, new results, and insight. *Industrial & Engineering Chemistry Research, 56*(18), 5360–5394.
19. Zhang, R. D., Lu, J. Y., Qu, H. Y., & Gao, F. R. (2014). State space model predictive fault-tolerant control for batch processes with partial actuator failure. *Journal of Process Control, 24*(5), 613–620.

Chapter 3
Predictive Functional Control Based on Extended State Space Model

3.1 Introduction

Based on the fact that the control law of PFC is a linear combination of the preset basis functions, the computational complexity for solving the corresponding optimal control law is decreased greatly [1, 2]. For the fast servo systems that require quick and accurate response of controllers, such as industrial robots, artillery systems, radar systems, etc., PFC is a good choice [3–5]. During the past decades, many kinds of models have been employed for PFC schemes, such as transfer function models, state space models, and so on, and there are a lot of developments for PFC strategies [6–12].

In conventional state space model based PFC methods, only the tracking goal is considered in the relevant performance index for tracking problems, and other useful dynamics in the state space models are ignored [13, 14]. It is meaningful to make full use of such information in the state space model to enhance the ensemble control performance of PFC strategies. The ESS model in which both the tracking error and the state variables are considered can also be introduced into the PFC algorithm. Based on the ESS model, more degrees of freedom are obtained for the corresponding controller design such that improved control performance is anticipated [15–17]. The details will be shown in this chapter.

R. Zhang et al., *Model Predictive Control*,
https://doi.org/10.1007/978-981-13-0083-7_3

3.2 Extended State Space Predictive Functional Control

3.2.1 Extended State Space Model [18]

In order to simplify the derivation process, the following SISO state space model is considered.

$$\begin{aligned} x_m(k+1) &= A_m x_m(k) + B_m u(k-d) \\ y_m(k+1) &= C_m x_m(k+1) \end{aligned} \tag{3.1}$$

where $x_m(k)$, $u(k)$ and $y_m(k)$ are the state variable, the input and output of the model at time instant k. A_m, B_m, C_m are the system matrices with appropriate dimensions, respectively. d is the dead time.

For the original state space model in Eq. (3.1), the following transformed form can be obtained by introducing a new state vector as $x_1(k) = [x_m(k)^{\mathrm{T}}, u(k-1), \ldots, u(k-d)]^{\mathrm{T}}$

$$\begin{aligned} x_1(k+1) &= A_1 x_1(k) + B_1 u(k) \\ y_m(k+1) &= C_1 x_1(k+1) \end{aligned} \tag{3.2}$$

where

$$A_1 = \begin{bmatrix} A_m & 0 \cdots & 0 & B_m \\ 0 & 0 \cdots & 0 & 0 \\ 0 & 1 \; 0 & \cdots & 0 \\ \vdots & \vdots \; \vdots & \ddots & \vdots \; \vdots \\ 0 & 0 \cdots & 1 & 0 \end{bmatrix}; \quad B_1 = \begin{bmatrix} 0 \\ 1 \\ 0 \\ \vdots \\ 0 \end{bmatrix}; \quad C_1 = \begin{bmatrix} C_m^{\mathrm{T}} \\ 0 \\ \vdots \\ 0 \\ 0 \end{bmatrix}^{\mathrm{T}}$$

By adding the difference operator Δ to Eq. (3.2), the following state space model is obtained

$$\begin{aligned} \Delta x_1(k+1) &= A_1 \Delta x_1(k) + B_1 \Delta u(k) \\ \Delta y_m(k+1) &= C_1 \Delta x_1(k+1) \end{aligned} \tag{3.3}$$

Denote the set-point as y_s and select the smoothing factor as α, then the corresponding reference trajectory can be described as

$$\begin{aligned} r(k) &= y(k) \\ r(k+i) &= \alpha^i y(k) + (1-\alpha^i) y_s \quad i = 1, 2, \ldots, P \end{aligned} \tag{3.4}$$

where P is the prediction horizon, and $y(k)$ is the process output.

The output tracking error at time instant k is defined as

$$e(k) = y(k) - r(k) \tag{3.5}$$

Synthesizing Eqs. (3.3)–(3.5), the output tracking error prediction at time instant $k + 1$ can be calculated as

$$e(k+1) = e(k) + C_1 A_1 \Delta x_1(k) + C_1 B_1 \Delta u(k) - \Delta r(k+1) \tag{3.6}$$

Here, we further construct an extended state vector that contains the tracking error as

$$z(k) = [\Delta x_1(k)^{\mathrm{T}}, e(k)]^{\mathrm{T}} \tag{3.7}$$

then the relevant ESS model is

$$z(k+1) = Az(k) + B\Delta u(k) + C\Delta r(k+1) \tag{3.8}$$

where

$$A = \begin{bmatrix} A_1 & 0 \\ C_1 A_1 & 1 \end{bmatrix}; \quad B = \begin{bmatrix} B_1 \\ C_1 B_1 \end{bmatrix}; \quad C = \begin{bmatrix} 0 \\ -1 \end{bmatrix} \tag{3.9}$$

Here, the 0 in A, C are zero vectors with appropriate dimensions.

Note that $\Delta u(k) = u(k) - u(k-1)$, then the ESS model in Eq. (3.8) can be rewritten as

$$z(k+1) = Az(k) + Bu(k) - Bu(k-1) + C\Delta r(k+1) \tag{3.10}$$

3.2.2 Controller Design

Generally, the control law of PFC can be expressed as the following formula [19–21]

$$u(k+i) = \sum_{j=1}^{N} \mu_j f_j(i) \tag{3.11}$$

where $u(k+i)$ is the control law at time instant $k+i$. $f_j(i)$ is the value of the basis function f_j at time instant $k+i$, and μ_j is the corresponding weighting coefficient. N is the number of the basis functions.

For sake of brevity, we define that

$$\begin{aligned} T_i &= [f_1(i), f_2(i), \ldots, f_N(i)], \quad (i = 0, 1, \ldots, P-1) \\ \eta &= [\mu_1, \mu_2, \ldots, \mu_N]^{\mathrm{T}} \end{aligned} \tag{3.12}$$

then the control law in Eq. (3.11) can be transformed as

$$u(k+i) = T_i \eta \tag{3.13}$$

Based on Eq. (3.10) and Eq. (3.13), the state prediction from time instant k is derived as

$$Z = Sz(k) + \varphi\eta - Fu(k-1) + \theta\Delta R \tag{3.14}$$

where

$$S = \begin{bmatrix} A \\ A^2 \\ \vdots \\ A^P \end{bmatrix}; \quad F = \begin{bmatrix} B \\ AB \\ \vdots \\ A^{P-1}B \end{bmatrix}; \quad \phi = \begin{bmatrix} BT_0 \\ (AB - B)T_0 + BT_1 \\ (A^2B - AB)T_0 + (AB - B)T_1 + BT_2 \\ \vdots \\ \sum_{k=1}^{P-1} (A^kB - A^{k-1}B)T_{P-1-k} + BT_{P-1} \end{bmatrix}$$

$$\theta = \begin{bmatrix} C & 0 & 0 & 0 & 0 \\ AC & C & 0 & 0 & 0 \\ A^2C & AC & C & 0 & 0 \\ \vdots & \vdots & \vdots & \ddots & \vdots \\ A^{P-1}C & A^{P-2}C & A^{P-3}C & \cdots & C \end{bmatrix}; \quad Z = \begin{bmatrix} z(k+1) \\ z(k+2) \\ \vdots \\ z(k+P) \end{bmatrix}; \quad \Delta R = \begin{bmatrix} \Delta r(k+1) \\ \Delta r(k+2) \\ \vdots \\ \Delta r(k+P) \end{bmatrix}$$

The following objective function in which the prediction error is considered to compensate for the effects caused by disturbance and uncertainty is chosen for the ESS model based PFC

$$J(k) = (Z + E_{\mathrm{pre}})^{\mathrm{T}} Q (Z + E_{\mathrm{pre}}) \tag{3.15}$$

where

$$E_{\mathrm{pre}} = [E, E, \ldots, E]^{\mathrm{T}}; \quad E = [\,0 \; e_{\mathrm{pre}}(k)\,]$$

$e_{\mathrm{pre}}(k) = y(k) - y_m(k)$ is the prediction error, and 0 in E is a zero vector with appropriate dimensions. Q is the relevant weighting matrix for the state variables.

Remark 3.1 In Eq. (3.15), it is obvious that the state variables and the output tracking error can be regulated by the corresponding weighting coefficients separately, and more degrees of freedom can be offered for the relevant controller design.

Combining Eqs. (3.14) and (3.15), the optimal control law can be obtained by minimizing the performance index J

$$\eta = -(\varphi^{\mathrm{T}} Q \varphi)^{-1} \varphi^{\mathrm{T}} Q (Sz(k) + \theta \Delta R - Fu(k-1) + E_{\mathrm{pre}}) \tag{3.16}$$

Further, define

$$\begin{aligned}
\mu_1 &= -(1, 0, \ldots, 0)(\varphi^{\mathrm{T}} Q \varphi)^{-1} \varphi^{\mathrm{T}} Q (Sz(k) - Fu(k-1) + \theta \Delta R + E_{\mathrm{pre}}) \\
&= -h_1 z(k) + h_{u1} u(k-1) - m_1 (\theta \Delta R + E_{\mathrm{pre}}) \\
\mu_2 &= -(0, 1, \ldots, 0)(\varphi^{\mathrm{T}} Q \varphi)^{-1} \varphi^{\mathrm{T}} Q (Sz(k) - Fu(k-1) + \theta \Delta R + E_{\mathrm{pre}}) \\
&= -h_2 z(k) + h_{u2} u(k-1) - m_2 (\theta \Delta R + E_{\mathrm{pre}}) \\
&\vdots \\
\mu_N &= -(0, 0, \ldots, 1)(\varphi^{\mathrm{T}} Q \varphi)^{-1} \varphi^{\mathrm{T}} Q (Sz(k) - Fu(k-1) + \theta \Delta R + E_{\mathrm{pre}}) \\
&= -h_N z(k) + h_{uN} u(k-1) - m_N (\theta \Delta R + E_{\mathrm{pre}})
\end{aligned} \tag{3.17}$$

then the control law at time instant k can be expressed as

$$u(k) = \sum_{j=1}^{N} \mu_j f_j(0) = -Hz(k) + H_u u(k-1) - M(\theta \Delta R + E_{\mathrm{pre}}) \tag{3.18}$$

where

$$H = \sum_{j=1}^{N} f_j(0) h_k, \quad (k = 1, 2, \ldots, N)$$

$$H_u = \sum_{j=1}^{N} f_j(0) h_{uk}, \quad (k = 1, 2, \ldots, N)$$

$$M = \sum_{j=1}^{N} f_j(0) m_k, \quad (k = 1, 2, \ldots, N)$$

3.3 Summary

In this chapter, the ESS model is introduced for PFC scheme. By employing the ESS model, more degrees of freedom for the corresponding controller design are offered and better control performance is anticipated. As to other models, such as

the input–output model, the idea of extended state space models can also be obtained and employed for MPC strategies, namely, extended non-minimal state space models, which will be discussed in the next chapter.

References

1. Yang, B., Xu, Z. H., Yang, Y., & Gao, F. R. (2015). Application of two-dimensional predictive functional control in injection molding. *Industrial & Engineering Chemistry Research, 54*(41), 10088–10102.
2. Zhang, B., & Zhang, W. D. (2006). Adaptive predictive functional control of a class of nonlinear systems. *ISA Transactions, 45*(2), 175–183.
3. Vivas, A., & Poignet, P. (2005). Predictive functional control of a parallel robot. *Control Engineering Practice, 13*(7), 863–874.
4. Li, L., Wang, X. Y., Hu, X. S., Chen, Z., Song, J., & Muhammad, F. (2016). A modified predictive functional control with sliding mode observer for automated dry clutch control of vehicle. *Journal of Dynamic Systems Measurement and Control-Transactions of The ASME, 138*(6).
5. Bigdeli, N., & Haeri, M. (2009). Predictive functional control for active queue management in congested TCP/IP networks. *ISA Transactions, 48*(1), 107–121.
6. Zabet, K., Rossiter, J. A., Haber, R., & Abdullah, M. (2017). Pole-placement predictive functional control for under-damped systems with real numbers algebra. *ISA Transactions, 71,* 403–414.
7. Tao, J. L., Yu, Z. H., Zhu, Y., & Ma, L. H. (2015). A linear quadratic structure based predictive functional control design for industrial processes against partial actuator failures. *Chemometrics and Intelligent Laboratory Systems, 146,* 263–269.
8. Shi, H. Y., Su, C. L., Cao, J. T., Li, P., Liang, J. P., & Zhong, G. C. (2015). Nonlinear adaptive predictive functional control based on the Takagi-Sugeno model for average cracking outlet temperature of the ethylene cracking furnace. *Industrial & Engineering Chemistry Research, 54*(6), 1849–1860.
9. Zhang, J. M. (2014). A non-minimal state space formulation based predictive functional control design for inverse-response processes. *Chemometrics and Intelligent Laboratory Systems, 139,* 70–75.
10. Zhang, Q., Wang, Q. J., & Li, G. L. (2016). Nonlinear modeling and predictive functional control of Hammerstein system with application to the turntable servo system. *Mechanical Systems and Signal Processing, 72–73,* 383–394.
11. Dovzan, D., & Skrjanc, I. (2012). Control of mineral wool thickness using predictive functional control. *Robotics and Computer-Integrated Manufacturing, 28*(3), 344–350.
12. Liu, H. X., & Li, S. H. (2012). Speed control for PMSM servo system using predictive functional control and extended state observer. *IEEE Transactions on Industrial Electronics, 59*(2), 1171–1183.
13. Zhang, R. D., & Gao, F. R. (2013). Multivariable decoupling predictive functional control with non-zero-pole cancellation and state weighting: Application on chamber pressure in a coke furnace. *Chemical Engineering Science, 94,* 30–43.
14. Zhang, R. D., Xue, A. K., Wang, S. D., Zhang, J. M., & Gao, F. R. (2012). Partially decoupled approach of extended non-minimal state space predictive functional control for MIMO processes. *Journal of Process Control, 22*(5), 837–851.
15. Zhang, R. D., Xue, A. K., Wang, S. Q., & Zhang, J. M. (2012). An improved state-space model structure and a corresponding predictive functional control design with improved control performance. *International Journal of Control, 85*(8), 1146–1161.
16. Wu, S. (2015). State space predictive functional control optimization based new PID design for multivariable processes. *Chemometrics and Intelligent Laboratory Systems, 143,* 16–27.

17. Zhang, R. D., Zou, H. B., Xue, A. K., & Gao, F. R. (2014). GA based predictive functional control for batch processes under actuator faults. *Chemometrics and Intelligent Laboratory Systems, 137,* 67–73.
18. Zhang, R. D., Lu, R. Q., & Xue, A. K. (2014). Predictive functional control for linear systems under partial actuator faults and application on an injection molding batch process. *Industrial & Engineering Chemistry Research, 53*(2), 723–731.
19. Rossiter, J. A., Haber, R., & Zabet, K. (2016). Pole-placement predictive functional control for over-damped systems with real poles. *ISA Transactions, 61,* 229–239.
20. Kassem, A. M. (2012). Robust voltage control of a stand alone wind energy conversion system based on functional model predictive approach. *International Journal of Electrical Power & Energy Systems, 41*(1), 124–132.
21. Fallahsohi, H., Changenet, C., Place, S., Ligeret, C., & Lin-Shi, X. (2010). Predictive functional control of an expansion value for minimizing the superheat of an evaporator. *International Journal of Refrigeration-Revue Internationale Du Froid, 33*(2), 409–418.

Chapter 4
Model Predictive Control Based on Extended Non-minimal State Space Model

4.1 Introduction

Input–output models are common in industrial processes, and they can be easily obtained by model identification algorithms, such as recursive least-square identification, neural network modeling, support vector machine, etc. [1–5]. Based on input–output models, especially the first-order process model, there are numerous applications of MPC strategies for various industrial processes [6–8]. It is a fact that the derivation process of MPC schemes in which high-order input–output models are employed is complicated, and the corresponding system analysis is also complex. In order to solve this problem, the introduction of state space models is an effective tool because the relevant theoretical derivations are simpler [9].

It is known that input–output models can be transformed into state space models through many methods, and there were lots of significant results for the state space model based MPC algorithms during the past decades [10–15]. As mentioned in the above chapters, the degrees of freedom for most conventional state space model based MPC schemes are limited. In this chapter, the extended non-minimal state space (ENMSS) model [16, 17] that is converted from the input–output model is presented for the subsequent MPC design. By using such models in which the state variables can be regulated additionally, more degrees of freedom for the corresponding controller design are provided and enhanced ensemble control performance can be anticipated.

In order to make this chapter more coherent, the conventional non-minimal state space (NMSS) model based MPC strategy is described first, then the ENMSS model based MPC scheme is discussed in detail. To verify the effectiveness of the ENMSS model based MPC, case studies on a double integrating process and a glasshouse micro-climate process are presented finally.

R. Zhang et al., *Model Predictive Control*,
https://doi.org/10.1007/978-981-13-0083-7_4

4.2 Input–Output Model Based NMSS Model Predictive Control

In this section, NMSS and ENMSS model based MPC schemes will be expressed successively, thus the transformation from the input–output model to the ENMSS model will be legible for readers.

4.2.1 Conventional NMSS Model Predictive Control [18]

Consider the SISO process with the following input–output model

$$\begin{aligned} &y(k+1) + H_1 y(k) + H_2 y(k-1) + \cdots + H_m y(k-m+1) \\ &\quad = L_1 u(k) + L_2 u(k-1) + \cdots + L_n u(k-n+1) \end{aligned} \tag{4.1}$$

where $y(k)$ and $u(k)$ are the process output and input at time instant k, respectively. $H_1, \ldots, H_m$ and $L_1, \ldots, L_n$ are the corresponding coefficients.

For the input–output model shown in Eq. (4.1), it can be converted into the following form by adding the difference operator Δ

$$\begin{aligned} &\Delta y(k+1) + H_1 \Delta y(k) + H_2 \Delta y(k-1) + \cdots + H_m \Delta y(k-m+1) \\ &\quad = L_1 \Delta u(k) + L_2 \Delta u(k-1) + \cdots + L_n \Delta u(k-n+1) \end{aligned} \tag{4.2}$$

In order to transform the input–output model in Eq. (4.2) into the NMSS model, the following NMSS vector $\Delta x_m(k)$ is selected

$$\begin{aligned} \Delta x_m(k)^{\mathrm{T}} = [&\Delta y(k), \Delta y(k-1), \ldots, \Delta y(k-m+1), \\ &\Delta u(k-1), \Delta u(k-2), \ldots, \Delta u(k-n+1)] \end{aligned} \tag{4.3}$$

then the corresponding NMSS model is

$$\begin{aligned} \Delta x_m(k+1) &= A_m \Delta x_m(k) + B_m \Delta u(k) \\ \Delta y(k+1) &= C_m \Delta x_m(k+1) \end{aligned} \tag{4.4}$$

where

$$A_m = \begin{bmatrix} -H_1 & -H_2 & \cdots & -H_{m-1} & -H_m & L_2 & \cdots & L_{n-1} & L_n \\ 1 & 0 & \cdots & 0 & 0 & 0 & \cdots & 0 & 0 \\ 0 & 1 & \cdots & 0 & 0 & 0 & \cdots & 0 & 0 \\ \vdots & \vdots & \cdots & \vdots & \vdots & \vdots & \cdots & \vdots & \vdots \\ 0 & 0 & \cdots & 1 & 0 & 0 & \cdots & 0 & 0 \\ 0 & 0 & \cdots & 0 & 0 & 0 & \cdots & 0 & 0 \\ 0 & 0 & \cdots & 0 & 0 & 1 & \cdots & 0 & 0 \\ \vdots & \vdots & \cdots & \vdots & \vdots & \vdots & \cdots & \vdots & \vdots \\ 0 & 0 & \cdots & 0 & 0 & 0 & \cdots & 1 & 0 \end{bmatrix}$$

$$B_m = [\, L_1 \; 0 \; 0 \cdots 1 \; 0 \cdots 0 \,]^{\mathrm{T}}$$

$$C_m = [\, 1 \; 0 \; 0 \cdots 0 \; 0 \; 0 \; 0 \,]$$

Note that if we reconstruct the NMSS vector to contain the process output $y(k)$, then Eq. (4.4) can be rewritten as

$$\begin{aligned} x(k+1) &= Ax(k) + B\Delta u(k) \\ y(k+1) &= Cx(k+1) \end{aligned} \tag{4.5}$$

where

$$x(k) = \begin{bmatrix} \Delta x_m(k) \\ y(k) \end{bmatrix}; \quad A = \begin{bmatrix} A_m & 0 \\ C_m A_m & 1 \end{bmatrix}; \quad B = \begin{bmatrix} B_m \\ C_m B_m \end{bmatrix}; \quad C = \begin{bmatrix} 0 \; 1 \end{bmatrix}$$

Here, 0 in A, C are zero vectors with appropriate dimensions.

Define the set-point as y_s , and the reference trajectory is further defined as follows:

$$\begin{aligned} s(k) &= y(k) \\ s(k+i) &= \alpha^i y(k) + (1-\alpha^i) y_s \quad i = 1, 2, \ldots, P \end{aligned} \tag{4.6}$$

where α is the smoothing factor of the reference trajectory, and P is the prediction horizon.

On the basis of Eq. (4.5), the state prediction from time instant k can be derived easily. Denote the control horizon as M and

$$X = \begin{bmatrix} x(k+1) \\ x(k+2) \\ \vdots \\ x(k+P) \end{bmatrix}; \quad \Delta U = \begin{bmatrix} \Delta u(k) \\ \Delta u(k+1) \\ \vdots \\ \Delta u(k+M-1) \end{bmatrix}; \quad Y = \begin{bmatrix} y(k+1) \\ y(k+2) \\ \vdots \\ y(k+P) \end{bmatrix}; \quad S = \begin{bmatrix} s(k+1) \\ s(k+2) \\ \vdots \\ s(k+P) \end{bmatrix} \tag{4.7}$$

then the prediction is

$$\begin{aligned} X &= Fx(k) + \Phi\Delta U \\ Y &= Tx(k) + G\Delta U \end{aligned} \tag{4.8}$$

where

$$F = \begin{bmatrix} A \\ A^2 \\ \vdots \\ A^P \end{bmatrix}; \quad \Phi = \begin{bmatrix} B & 0 & 0 & \cdots & 0 \\ AB & B & 0 & \cdots & 0 \\ A^2B & AB & B & \cdots & 0 \\ \vdots & \vdots & \vdots & \ddots & \vdots \\ A^{P-1}B & A^{P-2}B & A^{P-3}B & \cdots & A^{P-M}B \end{bmatrix}$$

$$T = \begin{bmatrix} CA \\ CA^2 \\ \vdots \\ CA^P \end{bmatrix}; \quad G = \begin{bmatrix} CB & 0 & 0 & \cdots & 0 \\ CAB & CB & 0 & \cdots & 0 \\ CA^2B & CAB & CB & \cdots & 0 \\ \vdots & \vdots & \vdots & \ddots & \vdots \\ CA^{P-1}B & CA^{P-2}B & CA^{P-3}B & \cdots & CA^{P-M}B \end{bmatrix}$$

In order to achieve set-point tracking, we select the following performance index

$$J = (S - Y)^{\mathrm{T}} Q (S - Y) + \Delta U^{\mathrm{T}} L \Delta U \tag{4.9}$$

where Q, L are the relevant weighting matrices with appropriate dimensions.

Finally, the optimal control law can be calculated by minimizing the cost function J

$$\Delta U = -(G^{\mathrm{T}} Q G + L)^{-1} G^{\mathrm{T}} Q (Tx(k) - S) \tag{4.10}$$

Define

$$\begin{aligned} K_F &= (G^{\mathrm{T}} Q G + L)^{-1} G^{\mathrm{T}} Q T \\ K_S &= (G^{\mathrm{T}} Q G + L)^{-1} G^{\mathrm{T}} Q \end{aligned} \tag{4.11}$$

then the optimal control law at time instant k can be expressed as

$$\Delta u(k) = -k_F x(k) + k_s S \tag{4.12}$$

where k_F and k_s are the first rows of K_F and K_S, respectively.

4.2.2 Extended NMSS Model Predictive Control [19]

Consider the same input–output model shown in Eq. (4.1), the following formulation can be obtained by introducing the difference operator Δ

$$\begin{aligned}&\Delta y(k+1) + H_1 \Delta y(k) + H_2 \Delta y(k-1) + \cdots + H_m \Delta y(k-m+1) \\ &\quad = L_1 \Delta u(k) + L_2 \Delta u(k-1) + \cdots + L_n \Delta u(k-n+1)\end{aligned} \tag{4.13}$$

Construct the NMSS vector as

$$\begin{aligned}\Delta x(k)^{\mathrm{T}} = [&\Delta y(k), \Delta y(k-1), \ldots, \Delta y(k-m+1), \\ &\Delta u(k-1), \Delta u(k-2), \ldots, \Delta u(k-n+1)]\end{aligned} \tag{4.14}$$

then the following NMSS model is obtained.

$$\begin{aligned}\Delta x(k+1) &= A \Delta x(k) + B \Delta u(k) \\ \Delta y(k+1) &= C \Delta x(k+1)\end{aligned} \tag{4.15}$$

where

$$A = \begin{bmatrix} -H_1 & -H_2 & \cdots & -H_{m-1} & -H_m & L_2 & \cdots & L_{n-1} & L_n \\ 1 & 0 & \cdots & 0 & 0 & 0 & \cdots & 0 & 0 \\ 0 & 1 & \cdots & 0 & 0 & 0 & \cdots & 0 & 0 \\ \vdots & \vdots & \cdots & \vdots & \vdots & \vdots & \cdots & \vdots & \vdots \\ 0 & 0 & \cdots & 1 & 0 & 0 & \cdots & 0 & 0 \\ 0 & 0 & \cdots & 0 & 0 & 0 & \cdots & 0 & 0 \\ 0 & 0 & \cdots & 0 & 0 & 1 & \cdots & 0 & 0 \\ \vdots & \vdots & \cdots & \vdots & \vdots & \vdots & \cdots & \vdots & \vdots \\ 0 & 0 & \cdots & 0 & 0 & 0 & \cdots & 1 & 0 \end{bmatrix}$$

$$B = \begin{bmatrix} L_1 & 0 & 0 & \cdots & 1 & 0 & \cdots & 0 \end{bmatrix}^{\mathrm{T}}$$

$$C = \begin{bmatrix} 1 & 0 & 0 & \cdots & 0 & 0 & 0 & 0 \end{bmatrix}$$

Here, we select P as the prediction horizon, y_s as the set-point and the reference trajectory as

$$\begin{aligned}r(k) &= y(k) \\ r(k+i) &= \alpha^i y(k) + (1-\alpha^i) y_s \quad i = 1, 2, \ldots, P\end{aligned} \tag{4.16}$$

where α is the smoothing factor of the reference trajectory.

Here, the tracking error at time instant k is defined as

$$e(k) = y(k) - r(k) \tag{4.17}$$

Based on Eqs. (4.15) and (4.17), the output tracking error prediction at time instant $k + 1$ can be obtained further.

$$e(k+1) = e(k) + CA\Delta x(k) + CB\Delta u(k) - \Delta r(k+1) \tag{4.18}$$

In order to obtain the ENMSS model, the following state vector is chosen.

$$z(k) = \begin{bmatrix} \Delta x(k) \\ e(k) \end{bmatrix} \tag{4.19}$$

then the relevant ENMSS model is presented as

$$z(k+1) = A_m z(k) + B_m \Delta u(k) + C_m \Delta r(k+1) \tag{4.20}$$

where

$$A_m = \begin{bmatrix} A & 0 \\ CA & 1 \end{bmatrix}; \quad B_m = \begin{bmatrix} B \\ CB \end{bmatrix}; \quad C_m = \begin{bmatrix} 0 \\ -1 \end{bmatrix} \tag{4.21}$$

Here, the 0 in A_m, C_m are zero vectors with appropriate dimensions.

On the basis of Eq. (4.20), we can obtain the state prediction from time instant k. Here, we define

$$Z = \begin{bmatrix} z(k+1) \\ z(k+2) \\ \vdots \\ z(k+P) \end{bmatrix}; \quad \Delta U = \begin{bmatrix} \Delta u(k) \\ \Delta u(k+1) \\ \vdots \\ \Delta u(k+M-1) \end{bmatrix}; \quad \Delta R = \begin{bmatrix} \Delta r(k+1) \\ \Delta r(k+2) \\ \vdots \\ \Delta r(k+P) \end{bmatrix} \tag{4.22}$$

then the corresponding state prediction is

$$Z = Sz(k) + F\Delta U + \theta \Delta R \tag{4.23}$$

where

$$S = \begin{bmatrix} A_m \\ A_m^2 \\ \vdots \\ A_m^P \end{bmatrix}; \; F = \begin{bmatrix} B_m & 0 & 0 & \cdots & 0 \\ A_m B_m & B_m & 0 & \cdots & 0 \\ A_m^2 B_m & A_m B_m & B_m & \cdots & 0 \\ \vdots & \vdots & \vdots & \ddots & \vdots \\ A_m^{P-1} B_m & A_m^{P-2} B_m & A_m^{P-3} B_m & \cdots & A_m^{P-M} B_m \end{bmatrix}$$

$$\theta = \begin{bmatrix} C_m & 0 & 0 & 0 & 0 \\ A_m C_m & C_m & 0 & 0 & 0 \\ A_m^2 C_m & A_m C_m & C_m & 0 & 0 \\ \vdots & \vdots & \vdots & \ddots & \vdots \\ A_m^{P-1} C_m & A_m^{P-2} C_m & A_m^{P-3} C_m & \cdots & C_m \end{bmatrix}$$

Consider the following objective function for the ENMSS model based MPC strategy

$$J(k) = Z^{\mathrm{T}} Q Z + \Delta U^{\mathrm{T}} L \Delta U \tag{4.24}$$

where Q, L are the relevant weighting matrices for the state variables and control input increments, respectively.

By taking a derivative of $J(k)$ and synthesizing Eqs. (4.23) and (4.24), the optimal control law is derived as

$$\Delta U = -(F^{\mathrm{T}} Q F + L)^{-1} F^{\mathrm{T}} Q (S z(k) + \theta \Delta R)) \tag{4.25}$$

Denote

$$\begin{aligned} K_F &= (F^{\mathrm{T}} Q F + L)^{-1} F^{\mathrm{T}} Q S \\ K_S &= (F^{\mathrm{T}} Q F + L)^{-1} F^{\mathrm{T}} Q \theta \end{aligned} \tag{4.26}$$

then the optimal control law at time instant k can be described as

$$\Delta u(k) = -k_F z(k) - k_s \Delta R \tag{4.27}$$

where k_F and k_s are the first rows of K_F and K_S, respectively.

4.3 Case Studies

In this section, a SISO double integrating process and a multiple-input multiple-output (MIMO) glasshouse micro-climate process are introduced to test the effectiveness of the ENMSS model based MPC. Meanwhile, the conventional NMSS model based MPC scheme is also adopted as the comparison to prove the improved control performance of the ENMSS model based MPC.

Table 4.1 The control parameters for two MPC strategies

Parameters	Proposed	Conventional
P	20	20
M	3	3
α	0.65	0.65
$L = \text{diag}(L_1, L_2, L_3)$	$L_i = 1 (i = 1, 2, 3)$	$L_i = 1 (i = 1, 2, 3)$
$Q = \text{diag}(Q_1, Q_2, \ldots, Q_{20})$	$Q_j = \text{diag}(1, 1, 0, 1)$ $(j = 1, 2, \ldots, 20)$	$Q_j = 1$ $(j = 1, 2, \ldots, 20)$

4.3.1 SISO Case Study

The SISO double integrating process with the following discrete-time transfer function model is considered [18]

$$G(z) = \frac{0.5(z+1)}{(z-1)^2} \tag{4.28}$$

Taking into account the fact that the inevitable disturbance and uncertainty in practice may cause model/plant mismatches, here the following model/plant mismatched cases are employed to evaluate the control performance of both MPC schemes.

Case 1:

$$G(z) = \frac{0.41(z-0.86)}{(z-1.12)^2} \tag{4.29}$$

Case 2:

$$G(z) = \frac{0.53(z-0.82)}{(z-1.19)^2} \tag{4.30}$$

For the two MPC strategies, the set-point is selected as 1 and the load disturbance with amplitude of -0.1 is added to the process at time instant $k = 150$. The control parameters for both methods are listed in Table 4.1.

Due to the fact that there is only the tracking error considered in the performance index of conventional NMSS model based MPC, the elements in Q_j are less than those of ENMSS model based MPC, which implies that more degrees of freedom are provided for the ENMSS model based MPC.

The responses of both methods under the two cases are shown in Figs. 4.1 and 4.2. It can be easily seen that although two MPC strategies achieve the set-point tracking and disturbance rejection successfully in Fig. 4.1a, the overshoot and oscillations in the responses of the ENMSS model based MPC are smaller, which indicates that improved control performance is obtained in the ENMSS model based MPC. In

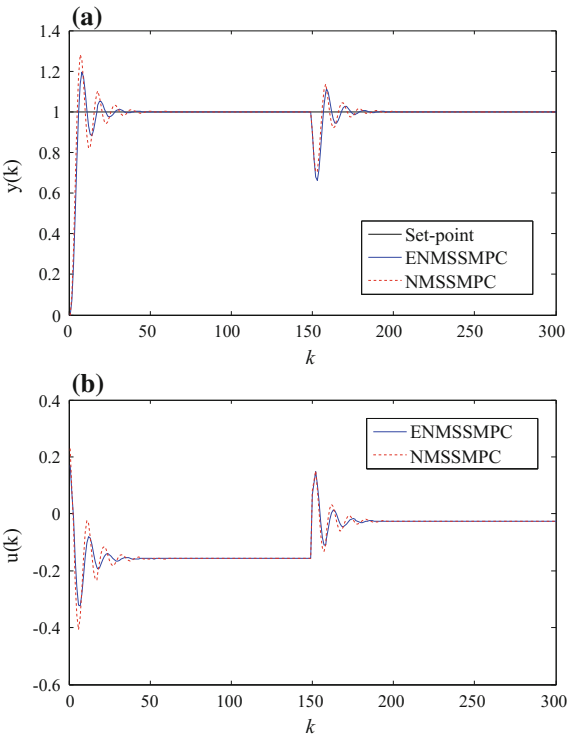

Fig. 4.1 **a** Closed-loop output responses for both MPC methods under case 1. **b** Closed-loop input responses for both MPC methods under case 1

Fig. 4.2, the results are similar to those in Fig. 4.1. The overshoot and oscillations in the responses of the NMSS model based MPC are bigger. From an overall perspective, the ENMSS model based MPC provides enhanced ensemble control performance.

4.3.2 MIMO Case Study

Here, we consider the following MIMO glasshouse micro-climate process with the following discrete model [18]

$$\begin{bmatrix} y_1(k) \\ y_2(k) \end{bmatrix} = \begin{bmatrix} \dfrac{-0.2929z^{-2}}{1 - 0.8669z^{-1}} & \dfrac{0.1237z^{-1} + 0.04935z^{-2}}{1 - 0.8669z^{-1}} \\ \dfrac{-0.05833z^{-2} - 0.2214z^{-3}}{1 - 0.9001z^{-1}} & \dfrac{0.2933z^{-1} + 0.1496z^{-2}}{1 - 0.897z^{-1}} \end{bmatrix} \begin{bmatrix} u_1(k) \\ u_2(k) \end{bmatrix} \tag{4.31}$$

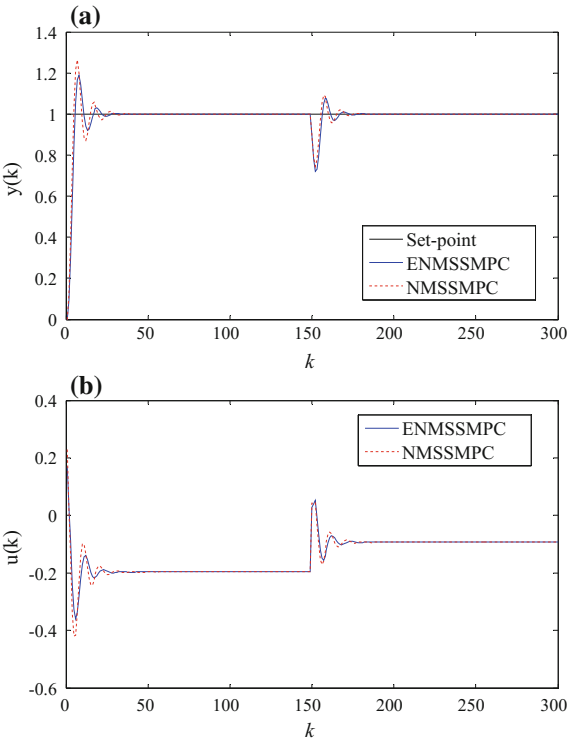

Fig. 4.2 **a** Closed-loop output responses for two MPC approaches under case 2. **b** Closed-loop input responses for two MPC approaches under case 2

Similar to Sect. 4.3.1, the model/plant mismatched case is introduced to verify the control performance of both MPC schemes, and the details are

Case 3:

$$\begin{bmatrix} y_1(k) \\ y_2(k) \end{bmatrix} = \begin{bmatrix} \dfrac{-0.3175z^{-2}}{1 - 0.7912z^{-1}} & \dfrac{0.1049z^{-1} + 0.05614z^{-2}}{1 - 0.7417z^{-1}} \\ \dfrac{-0.05671z^{-2} - 0.2553z^{-3}}{1 - 0.8123z^{-1}} & \dfrac{0.3028z^{-1} + 0.1601z^{-2}}{1 - 0.7735z^{-1}} \end{bmatrix} \begin{bmatrix} u_1(k) \\ u_2(k) \end{bmatrix} \tag{4.32}$$

As to the two MPC strategies, the set-point is chosen as 1 and the output disturbances with amplitude of -0.05 and -0.1 are added to the two process outputs, respectively. The control parameters for the two MPC methods are listed in Table 4.2.

Note that both the tracking errors and the state variables can be weighted in the performance index of the ENMSS model based MPC, thus the elements in Q_j are more than those of NMSS model based MPC.

Table 4.2 The control parameters for two MPC methods

Parameters	Proposed	Conventional
P	8	8
M	1	1
α	0.6	0.6
L	$L = \text{diag}(0.1, 0.1)$	$L = \text{diag}(0.1, 0.1)$
$Q = \text{diag}(Q_1, Q_2, \ldots, Q_8)$	$Q_j = \text{diag}(2, 2, 1, 1, 0, 0, 0, 0, 0, 0, 1, 1)$ $(j = 1, 2, \ldots, 8)$	$Q_j = \text{diag}(1, 1)$ $(j = 1, 2, \ldots, 8)$

Figure 4.3 shows the responses of both MPC schemes under case 3. For y_1, it is obvious that the overshoot and oscillations in the responses of ENMSS model based MPC are smaller, which proves that improved ensemble control performance is offered in the ENMSS model based MPC. At the same time, the signals of u_1 for the ENMSS model based MPC are smoother than those of the conventional NMSS model based MPC, which verifies the aforementioned viewpoints further. As to y_2 and u_2, the situations are similar to those of y_1 and u_1. In a word, the ENMSS model based MPC provides better ensemble control performance.

4.4 Summary

In this chapter, the conventional NMSS and ENMSS models based MPC strategies are introduced. Meanwhile, the derivation process of transforming input–output models into ENMSS models is also described in detail. By adopting the ENMSS model, more degrees of freedom are obtained and the corresponding controller design is more flexible due to the fact that both the tracking error and the state variables can be adjusted separately in the relevant performance index. The case studies on a SISO double integrating process and a MIMO glasshouse micro-climate process demonstrate the effectiveness of the ENMSS model based MPC. Further, the ENMSS model can also be adopted for PFC strategy, and the details will be discussed in the next chapter.

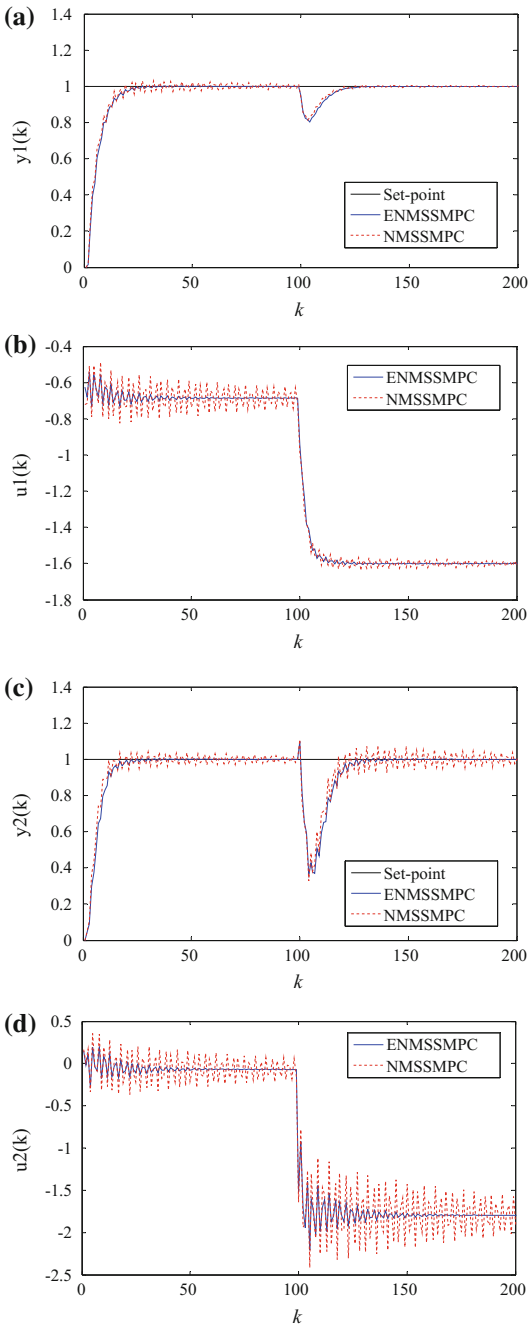

Fig. 4.3 **a** Closed-loop responses for y_1 under case 3. **b** Closed-loop responses for u_1 under case 3. **c** Closed-loop responses for y_2 under case 3. **d** Closed-loop responses for u_2 under case 3

References

1. Abbaszadeh, A., Khaburi, D. A., & Rodriguez, J. (2017). Predictive control of permanent magnet synchronous motor with non-sinusoidal flux distribution for torque ripple minimisation using the recursive least square identification method. *IET Electric Power Applications, 11*(5), 847–856.
2. Cao, Z. X., Yang, Y., Lu, J. Y., & Gao, F. R. (2014). Constrained two dimensional recursive least squares model identification for batch processes. *Journal of Process Control, 24*(6), 871–879.
3. Wang, Q. J., Dai, W., Ma, X. P., & Yang, C. Y. (2018). Multiple models and neural networks based adaptive PID decoupling control of mine main fan switchover system. *IET Control Theory and Applications, 12*(4), 446–455.
4. Zhang, R. D., & Tao, J. (2018). A nonlinear fuzzy neural network modeling approach using an improved genetic algorithm. *IEEE Transactions on Industrial Electronics, 65*(7), 5882–5892.
5. Mao, X. F., Wang, Y. J., Liu, X. D., & Guo, Y. G. (2018). A hybrid feedforward-feedback hysteresis compensator in piezoelectric actuators based on least-squares support vector machine. *IEEE Transactions on Industrial Electronics, 65*(7), 5704–5711.
6. Abbas, H. S., Hanema, J., Toth, R., Mohammadpour, J., & Meskin, N. (2018). An improved robust model predictive control for linear parameter-varying input-output models. *International Journal of Robust and Nonlinear Control, 28*(3), 859–880.
7. Ding, B. C., & Zou, T. (2014). A synthesis approach for output feedback robust model predictive control based-on input-output model. *Journal of Process Control, 24*(3), 60–72.
8. Chen, J. H., & Lin, Y. H. (2012). Multibatch model predictive control for repetitive batch operation with input-output linearization. *Industrial & Engineering Chemistry Research, 51*(28), 9598–9608.
9. Tao, J. L., Zhu, Y., & Fan, Q. R. (2014). Improved state space model predictive control design for linear systems with partial actuator failure. *Industrial & Engineering Chemistry Research, 53*(9), 3578–3586.
10. Gallego, A. J., & Camacho, E. F. (2012). Adaptative state-space model predictive control of a parabolic-trough field. *Control Engineering Practice, 20*(9), 904–911.
11. Falugi, P., Olaru, S., & Dumur, D. (2010). Multi-model predictive control based on LMI: from the adaptation of the state-space model to the analytic description of the control law. *International Journal of Control, 83*(8), 1548–1563.
12. Miranda, H., Cortes, P., Yuz, J. I., & Rodriguez, J. (2009). Predictive torque control of induction machines based on state-space models. *IEEE Transactions on Industrial Electronics, 56*(6), 1916–1924.
13. Simkoff, J. M., Wang, S., Baldea, M., Chiang, L. H., Castillo, I., Bindlish, R., et al. (2018). Plant-model mismatch estimation from closed-loop data for state-space model predictive control. *Industrial & Engineering Chemistry Research, 57*(10), 3732–3741.
14. Zou, T., Wu, S., & Zhang, R. D. (2018). Improved state space model predictive fault-tolerant control for injection molding batch processes with partial actuator faults using GA optimization. *ISA Transactions, 73,* 147–153.
15. Lawrynczuk, M. (2017). Nonlinear predictive control of a boiler-turbine unit: A state-space approach with successive on-line model linearisation and quadratic optimisation. *ISA Transactions, 67,* 476–495.
16. Zhang, R. D., Cao, Z. X., Bo, C. M., Li, P., & Gao, F. R. (2014). New PID controller design using extended nonminimal state space model based predictive functional control structure. *Industrial & Engineering Chemistry Research, 53*(8), 3283–3292.
17. Zhang, R. D., Zou, Q., Cao, Z. X., & Gao, F. R. (2017). Design of fractional order modeling based extended non-minimal state space MPC for temperature in an industrial electric heating furnace. *Journal of Process Control, 56,* 13–22.

18. Wang, L. P., & Young, P. C. (2006). An improved structure for model predictive control using non-minimal state space realisation. *Journal of Process Control, 16*(4), 355–371.
19. Zhang, R. D., Xue, A. K., Wang, S. Q., & Ren, Z. Y. (2011). An improved model predictive control approach based on extended non-minimal state space formulation. *Journal of Process Control, 21*(8), 1183–1192.

Chapter 5
Predictive Functional Control Based on Extended Non-minimal State Space Model

5.1 Introduction

It is a fact that the computational complexity of PFC is smaller than that of other MPC algorithms, so it draws a lot of attention from various industries, especially for those fast process systems [1–3]. As for the input-output model based PFC, there are lots of developments on both theory and applications [4, 5]. However, the higher order input-output model that is necessary in practice sometimes will make the controller design and the analysis of corresponding PFC approaches complicated, which may block the industrial application.

It is clear that state space models can be obtained from input-output models in many ways and the state space model based theoretical derivation is straightforward [6–8]. Many researchers have contributed to the development of state space model based PFC strategies [9–13]. In order to improve the control performance of relevant state space model based PFC algorithms such that the stricter and higher requirements can be satisfied, a lot of significant viewpoints have been presented [14–19]. Note that for most state space model based PFC schemes, the degrees of freedom for the controller design are limited due to the fact that only the controlled variables are considered in the corresponding performance index. In this chapter, the ENMSS model [20, 21] in which other state variables can also be taken into account is introduced for the PFC scheme, and more degrees of freedom are obtained for the controller design.

R. Zhang et al., *Model Predictive Control*,
https://doi.org/10.1007/978-981-13-0083-7_5

5.2 Input-Output Model Based ENMSS Predictive Functional Control

5.2.1 Extended Non-minimal State Space Model [22]

For simplicity, a SISO system is considered here, and its input-output model is

$$\begin{aligned} &y(k+1)+H_1y(k)+H_2y(k-1)+\cdots+H_my(k-m+1)\\ &=L_1u(k)+L_2u(k-1)+\cdots+L_nu(k-n+1) \end{aligned} \tag{5.1}$$

where $y(k)$ is the process output at time instant k, and $u(k)$ is the control input at time instant k. $H_1, \ldots, H_m$ and $L_1, \ldots, L_n$ are the relevant coefficients.

By adding the difference operator Δ to Eq. (5.1), the following model is obtained

$$\begin{aligned} &\Delta y(k+1)+H_1\Delta y(k)+H_2\Delta y(k-1)+\cdots+H_m\Delta y(k-m+1)\\ &=L_1\Delta u(k)+L_2\Delta u(k-1)+\cdots+L_n\Delta u(k-n+1) \end{aligned} \tag{5.2}$$

In order to obtain the relevant state space model, we construct the NMSS vector as

$$\begin{aligned} \Delta x(k)^{\mathrm{T}}=&[\Delta y(k),\Delta y(k-1),\ldots,\Delta y(k-m+1),\\ &\Delta u(k-1),\Delta u(k-2),\ldots,\Delta u(k-n+1)] \end{aligned} \tag{5.3}$$

then the following NMSS model is obtained

$$\begin{aligned} \Delta x(k+1)&=A\Delta x(k)+B\Delta u(k)\\ \Delta y(k+1)&=C\Delta x(k+1) \end{aligned} \tag{5.4}$$

where

$$A=\begin{bmatrix} -H_1 & -H_2 & \cdots & -H_{m-1} & -H_m & L_2 & \cdots & L_{n-1} & L_n\\ 1 & 0 & \cdots & 0 & 0 & 0 & \cdots & 0 & 0\\ 0 & 1 & \cdots & 0 & 0 & 0 & \cdots & 0 & 0\\ \vdots & \vdots & \cdots & \vdots & \vdots & \vdots & \cdots & \vdots & \vdots\\ 0 & 0 & \cdots & 1 & 0 & 0 & \cdots & 0 & 0\\ 0 & 0 & \cdots & 0 & 0 & 0 & \cdots & 0 & 0\\ 0 & 0 & \cdots & 0 & 0 & 1 & \cdots & 0 & 0\\ \vdots & \vdots & \cdots & \vdots & \vdots & \vdots & \cdots & \vdots & \vdots\\ 0 & 0 & \cdots & 0 & 0 & 0 & \cdots & 1 & 0 \end{bmatrix}$$

$$B=\begin{bmatrix} L_1 & 0 & 0 & \cdots & 1 & 0 & \cdots & 0 \end{bmatrix}^{\mathrm{T}}$$

$$C = \begin{bmatrix} 1\ 0\ 0 \cdots 0\ 0\ 0\ 0 \end{bmatrix}$$

Define the set-point as y_s and the reference trajectory as

$$\begin{aligned} r(k) &= y(k) \\ r(k+i) &= \alpha^i y(k) + (1-\alpha^i) y_s \quad i = 1, 2, \ldots, P \end{aligned} \tag{5.5}$$

where P is the prediction horizon, and α is the smoothing factor of the reference trajectory.

The output tracking error at time instant k is further defined as

$$e(k) = y(k) - r(k) \tag{5.6}$$

Then the output tracking error prediction at time instant $k+1$ can be derived based on Eqs. (5.4) and (5.6) as follows

$$e(k+1) = e(k) + CA\Delta x(k) + CB\Delta u(k) - \Delta r(k+1) \tag{5.7}$$

By extending the state vector to contain the tracking error dynamics, i.e.,

$$z(k) = \begin{bmatrix} \Delta x(k) \\ e(k) \end{bmatrix} \tag{5.8}$$

the ENMSS model is obtained

$$z(k+1) = A_m z(k) + B_m \Delta u(k) + C_m \Delta r(k+1) \tag{5.9}$$

where

$$A_m = \begin{bmatrix} A & 0 \\ CA & 1 \end{bmatrix}; \quad B_m = \begin{bmatrix} B \\ CB \end{bmatrix}; \quad C_m = \begin{bmatrix} 0 \\ -1 \end{bmatrix} \tag{5.10}$$

The 0 in A_m, C_m are zero vectors with appropriate dimensions.

Note that $\Delta u(k) = u(k) - u(k-1)$, then Eq. (5.9) can be replaced by the following formulation

$$z(k+1) = A_m z(k) + B_m u(k) - B_m u(k-1) + C_m \Delta r(k+1) \tag{5.11}$$

5.2.2 Controller Design

The following control law that is a linear combination of basis functions is introduced for PFC

$$u(k+i) = \sum_{j=1}^{N} \mu_j f_j(i) \tag{5.12}$$

where $u(k+i)$ is the control law at time instant $k+i$. N is the number of the basis functions. μ_j is the relevant weighting coefficient, and $f_j(i)$ is the value of the basis function f_j at time instant $k+i$.

Denote

$$\begin{aligned} T_i &= [f_1(i), f_2(i), \ldots, f_N(i)], (i = 0, 1, \ldots, P-1) \\ \eta &= [\mu_1, \mu_2, \ldots, \mu_N]^{\mathrm{T}} \end{aligned} \tag{5.13}$$

then the control law in Eq. (5.12) can be simplified as

$$u(k+i) = T_i \eta \tag{5.14}$$

By defining

$$Z = \begin{bmatrix} z(k+1) \\ z(k+2) \\ \vdots \\ z(k+P) \end{bmatrix}; \quad \Delta R = \begin{bmatrix} \Delta r(k+1) \\ \Delta r(k+2) \\ \vdots \\ \Delta r(k+P) \end{bmatrix} \tag{5.15}$$

the state prediction from time instant k can be obtained on the basis of Eqs. (5.11) and (5.14)

$$Z = Sz(k) + \varphi\eta - Fu(k-1) + \theta\Delta R \tag{5.16}$$

where

$$S = \begin{bmatrix} A_m \\ A_m^2 \\ \vdots \\ A_m^P \end{bmatrix}; \quad F = \begin{bmatrix} B_m \\ A_m B_m \\ \vdots \\ A_m^{P-1} B_m \end{bmatrix}; \quad \varphi = \begin{bmatrix} B_m T_0 \\ (A_m B_m - B_m) T_0 + B_m T_1 \\ (A_m^2 B_m - A_m B_m) T_0 + (A_m B_m - B_m) T_1 + B_m T_2 \\ \vdots \\ \sum_{k=1}^{P-1} (A_m^k B_m - A_m^{k-1} B_m) T_{P-1-k} + B_m T_{P-1} \end{bmatrix}$$

$$\theta = \begin{bmatrix} C_m & 0 & 0 & 0 & 0 \\ A_m C_m & C_m & 0 & 0 & 0 \\ A_m^2 C_m & A_m C_m & C_m & 0 & 0 \\ \vdots & \vdots & \vdots & \ddots & \vdots \\ A_m^{P-1} C_m & A_m^{P-2} C_m & A_m^{P-3} C_m & \cdots & C_m \end{bmatrix}$$

Here we select the following performance index for the ENMSS model based PFC

$$J(k) = Z^{\mathrm{T}} Q Z \tag{5.17}$$

where Q is the weighting matrix for the state variables.

By minimizing the cost function in Eq. (5.17) and combining Eqs. (5.16) and (5.17), we can obtain the following optimal control law

$$\eta = -(\varphi^{\mathrm{T}} Q \varphi)^{-1} \varphi^{\mathrm{T}} Q (Sz(k) + \theta \Delta R - Fu(k-1)) \tag{5.18}$$

Define

$$\begin{aligned} \mu_1 &= -(1, 0, \ldots, 0)(\varphi^{\mathrm{T}} Q \varphi)^{-1} \varphi^{\mathrm{T}} Q (Sz(k) - Fu(k-1) + \theta \Delta R) \\ &= -h_1 z(k) + h_{u1} u(k-1) - m_1 \Delta R \\ \mu_2 &= -(0, 1, \ldots, 0)(\varphi^{\mathrm{T}} Q \varphi)^{-1} \varphi^{\mathrm{T}} Q (Sz(k) - Fu(k-1) + \theta \Delta R) \\ &= -h_2 z(k) + h_{u2} u(k-1) - m_2 \Delta R \\ &\vdots \\ \mu_N &= -(0, 0, \ldots, 1)(\varphi^{\mathrm{T}} Q \varphi)^{-1} \varphi^{\mathrm{T}} Q (Sz(k) - Fu(k-1) + \theta \Delta R) \\ &= -h_N z(k) + h_{uN} u(k-1) - m_N \Delta R \end{aligned} \tag{5.19}$$

then the optimal control input at time instant k is expressed as

$$u(k) = \sum_{j=1}^{N} \mu_j f_j(0) = -Hz(k) + H_u u(k-1) - M \Delta R \tag{5.20}$$

where

$$H = \sum_{j=1}^{N} f_j(0) h_k, (k = 1, 2, \ldots, N)$$

$$H_u = \sum_{j=1}^{N} f_j(0) h_{uk}, (k = 1, 2, \ldots, N)$$

$$M = \sum_{j=1}^{N} f_j(0) m_k, (k = 1, 2, \ldots, N)$$

5.3 Summary

In this chapter, the ENMSS model based PFC is described. The input–output model is transformed into the ENMSS model in which the process state variables and the tracking error can be regulated separately for PFC, then more degrees of freedom are offered for the subsequent controller design, such that improved control performance is expected. As to the constraint dealing in MPC strategies, it is also a vital topic and the details will be discussed in the next chapter.

References

1. Bigdeli, N., & Haeri, M. (2009). Predictive functional control for active queue management in congested TCP/IP networks. *ISA Transactions, 48*(1), 107–121.
2. Skrjanc, I. (2007). A decomposed-model predictive functional control approach to air-vehicle pitch-angle control. *Journal of Intelligent and Robotic Systems, 48*(1), 115–127.
3. Tian, J. Y., Zhang, S. F., Zhang, Y. H., Li, T., & Yang, H. B. (2016). Enhanced predictive functional control based on equivalent input disturbance and generalized extended state observer for nonlinear systems with fast dynamics. *Proceedings of The Institution of Mechanical Engineers part G-Journal of Aerospace Engineering, 230*(10), 1943–1963.
4. Khadir, M. T., & Ringwood, J. V. (2008). Extension of first order predictive functional controllers to handle higher order internal models. *International Journal of Applied Mathematics and Computer Science, 18*(2), 229–239.
5. Zou, Z. Y., Zhao, D. D., Huang, Y., Pan, Y. S., Guo, Y. Q., Yu, M. (2013). Design of a new predictive functional control algorithm based on linear difference equation model. In *Proceedings of the 2013 Fourth International Conference on Intelligent Control and Information Processing (ICICIP)* (pp. 661–665).
6. Wang, L. P., Young, P. C., Gawthrop, P. J., & Taylor, C. J. (2009). Non-minimal state-space model-based continuous-time model predictive control with constraints. *International Journal of Control, 82*(6), 1122–1137.
7. Zhang, J. M. (2014). A non-minimal state space formulation based predictive functional control design for inverse-response processes. *Chemometrics and Intelligent Laboratory Systems, 139,* 70–75.
8. Lu, K. D., Zhou, W. N., Zeng, G. Q., & Du, W. (2018). Design of PID controller based on a self-adaptive state-space predictive functional control using external optimization method. *Journal of The Franklin Institute-Engineering and Applied Mathematics, 355*(5), 2197–2220.
9. Skrjanc, I., & Blazic, S. (2005). Predictive functional control based on fuzzy model: Design and stability study. *Journal of the Intelligent & Robotic Systems, 43*(2–4), 283–299.
10. Tang, W. Q., & Cai, Y. L. (2012). Predictive functional control-based missile autopilot design. *Journal of Guidance, Control and Dynamics, 35*(5), 1450–1455.
11. Tao, J. L., Yu, Z. H., Zhu, Y., & Ma, L. H. (2015). A linear quadratic structure based predictive functional control design for industrial processes against partial actuator failures. *Chemometrics and Intelligent Laboratory Systems, 146,* 263–269.

12. Zhang, R. D., Zou, H. B., Xue, A. K., & Gao, F. R. (2014). GA based predictive functional control for batch processes under actuator faults. *Chemometrics and Intelligent Laboratory Systems, 137,* 67–73.
13. Skrjanc, I., & Matko, D. (2001). Fuzzy predictive functional control in the state space domain. *Journal of Intelligent and Robotic Systems, 31*(1–3), 283–297.
14. Simkoff, J. M., Wang, S., Baldea, M., Chiang, L. H., Castillo, I., Bindlish, R., et al. (2018). Plant-model mismatch estimation from closed-loop data for state-space model predictive control. *Industrial & Engineering Chemistry Research, 57*(10), 3732–3741.
15. Tatjewski, P. (2014). Disturbance modeling and state estimation for offset-free predictive control with state-space process models. *International Journal of Applied Mathematics and Computer Science, 24*(2), 313–323.
16. Gallego, A. J., & Camacho, E. F. (2012). Adaptive state-space model predictive control of a parabolic-trough field. *Control Engineering Practice, 20*(9), 904–911.
17. Miranda, H., Cortes, P., Yuz, J. I., & Rodriguez, J. (2009). Predictive torque control of induction machines based on state-space models. *IEEE Transactions on Industrial Electronics, 56*(6), 1916–1924.
18. Lawrynczuk, M. (2017). Nonlinear predictive control of a boiler-turbine unit: A state-space approach with successive on-line model linearisation and quadratic optimisation. *ISA Transactions, 67,* 476–495.
19. Zhang, R. D., Xue, A. K., Wang, S. Q., & Zhang, J. M. (2014). An improved state-space model structure and a corresponding predictive functional control design with improved control performance. *International Journal of Control, 85*(8), 1146–1161.
20. Zhang, R. D., Zou, Q., Cao, Z. X., & Gao, F. R. (2017). Design of fractional order modeling based extended non-minimal state space MPC for temperature in an industrial electric heating furnace. *Journal of Process Control, 56,* 13–22.
21. Zhang, R. D., & Gao, F. R. (2015). An improved decoupling structure based state space MPC design with improved performance. *Systems & Control Letters, 75,* 77–83.
22. Zhang, R. D., & Gao, F. R. (2013). Multivariable decoupling predictive functional control with non-zero-pole cancellation and state weighting: Application on chamber pressure in a coke furnace. *Chemical Engineering Science, 94,* 30–43.

Chapter 6
Model Predictive Control Under Constraints

6.1 Introduction

In practical industrial processes, many constraints are considered for operation safety, device limitations, equipment requirements, and so on. As to the constraints dealing in MPC strategies, there were a lot of fruits during the past decades [1–5]. In order to obtain the control law for constrained MPC schemes, many optimization approaches have been employed, such as linear programming [6–8], quadratic programming [9–11], linear matrix inequalities [12–14], etc.

It is a fact that the working conditions are continuously changing and the preset constraints may be too rigorous in practice, which affects the solution of the corresponding constrained optimization problem greatly [15–17]. Meanwhile, the computational time is another point that needs to be taken into account to meet practical requirements [18, 19]. Based on these backgrounds, how to obtain the solution for constrained MPC approaches effectively and accurately is still an open issue. In this chapter, a basic constraints handling approach is described for the ENMSS model based MPC. The constraints on control input and output will be transformed properly, and a new linear programming problem will be considered for the constrained MPC scheme. Finally, the optimal control law for the constrained optimization problem can be obtained by employing the simplex method.

6.2 Constraints Handling in Model Predictive Control [20]

In this section, a kind of constraints handing methods is introduced and the ENMSS based MPC scheme is adopted as the example.

Here, the prediction horizon and the control horizon will both be chosen as P to simplify the derivation. Refer to Sect. 4.2.2, it is clear that the optimal control law for the unconstrained ENMSS model based MPC is

R. Zhang et al., *Model Predictive Control*,
https://doi.org/10.1007/978-981-13-0083-7_6

$$\Delta U = -(F^{\mathrm{T}} Q F + L)^{-1} F^{\mathrm{T}} Q(Sz(k) + \theta \Delta R)) \tag{6.1}$$

Consider the following constraints for the controlled system

$$y_{\min} \le y(k) \le y_{\max}, u_{\min} \le u(k) \le u_{\max} \tag{6.2}$$

where $y_{\min}, y_{\max}$ are the corresponding constrained bounds for the process output, and $u_{\min}, u_{\max}$ are the lower and upper bounds for the control input. Note that the control law in Eq. (6.1) may not satisfy the constraints in Eq. (6.2).

In order to obtain the control law for the constrained MPC approach, a new vector $Z = [Z_1^{\mathrm{T}}, Z_2^{\mathrm{T}}, \ldots, Z_P^{\mathrm{T}}]^{\mathrm{T}}$ is introduced first.

$$Z = (F^{\mathrm{T}} Q F + L)\Delta U + F^{\mathrm{T}} Q(Sz(k) + \theta \Delta R) \tag{6.3}$$

Meanwhile, the following performance index is considered.

$$J[\Delta U] = \min \sum_{i=1}^{P} |Z_i| \tag{6.4}$$

Remark 6.1 The objective function in Eq. (6.4) aims at achieving the set-point tracking and guaranteeing the steady control input together.

Denote

$$Z_i = Z_i^+ - Z_i^- \tag{6.5}$$

where $Z_i^+ > 0$ and $Z_i^- > 0$.

Based on Eq. (6.5), the cost function in Eq. (6.4) can be replaced by the following formulation

$$J[\Delta U] = \min \sum_{i=1}^{P} \left| Z_i^+ - Z_i^- \right| \tag{6.6}$$

Then, the following linear programming problem is obtained for the constrained MPC strategy.

$$\min \sum_{i=1}^{P} \left| Z_i^+ - Z_i^- \right| \tag{6.7}$$

subject to

$$\begin{aligned} &y_{\min} \le y(k+i) \le y_{\max} (i = 1, 2, \ldots, P) \\ &u_{\min} \le u(k+i-1) \le u_{\max} (i = 1, 2, \ldots, P) \end{aligned} \tag{6.8}$$

As to the constrained control input in Eq. (6.8), it can be decomposed with the manipulated vector ΔU as follows.

$$\begin{bmatrix} u(k) \\ u(k+1) \\ \vdots \\ u(k+P-1) \end{bmatrix} = \begin{bmatrix} 1 \\ 1 \\ \vdots \\ 1 \end{bmatrix} u(k-1) + \begin{bmatrix} 1 & 0 & \cdots & 0 \\ 1 & 1 & \cdots & 0 \\ \vdots & \vdots & \ddots & \vdots \\ 1 & 1 & 1 & 1 \end{bmatrix} \begin{bmatrix} \Delta u(k) \\ \Delta u(k+1) \\ \vdots \\ \Delta u(k+P-1) \end{bmatrix} \tag{6.9}$$

Further, the constrained control input can be converted into the following constraints for the manipulated vector ΔU

$$C_1 u_{\min} - C_2 u(k-1) \leq C\Delta U \leq C_1 u_{\max} - C_2 u(k-1) \tag{6.10}$$

where C, C_1, C_2 are the relevant matrices.

Note that the following equation is achieved for the process output based on Eq. (4.15) in Sect. 4.2.2

$$y(k) = \bar{C} \begin{bmatrix} \Delta x(k) \\ y(k) \end{bmatrix} \tag{6.11}$$

where $\bar{C} = [\,0\ 1\,]$, and 0 in $\bar{C}$ is a zero vector with appropriate dimensions.

Then, the constrained process output in Eq. (6.8) can be expressed as follows

$$Y = \begin{bmatrix} y(k+1) \\ y(k+2) \\ \vdots \\ y(k+P) \end{bmatrix} = \hat{C} \begin{bmatrix} \Delta x(k) \\ y(k) \end{bmatrix} + \hat{C} F \Delta U \tag{6.12}$$

where $\hat{C}$ is a P-diagonal matrix with matrix $\bar{C}$ sitting on its diagonal.

Further, the output constraints in Eq. (6.8) can be presented by the following equation

$$C_3 y_{\min} - \hat{C} \begin{bmatrix} \Delta x(k) \\ y(k) \end{bmatrix} \leq \hat{C} F \Delta U \leq C_4 y_{\max} - \hat{C} \begin{bmatrix} \Delta x(k) \\ y(k) \end{bmatrix} \tag{6.13}$$

where C_3, C_4 are the relevant matrices.

Finally, the constraints on Z can be calculated by combining Eqs. (6.3), (6.10), and (6.13). Meanwhile, the linear programming problem in Eq. (6.7) can be solved by simplex algorithms.

6.3 Summary

In this chapter, a constraints handling approach is introduced for the ENMSS model based MPC briefly. The constraints for the inputs and outputs are transformed into the constraints for the manipulated vector and a corresponding linear programming problem is considered in this constraints handling method. Finally, the optimal control law is obtained by solving the linear programming problem through simplex methods.

References

1. Zhang, J. F., Jia, X. L., Zhang, R. D., & Zuo, Y. (2018). A model predictive control framework for constrained uncertain positive systems. *International Journal of Systems Science, 49*(4), 884–896.
2. Avanzini, G. B., Zanchettin, A. M., & Rocco, P. (2018). Constrained model predictive control for mobile robotic manipulators. *Robotica, 36*(1), 19–38.
3. Kheawhom, S., & Bumroongsri, P. (2018). Interpolation techniques for robust constrained model predictive control based on polyhedral invariant set. *IMA Journal of Mathematical Control and Information, 34*(2), 501–519.
4. Liu, K. L., Li, K., & Zhang, C. (2017). Constrained generalized predictive control of battery charging process based on a coupled thermoelectric model. *Journal of Power Sources, 347,* 145–158.
5. Tarczewski, T., & Grzesiak, L. M. (2016). Constrained state feedback speed control of PMSM based on model predictive approach. *IEEE Transactions on Industrial Electronics, 63*(6), 3867–3875.
6. Deng, K., Sun, Y., Li, S. S., Lu, Y., Brouwer, J., Mehta, P. G., et al. (2015). Model predictive control of central chiller plant with thermal energy storage via dynamic programming and mixed-integer linear programming. *IEEE Transactions on Automation Science and Engineering, 12*(2), 565–579.
7. Vichik, S., & Borrelli, F. (2014). Solving linear and quadratic programs with an analog circuit. *Computers & Chemical Engineering, 70,* 160–171.
8. Jones, C. N., Grieder, P., & Rakovic, S. V. (2006). A logarithmic-time solution to the point location problem for parametric linear programming. *Automatica, 42*(12), 2215–2218.
9. Ke, F., Li, Z. J., Xiao, H. Z., & Zhang, X. B. (2017). Visual servoing of constrained mobile robots based on model predictive control. *IEEE Transactions on Systems Man Cybernetics:Systems, 47*(7), 1428–1438.
10. Harrison, C. A., & Qin, S. J. (2009). Minimum variance performance map for constrained model predictive control. *Journal of Process Control, 19*(7), 1199–1204.
11. Baker, R., & Swartz, C. L. E. (2008). Interior point solution of multilevel quadratic programming problems in constrained model predictive control applications. *Industrial & Engineering Chemistry Research, 47*(1), 81–91.
12. Bernardini, D., & Bemporad, A. (2012). Stabilizing model predictive control of stochastic constrained linear systems. *IEEE Transactions on Automatic Control, 57*(6), 1468–1480.
13. Lee, S. M., & Won, S. C. (2007). Robust constrained predictive control using a sector bounded nonlinear model. *IET Control Theory and Applications, 1*(4), 999–1007.
14. Bououden, S., Chadli, M., Zhang, L. X., & Yang, T. (2016). Constrained model predictive control for time-varying delay systems: Application to an active car suspension. *International Journal of Control, Automation and Systems, 14*(1), 51–58.

15. Sun, T. R., Pan, Y. P., Zhang, J., & Yu, H. Y. (2018). Robust model predictive control for constrained continuous-time nonlinear systems. *International Journal of Control, 91*(2), 359–368.
16. Jalal, R. E., & Rasmussen, B. P. (2017). Limited-communication distributed model predictive control for coupled and constrained subsystems. *IEEE Transactions on Control Systems Technology, 25*(5), 1807–1815.
17. Lu, L., Zou, Y. Y., & Niu, Y. G. (2017). Event-driven robust output feedback control for constrained linear systems via model predictive control method. *Circuits Systems and Signal Processing, 36*(2), 543–558.
18. Blanchini, F., Casagrande, D., Giordano, G., & Viaro, U. (2016). Robust constrained model predictive control of fast electromechanical systems. *Journal of The Franklin Institute-Engineering and Applied Mathematics, 353*(9), 2087–2103.
19. Mohammadkhani, M. A., Bayat, F., & Jalali, A. A. (2014). Design of explicit model predictive control for constrained linear systems with disturbances. *International Journal pf Control Automation and Systems, 12*(2), 294–301.
20. Zhang, R. D., Xue, A. K., Wang, S. Q., & Zhang, J. M. (2012). An improved state space model structure and a corresponding predictive functional control design with improved control performance. *International Journal of Control, 85*(8), 1146–1161.

Chapter 7
PID Control Using Extended Non-minimal State Space Model Optimization

7.1 Introduction

As a classic control strategy with simple structure, PID control has obtained a lot of applications in practical industrial processes [1–4]. It is known that the employment of traditional PID control in the processes with large time delay or strong nonlinearity may not achieve the desired control performance; meanwhile, there are challenges for conventional PID control to meet stricter and higher requirements with the rapid development of economy [5–9]. In order to enhance the control performance of PID control, many significant improvements have been presented [10–14].

MPC is a promising and effective advanced control algorithm for various industrial processes, however, limited by the cost, hardware, etc., its applications are not as wide as that of PID control [15–17]. Based on such backgrounds, it is meaningful to develop a new control approach that possesses the simple structure as PID control and the good control performance as MPC. In this chapter, the structure of the control law of PID control is introduced to the framework of ENMSS model based MPC scheme, where the PID control parameters are optimized finally. For the improved PID control, it inherits the same control performance of ENMSS model based MPC approach and the simple structure of conventional PID control. Case studies on a SISO industrial surfactant reactor and a MIMO glasshouse micro-climate process demonstrate the effectiveness of the novel PID control.

R. Zhang et al., *Model Predictive Control*,
https://doi.org/10.1007/978-981-13-0083-7_7

7.2 ENMSS Model Based PID Control Optimization

In this section, the optimization of SISO PID controller and MIMO PID controller using ENMSS model based MPC strategy will be described respectively. Meanwhile, the ENMSS model based PFC scheme is also introduced to optimize the SISO and MIMO PID controllers.

7.2.1 SISO PID Controller Optimized by ENMSS Model Predictive Control [18]

The SISO process with the following model is considered.

$$\begin{aligned} &y(k+1) + H_1 y(k) + H_2 y(k-1) + \cdots + H_m y(k-m+1) \\ &\quad = L_1 u(k) + L_2 u(k-1) + \cdots + L_n u(k-n+1) \end{aligned} \tag{7.1}$$

where $y(k)$, $u(k)$ are the process output and control input at time instant k, respectively. H_1, …, H_m and L_1, …, L_n are the relevant coefficients.

In order to make this book more concise, the repetitive derivation processes that can be referred to in Sect. 4.2.2 are omitted here. Following the procedures in Sect. 4.2.2, the state prediction from time instant k is obtained as follows.

$$Z = Sz(k) + F\Delta U + \theta \Delta R \tag{7.2}$$

where

$$S = \begin{bmatrix} A \\ A^2 \\ \vdots \\ A^P \end{bmatrix}; \quad F = \begin{bmatrix} B & 0 & 0 & \cdots & 0 \\ AB & B & 0 & \cdots & 0 \\ A^2B & AB & B & \cdots & 0 \\ \vdots & \vdots & \vdots & \ddots & \vdots \\ A^{P-1}B & A^{P-2}B & A^{P-3}B & \cdots & A^{P-M}B \end{bmatrix}$$

$$\theta = \begin{bmatrix} C & 0 & 0 & 0 & 0 \\ AC & C & 0 & 0 & 0 \\ A^2C & AC & C & 0 & 0 \\ \vdots & \vdots & \vdots & \ddots & \vdots \\ A^{P-1}C & A^{P-2}C & A^{P-3}C & \cdots & C \end{bmatrix}$$

Select the performance index for the ENMSS model based MPC as

$$J(k) = Z^{\mathrm{T}} Q Z + \Delta U^{\mathrm{T}} L \Delta U \tag{7.3}$$

where Q, L are the weighting matrices for the state variables and control input increments, respectively.

In this section, the PID controller to be introduced and optimized is of the incremental form, and its control law can be expressed as

$$\begin{aligned} u(k) &= u(k-1) + K_p(k)(e_1(k) - e_1(k-1)) + K_i(k)e_1(k) \\ &\quad + K_d(k)(e_1(k) - 2e_1(k-1) + e_1(k-2)) \\ e_1(k) &= y_s - y(k) \end{aligned} \tag{7.4}$$

where $K_p(k)$, $K_i(k)$, $K_d(k)$ are the proportional coefficient, the integral coefficient, and the derivative coefficient at time instant k, respectively. $e_1(k)$ is the error between the set-point and the process output at time instant k.

For simplicity, the formulation in Eq. (7.4) can be replaced by the following equation

$$\begin{aligned} u(k) &= u(k-1) + w(k)^{\mathrm{T}} E(k) \\ w(k) &= [w_1(k), w_2(k), w_3(k)]^{\mathrm{T}} \\ w_1(k) &= K_p(k) + K_i(k) + K_d(k), w_2(k) = -K_p(k) - 2K_d(k), w_3(k) = K_d(k) \\ E(k) &= [e_1(k), e_1(k-1), e_1(k-2)]^{\mathrm{T}} \end{aligned} \tag{7.5}$$

In order to simplify the derivation process further, here the control horizon is chosen as 1, then the optimal control law can be obtained by minimizing the objective function in Eq. (7.3).

$$w(k) = (-((F^{\mathrm{T}} Q F + L)E(k)^{\mathrm{T}} E(k))^{-1} F^{\mathrm{T}} Q(Sz(k) + \theta \Delta R))E(k) \tag{7.6}$$

Based on Eq. (7.6), the parameters of PID control can be obtained easily.

$$\begin{aligned} K_p(k) &= -w_2(k) - 2K_d(k) \\ K_i(k) &= w_1(k) - K_P(k) - K_d(k) \\ K_d(k) &= w_3(k) \end{aligned} \tag{7.7}$$

Remark 7.1 It is obvious that when $E(k)^{\mathrm{T}} E(k)$ approaches zero, i.e., the process output is close to the set-point, $w(k)$ will be infinite, which indicates that the parameters of PID control will be infinitely large and is not practical in practice. Hence, limitations should be set to avoid such situations and the details are as follows.

$$\begin{cases} K_p(k) = K_p(k-1) \\ K_i(k) = K_i(k-1) \ \cdots |e_1(k)| \le \delta \\ K_d(k) = K_d(k-1) \end{cases}$$
$$\begin{cases} K_p(k) = -w_2(k) - 2K_d(k) \\ K_i(k) = w_1(k) - K_P(k) - K_d(k) \cdots |e_1(k)| > \delta \\ K_d(k) = w_3(k) \end{cases} \tag{7.8}$$

where δ is a small permissible error. From Eq. (7.8), it can be easily seen that the parameters of PID control are not changed and remained as those of the previous sampling instant if the error $e_1(k)$ is in the range of δ.

Finally, the optimal control input at sampling instant k is obtained on the basis of Eq. (7.7) as

$$\begin{aligned} u(k) = u(k-1) &+ K_p(k)(e_1(k) - e_1(k-1)) + K_i(k)e_1(k) \\ &+ K_d(k)(e_1(k) - 2e_1(k-1) + e_1(k-2)) \end{aligned} \tag{7.9}$$

7.2.2 *SISO PID Controller Optimized by ENMSS Predictive Functional Control [19]*

Consider the SISO process in Eq. (5.1), the corresponding ENMSS model can be derived first as follows.

$$z(k+1) = A_m z(k) + B_m u(k) - B_m u(k-1) + C_m \Delta r(k+1) \tag{7.10}$$

where

$$A_m = \begin{bmatrix} A & 0 \\ CA & 1 \end{bmatrix}; \quad B_m = \begin{bmatrix} B \\ CB \end{bmatrix}; \quad C_m = \begin{bmatrix} 0 \\ -1 \end{bmatrix}$$

Note that the repeated derivation procedures are omitted here for brevity, and the relevant details can be referred to in Sect. 5.2.1.

Denote

$$Z = \begin{bmatrix} z(k+1) \\ z(k+2) \\ \vdots \\ z(k+P) \end{bmatrix}; \quad \Delta R = \begin{bmatrix} \Delta r(k+1) \\ \Delta r(k+2) \\ \vdots \\ \Delta r(k+P) \end{bmatrix} \tag{7.11}$$

then, based on Eq. (7.10), the state prediction from sampling time instant k is

$$Z = Sz(k) + Fu(k) - Fu(k-1) + \theta \Delta R \tag{7.12}$$

where

$$S = \begin{bmatrix} A_m \\ A_m^2 \\ \vdots \\ A_m^P \end{bmatrix}; \quad F = \begin{bmatrix} B_m \\ A_m B_m \\ \vdots \\ A_m^{P-1} B_m \end{bmatrix}$$

$$\theta = \begin{bmatrix} C_m & 0 & 0 & 0 & 0 \\ A_m C_m & C_m & 0 & 0 & 0 \\ A_m^2 C_m & A_m C_m & C_m & 0 & 0 \\ \vdots & \vdots & \vdots & \ddots & \vdots \\ A_m^{P-1} C_m & A_m^{P-2} C_m & A_m^{P-3} C_m & \cdots & C_m \end{bmatrix}$$

In order to achieve the set-point tracking, the following objective function is chosen

$$J(k) = Z^{\mathrm{T}} Q Z \tag{7.13}$$

where Q is the weighting matrix for the state variables.

Here, the following incremental PID controller is adopted.

$$\begin{aligned} u(k) &= u(k-1) + K_p(k)(e_1(k) - e_1(k-1)) + K_i(k)e_1(k) \\ &\quad + K_d(k)(e_1(k) - 2e_1(k-1) + e_1(k-2)) \\ e_1(k) &= y_s - y(k) \end{aligned} \tag{7.14}$$

where $K_p(k)$, $K_i(k)$, $K_d(k)$ are the proportional coefficient, the integral coefficient and the derivative coefficient at time instant k, respectively, $e_1(k)$ is the error between the set-point and the process output at time instant k.

In order to simplify the subsequent derivation process, the control law in Eq. (7.14) can be rewritten as

$$\begin{aligned} u(k) &= u(k-1) + w(k)^{\mathrm{T}} E(k) \\ w(k) &= [w_1(k), w_2(k), w_3(k)]^{\mathrm{T}} \\ w_1(k) &= K_p(k) + K_i(k) + K_d(k),\ w_2(k) = -K_p(k) - 2K_d(k),\ w_3(k) = K_d(k) \\ E(k) &= [e_1(k), e_1(k-1), e_1(k-2)]^{\mathrm{T}} \end{aligned} \tag{7.15}$$

By taking a derivative of the performance index in Eq. (7.13), the following optimal control law is obtained

$$w(k) = (-(F^{\mathrm{T}} Q F E(k)^{\mathrm{T}} E(k))^{-1} F^{\mathrm{T}} Q(Sz(k) + \theta \Delta R))E(k) \tag{7.16}$$

then the corresponding parameters of PID control can be calculated as

$$\begin{aligned} K_p(k) &= -w_2(k) - 2K_d(k) \\ K_i(k) &= w_1(k) - K_P(k) - K_d(k) \\ K_d(k) &= w_3(k) \end{aligned} \tag{7.17}$$

Note that the small permissible error δ and the relevant limitations in Eq. (7.8) are also needed here, and the optimal control input at time instant k is obtained finally

$$\begin{aligned} u(k) = u(k-1) &+ K_p(k)(e_1(k) - e_1(k-1)) + K_i(k)e_1(k) \\ &+ K_d(k)(e_1(k) - 2e_1(k-1) + e_1(k-2)) \end{aligned} \tag{7.18}$$

7.2.3 *MIMO PID Controller Optimized by ENMSS Model Predictive Control [20]*

Assume that the MIMO process has p inputs and q outputs. Refer to the similar derivation procedures in Sect. 4.2.2, the following state prediction can be derived first

$$Z = Sz(k) + F\Delta U + \theta \Delta R \tag{7.19}$$

where

$$S = \begin{bmatrix} A \\ A^2 \\ \vdots \\ A^P \end{bmatrix}; \quad F = \begin{bmatrix} B & 0 & 0 & \cdots & 0 \\ AB & B & 0 & \cdots & 0 \\ A^2B & AB & B & \cdots & 0 \\ \vdots & \vdots & \vdots & \ddots & \vdots \\ A^{P-1}B & A^{P-2}B & A^{P-3}B & \cdots & A^{P-M}B \end{bmatrix}$$

$$\theta = \begin{bmatrix} C & 0 & 0 & 0 & 0 \\ AC & C & 0 & 0 & 0 \\ A^2C & AC & C & 0 & 0 \\ \vdots & \vdots & \vdots & \ddots & \vdots \\ A^{P-1}C & A^{P-2}C & A^{P-3}C & \cdots & C \end{bmatrix}$$

The following objective function is selected for the ENMSS model based MPC strategy.

$$J(k) = Z^{\mathrm{T}} Q Z + \Delta U^{\mathrm{T}} L \Delta U \tag{7.20}$$

where Q, L are the weighting matrices for the state variables and control input increments, respectively.

The incremental PID controller with the following structure is introduced.

$$\begin{aligned} u(k) &= u(k-1) + k_p(k)(e_1(k) - e_1(k-1)) + k_i(k)e_1(k) \\ &\quad + k_d(k)(e_1(k) - 2e_1(k-1) + e_1(k-2)) \\ e_1(k) &= y_s - y(k) \\ e_1(k) &= \left[e_{11}(k)\ e_{12}(k) \cdots e_{1q}(k) \right]^{\mathrm{T}} \end{aligned} \tag{7.21}$$

where $k_p(k)$, $k_i(k)$, $k_d(k)$ are the proportional coefficient matrix, the integral coefficient matrix and the derivative coefficient matrix at time instant k, respectively. $e_1(k)$ is the error vector between the set-point vector and the process output vector at time instant k.

Suppose that p is equal or greater than q; meanwhile, the first q inputs are used to control the q outputs and the other $p - q$ inputs are zeros, then the following holds

$$k_n(k) = \begin{bmatrix} k_{n1}(k) & 0 & 0 & \cdots & \cdots\cdots & 0 \\ 0 & k_{n2}(k) & 0 & \vdots & \cdots & \vdots\ 0 \\ 0 & 0 & \ddots & 0 & \ddots & \vdots\ \vdots \\ \vdots & \vdots & 0 & k_{nq}(k) & 0 & \vdots\ \vdots \\ 0 & \cdots & 0 & 0 & 0 & \cdots 0 \\ \vdots & \vdots & \cdots & \ddots & \vdots & \ddots\ 0 \\ 0 & 0 & \cdots & \cdots & \cdots\cdots & 0 \end{bmatrix}, \quad (n = p, i, d) \tag{7.22}$$

Further, the incremental control law in Eq. (7.21) can be reconstructed as

$$u(k) = u(k-1) + E(k)^{\mathrm{T}} w(k) \tag{7.23}$$

where

$$E(k) = \begin{bmatrix} E_1(k) & 0 & 0 & \cdots 0 \\ 0 & E_2(k) & 0 & \cdots 0 \\ \vdots & \vdots & \vdots & \vdots\ \vdots \\ 0 & 0 & E_q(k) & \cdots 0 \end{bmatrix}_{3q \times p}$$

$$E_i(k) = \left[e_{1i}(k)\ e_{1i}(k-1)\ e_{1i}(k-2) \right]^{\mathrm{T}}$$

$$w(k) = \left[w_1(k)\ w_2(k) \cdots w_q(k) \right]^{\mathrm{T}}$$
$$w_i(k) = \left[w_{i1}(k)\ w_{i2}(k)\ w_{i3}(k) \right]$$

$$w_{i1}(k) = k_{pi}(k) + k_{ii}(k) + k_{di}(k);\ w_{i2}(k) = -k_{pi}(k) - 2k_{di}(k);\ w_{i3}(k) = k_{di}(k)$$

Synthesizing Eqs. (7.19–7.23), the relevant optimal control law can be derived by minimizing the cost function $J(k)$

$$w(k) = E(k)(-((F^{\mathrm{T}}QF + L)E(k)^{\mathrm{T}}E(k))^{-1}F^{\mathrm{T}}Q(Sz(k) + \theta\Delta R)) \tag{7.24}$$

Finally, the corresponding PID control parameters are obtained.

$$\begin{aligned} k_{pi}(k) &= -w_{i2}(k) - 2k_{di}(k) \\ k_{ii}(k) &= w_{i1}(k) - k_{pi}(k) - k_{di}(k) \\ k_{di}(k) &= w_{i3}(k) \end{aligned} \tag{7.25}$$

Based on Eq. (7.25), the optimal control input $u(k)$ in Eq. (7.21) can be calculated subsequently.

In order to avoid the case that the PID control parameters will be infinite when the process outputs reach the relevant set-points, the similar limitations as those in the aforementioned sections are considered, and the details are as follows.

$$\begin{cases} k_{pi}(k) = k_{pi}(k-1) \\ k_{ii}(k) = k_{ii}(k-1) \quad \cdots |e_{1i}(k)| \le \delta \\ k_{di}(k) = k_{di}(k-1) \end{cases}$$
$$\begin{cases} k_{pi}(k) = -w_{i2}(k) - 2k_{di}(k) \\ k_{ii}(k) = w_{i1}(k) - k_{pi}(k) - k_{di}(k) \quad \cdots |e_{1i}(k)| > \delta \\ k_{di}(k) = w_{i3}(k) \end{cases} \tag{7.26}$$

where δ is the small permissible error.

7.2.4 MIMO PID Controller Optimized by ENMSS Predictive Functional Control

Suppose that there are p inputs and q outputs in the MIMO process, and the following ENMSS model can be constructed first by referring to the similar derivation processes in Sect. 5.2.1.

$$z(k+1) = A_m z(k) + B_m u(k) - B_m u(k-1) + C_m \Delta r(k+1) \tag{7.27}$$

Define

$$Z = \begin{bmatrix} z(k+1) \\ z(k+2) \\ \vdots \\ z(k+P) \end{bmatrix}; \quad \Delta R = \begin{bmatrix} \Delta r(k+1) \\ \Delta r(k+2) \\ \vdots \\ \Delta r(k+P) \end{bmatrix} \tag{7.28}$$

then the state prediction from sampling time instant k can be expressed as

$$Z = Sz(k) + Fu(k) - Fu(k-1) + \theta \Delta R \tag{7.29}$$

where

$$S = \begin{bmatrix} A_m \\ A_m^2 \\ \vdots \\ A_m^P \end{bmatrix}; F = \begin{bmatrix} B_m \\ A_m B_m \\ \vdots \\ A_m^{P-1} B_m \end{bmatrix}$$

$$\theta = \begin{bmatrix} C_m & 0 & 0 & 0 & 0 \\ A_m C_m & C_m & 0 & 0 & 0 \\ A_m^2 C_m & A_m C_m & C_m & 0 & 0 \\ \vdots & \vdots & \vdots & \ddots & \vdots \\ A_m^{P-1} C_m & A_m^{P-2} C_m & A_m^{P-3} C_m & \cdots & C_m \end{bmatrix}$$

Choose the performance index for the ENMSS model base PFC as

$$J(k) = Z^{\mathrm{T}} Q Z \tag{7.30}$$

where Q is the weighting matrix for the state variables.

Select the incremental PID controller as the optimization target, and the corresponding control law is

$$\begin{aligned} u(k) &= u(k-1) + k_p(k)(e_1(k) - e_1(k-1)) + k_i(k)e_1(k) \\ &\quad + k_d(k)(e_1(k) - 2e_1(k-1) + e_1(k-2)) \\ e_1(k) &= y_s - y(k) \\ e_1(k) &= \left[e_{11}(k)\ e_{12}(k) \cdots e_{1q}(k) \right]^{\mathrm{T}} \end{aligned} \tag{7.31}$$

where $k_p(k)$, $k_i(k)$, $k_d(k)$ are the relevant block diagonal matrices and the details can be referred to in Eq. (7.22).

For simplicity, the control law in Eq. (7.31) can be replaced by the following formulation

$$u(k) = u(k-1) + E(k)^{\mathrm{T}} w(k) \tag{7.32}$$

where

$$\begin{aligned} E(k) &= \begin{bmatrix} E_1(k) & 0 & 0 & \cdots 0 \\ 0 & E_2(k) & 0 & \cdots 0 \\ \vdots & \vdots & \vdots & \vdots\ \vdots \\ 0 & 0 & E_q(k) & \cdots 0 \end{bmatrix}_{3q \times p} \\ E_i(k) &= \left[e_{1i}(k)\ e_{1i}(k-1)\ e_{1i}(k-2) \right]^{\mathrm{T}} \\ w(k) &= \left[w_1(k)\ w_2(k) \cdots w_q(k) \right]^{\mathrm{T}} \\ w_i(k) &= \left[w_{i1}(k)\ w_{i2}(k)\ w_{i3}(k) \right] \end{aligned}$$

$$w_{i1}(k) = k_{pi}(k) + k_{ii}(k) + k_{di}(k); \quad w_{i2}(k) = -k_{pi}(k) - 2k_{di}(k); \quad w_{i3}(k) = k_{di}(k)$$

Based on Eqs. (7.29–7.32), the optimal control law can be derived by taking a derivative of $J(k)$

$$w(k) = E(k)(-(F^{\mathrm{T}} Q F E(k)^{\mathrm{T}} E(k))^{-1} F^{\mathrm{T}} Q(Sz(k) + \theta \Delta R)) \tag{7.33}$$

Subsequently, the relevant parameters of PID control can be obtained

$$\begin{aligned} k_{pi}(k) &= -w_{i2}(k) - 2k_{di}(k) \\ k_{ii}(k) &= w_{i1}(k) - k_{pi}(k) - k_{di}(k) \\ k_{di}(k) &= w_{i3}(k) \end{aligned} \tag{7.34}$$

Finally, the optimal control input at time instant k can be calculated.

$$\begin{aligned} u(k) = u(k-1) + k_p(k)(e_1(k) - e_1(k-1)) + k_i(k)e_1(k) \\ + k_d(k)(e_1(k) - 2e_1(k-1) + e_1(k-2)) \end{aligned} \tag{7.35}$$

Refer to Sect. 7.2.3, the following limitation is also necessary

$$\begin{cases} \begin{cases} k_{pi}(k) = k_{pi}(k-1) \\ k_{ii}(k) = k_{ii}(k-1) \quad \cdots |e_{1i}(k)| \le \delta \\ k_{di}(k) = k_{di}(k-1) \end{cases} \\ \begin{cases} k_{pi}(k) = -w_{i2}(k) - 2k_{di}(k) \\ k_{ii}(k) = w_{i1}(k) - k_{pi}(k) - k_{di}(k) \quad \cdots |e_{1i}(k)| > \delta \\ k_{di}(k) = w_{i3}(k) \end{cases} \end{cases} \tag{7.36}$$

where δ is the small permissible error.

7.3 Case Studies

7.3.1 SISO Case Study

In this section, the temperature process of an industrial surfactant reactor is considered [18], and the corresponding transfer function model is

$$G(s) = \frac{2.8\mathrm{e}^{-28\,\mathrm{s}}}{1310\,\mathrm{s} + 1} \tag{7.37}$$

In order to verify the effectiveness of the improved PID controller, the conventional PID controller adjusted by inner model control (IMC) approach [21] is employed as the comparison.

The set-point is chosen as 1, and the output disturbance with amplitude of −0.05 is added to the process output for two approaches after the temperature control system has arrived at the steady state. For the traditional PID controller tuned by IMC method, we have $K_p = 9.93$, $T_i = 1324$, $T_d = 13.85$. As to the introduced ENMSS model based MPC, $P = 15$, $M = 1$, $Q = \text{diag}(Q_1, Q_2, \ldots, Q_{15})$, $Q_j = \text{diag}(0, 0, 0, 0, 0, 1)$, $(j = 1, 2, \ldots, 15)$, $\alpha = 0$, $L = 0.01$, $\delta = 10^{-5}$.

Meanwhile, two model/plant mismatched cases caused by the inevitable disturbance and uncertainty in practice are considered to evaluate the control performance of both schemes, and the details are

Case 1:

$$G(s) = \frac{3.0\text{e}^{-30\,\text{s}}}{1441\,\text{s} + 1} \tag{7.38}$$

Case 2:

$$G(s) = \frac{2.5\text{e}^{-27\,\text{s}}}{1153\,\text{s} + 1} \tag{7.39}$$

In Figs. 7.1 and 7.2, the responses for both PID controllers under cases 1–2 are shown. From an overall perspective, the PID controller optimized by ENMSS model based MPC scheme provides better ensemble control performance. It can be easily seen that both methods achieve the set-point tracking successfully in Fig. 7.1a, however, there are bigger overshoot and oscillations in the responses of the conventional PID control method. Meanwhile, the conventional PID control shows weaker recovery capacity under disturbances, which further proves that the PID control optimized by ENMSS model based MPC gives improved control performance. In Fig. 7.2, the situations are similar to those in Fig. 7.1, and the responses of PID control optimized by ENMSS model based MPC are smoother and with better recovery ability under disturbances.

7.3.2 MIMO Case Study

The following MIMO glasshouse micro-climate process is introduced in this section

$$\begin{bmatrix} y_1(k) \\ y_2(k) \end{bmatrix} = \begin{bmatrix} \dfrac{-0.2929z^{-2}}{1 - 0.8669z^{-1}} & \dfrac{0.1237z^{-1} + 0.04935z^{-2}}{1 - 0.8669z^{-1}} \\ \dfrac{-0.05833z^{-2} - 0.2214z^{-3}}{1 - 0.9001z^{-1}} & \dfrac{0.2933z^{-1} + 0.1496z^{-2}}{1 - 0.897z^{-1}} \end{bmatrix} \begin{bmatrix} u_1(k) \\ u_2(k) \end{bmatrix} \tag{7.40}$$

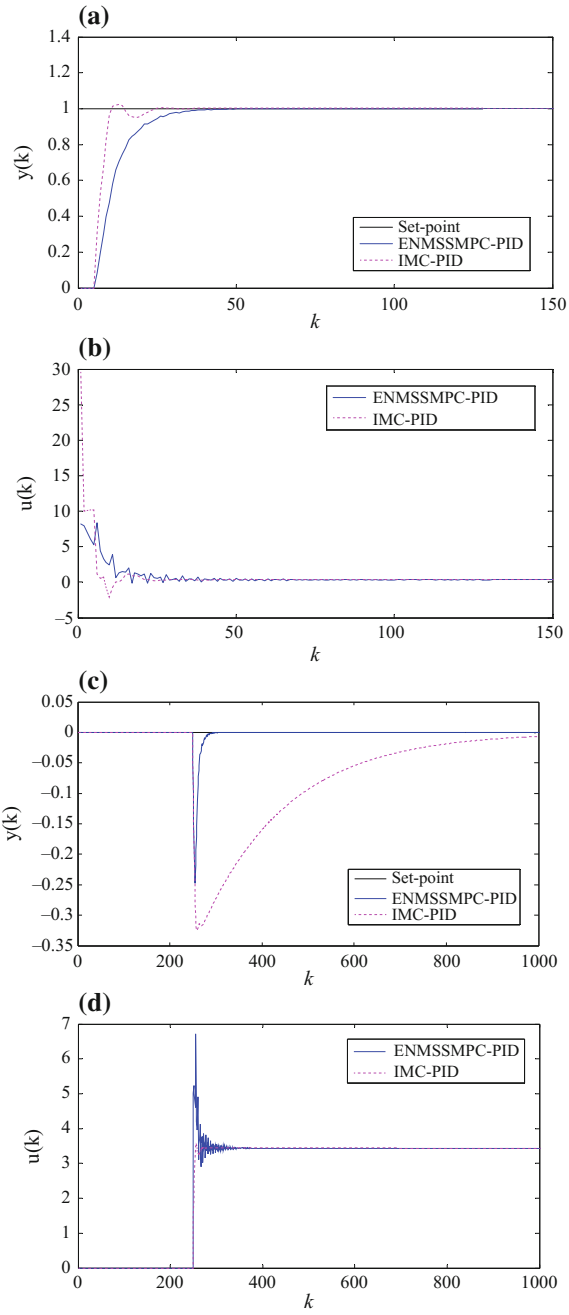

Fig. 7.1 **a** Closed-loop output responses for set-point tracking under case 1. **b** Closed-loop input responses for set-point tracking under case 1. **c** Closed-loop output responses for disturbance rejection under case 1. **d** Closed-loop input responses for disturbance rejection under case 1

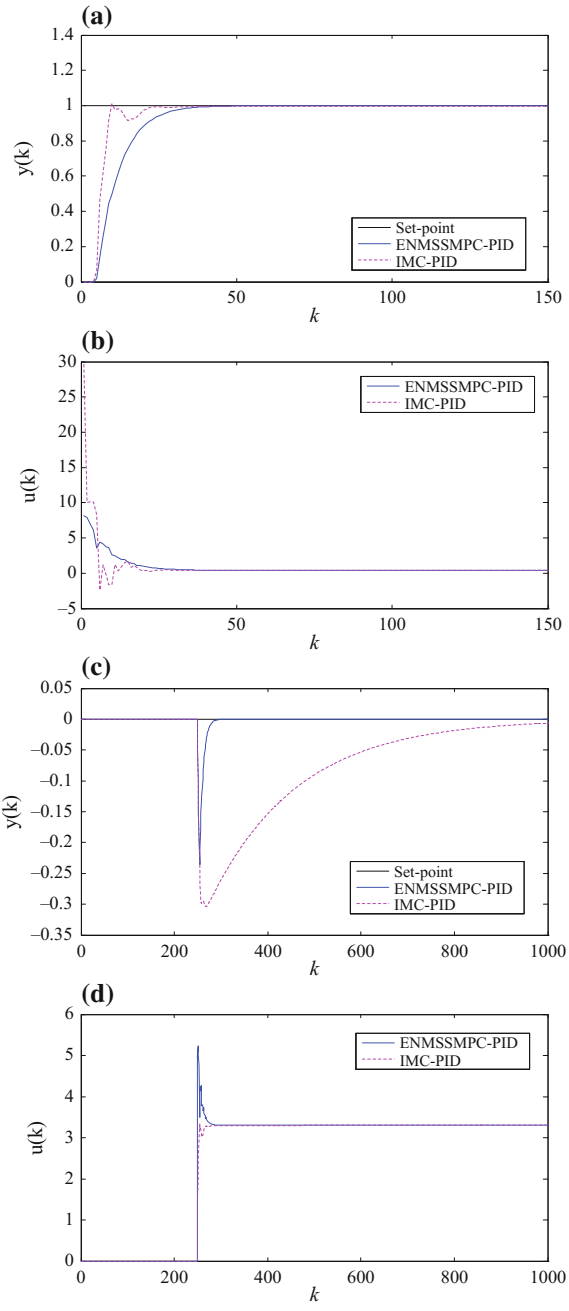

Fig. 7.2 **a** Closed-loop output responses for set-point tracking under case 2. **b** Closed-loop input responses for set-point tracking under case 2. **c** Closed-loop output responses for disturbance rejection under case 2. **d** Closed-loop input responses for disturbance rejection under case 2

Table 7.1 The control parameters for both MPC strategies

Parameters	ENMSSMPC	NMSSMPC
P	8	8
M	1	1
α	0.6	0.6
L	$L = \text{diag}(0.1, 0.1)$	$L = \text{diag}(0.1, 0.1)$
$Q = \text{diag}(Q_1, Q_2, \ldots, Q_8)$	$Q_j = \text{diag}(2, 2, 1, 1, 0, 0, 0, 0, 0, 0, 1, 1)(j = 1, 2, \ldots, 8)$	$Q_j = \text{diag}(1, 1)$ $(j = 1, 2, \ldots, 8)$
δ	10^{-6}	10^{-6}

Here, the PID controller optimized by NMSS model based MPC scheme is adopted as the comparison to test the control performance of PID controller optimized by ENMSS model based MPC, and the control parameters for both MPC methods are listed in Table 7.1.

The model/plant mismatch is also considered here, and the relevant case is

Case 3:

$$\begin{bmatrix} y_1(k) \\ y_2(k) \end{bmatrix} = \begin{bmatrix} \dfrac{-0.3056z^{-2}}{1 - 0.7899z^{-1}} & \dfrac{0.1035z^{-1} + 0.05521z^{-2}}{1 - 0.7502z^{-1}} \\ \dfrac{-0.05611z^{-2} - 0.2536z^{-3}}{1 - 0.8232z^{-1}} & \dfrac{0.3019z^{-1} + 0.1587z^{-2}}{1 - 0.7813z^{-1}} \end{bmatrix} \begin{bmatrix} u_1(k) \\ u_2(k) \end{bmatrix} \tag{7.41}$$

The responses of the two methods under case 3 are shown in Fig. 7.3. In terms of y_1, it is obvious that the responses of PID controller optimized by ENMSS model based MPC are smoother and with smaller overshoot and oscillations, which implies that improved control performance is provided by the PID controller optimized by ENMSS model based MPC. As to the responses of y_2, the situations are similar to those of y_1. The responses of PID controller optimized by NMSS model based MPC show bigger overshoot and oscillations. In a word, the PID controller optimized by ENMSS model based MPC offers better ensemble control performance.

7.4 Summary

In this chapter, the ENMSS model base MPC and PFC schemes are employed to optimize PID control. By introducing the structure of the PID control law into the framework of ENMSS model based MPC algorithm, an improved PID controller that inherits the simple structure of conventional PID control and the same control

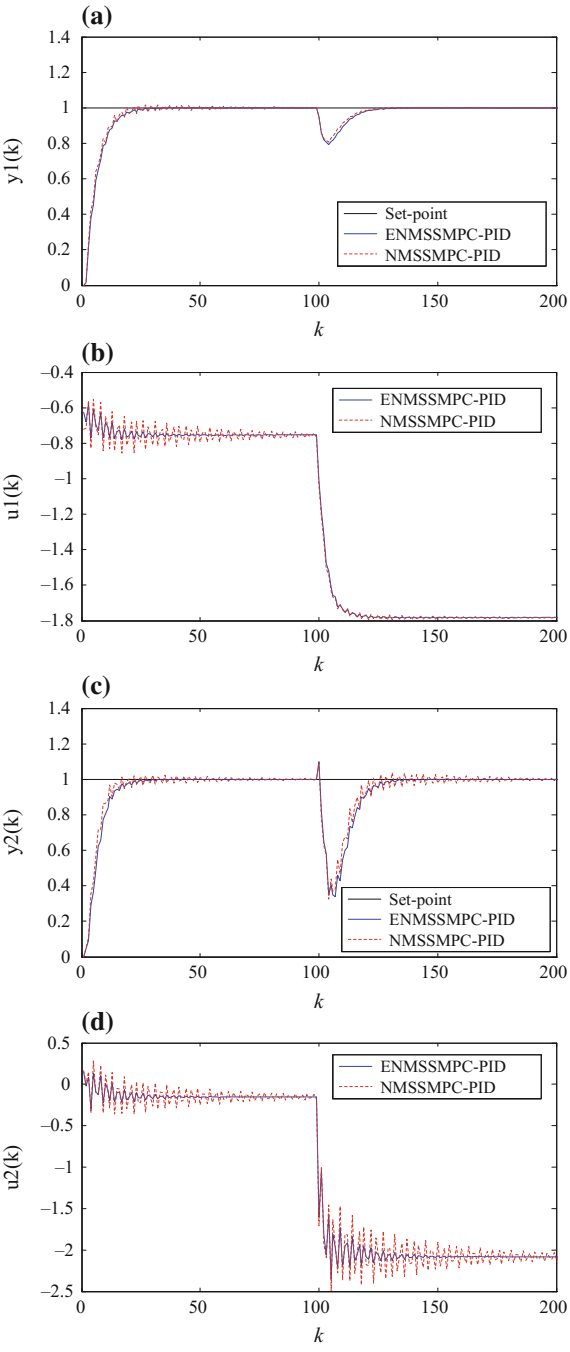

Fig. 7.3 **a** Closed-loop responses under case 3 for y_1. **b** Closed-loop responses under case 3 for u_1. **c** Closed-loop responses under case 3 for y_2. **d** Closed-loop responses under case 3 for u_2

performance of ENMSS model based MPC is developed. The effectiveness of the improved PID controller is tested on the control of a SISO industrial surfactant reactor and a MIMO glasshouse micro-climate process finally.

References

1. Bongulwar, M. R., & Patre, B. M. (2017). Design of PIλDμ controller for global power control of pressurized heavy water reactor. *ISA Transactions, 69,* 234–241.
2. Shi, C. X., & Yang, G. H. (2018). Robust consensus control for a class of multi-agent systems via distributed PID algorithm and weighted edge dynamics. *Applied Mathematics and Computation, 316,* 73–88.
3. Pachauri, N., Rani, A., & Singh, V. (2017). Bioreactor temperature control using modified fractional order IMC-PID for ethanol production. *Chemical Engineering Research and Design, 122,* 97–112.
4. Yuan, S., Zhao, C., & Guo, L. (2018). Uncoupled PID control of coupled multi-agent nonlinear uncertain systems. *Journal of Systems Science and Complexity, 31*(1), 4–21.
5. Zarei, M., Ghaderi, R., Kojuri, N., & Minuchehr, A. (2017). Robust PID control of power in lead cooled fast reactors: A direct synthesis framework. *Annals of Nuclear Energy, 102,* 200–209.
6. Shen, J., Xin, B., Cui, H. Q., & Gao, W. X. (2017). Control of single-axis rotation INS by tracking differentiator based fuzzy PID. *IEEE Transactions on Aerospace and Electronic Systems, 53*(6), 2976–2986.
7. Kuantama, E., Vesselenyi, T., Dzitac, S., & Tarca, R. (2017). PID and fuzzy-PID control model for quadcopter attitude with disturbance parameter. *International Journal of Computers Communications & Control, 12*(4), 519–532.
8. Song, Y. D., Huang, X. C., & Wen, C. Y. (2017). Robust adaptive fault-tolerant PID control of MIMO nonlinear systems with unknown control direction. *IEEE Transactions on Industrial Electronics, 64*(6), 4876–4884.
9. Zhang, R. M., Zeng, D. Q., Zhong, S. M., & Shi, K. B. (2017). Memory feedback PID control for exponential synchronisation of chaotic Lur'e systems. *International Journal of Systems Science, 48*(12), 2473–2484.
10. Soyguder, S., Karakose, M., & Alli, H. (2009). Design and simulation of self-tuning PID-type fuzzy adaptive control for an expert HVAC system. *Expert Systems with Applications, 36*(3), 4566–4573.
11. Ang, K. H., Chong, G., & Li, Y. (2005). PID control system analysis, design, and technology. *IEEE Transactions on Control Systems Technology, 13*(4), 559–576.
12. Paris, B., Eynard, J., Grieu, S., & Polit, M. (2011). Hybrid PID-fuzzy control scheme for managing energy resources in buildings. *Applied Soft Computing, 11*(8), 5068–5080.
13. Leosirikul, A., Chilin, D., Liu, J. F., Davis, J. F., & Christofides, P. D. (2012). Monitoring and retuning of low-level PID control loops. *Chemical Engineering Science, 69*(1), 287–295.
14. Khodabakhshian, A., & Hooshmand, R. (2010). A new PID controller design for automatic generation control of hydro power systems. *International Journal of Electrical Power & Energy Systems, 32*(5), 375–382.
15. Zhang, J. M. (2017). Design of a new PID controller using predictive functional control optimization for chamber pressure in a coke furnace. *ISA Transactions, 67,* 208–214.
16. Wu, S. (2015). Multivariable PID control using improved state space model predictive control optimization. *Industrial & Engineering Chemistry Research, 54*(20), 5505–5513.
17. Li, H. S., & Zhang, J. M. (2016). Improved PID design using new state space predictive functional control optimization based structure. *Chemometrics and Intelligent Laboratory Systems, 151,* 95–102.

18. Zhang, R. D., Wu, S., Lu, R. Q., & Gao, F. R. (2014). Predictive control optimization based PID control for temperature in an industrial surfactant reactor. *Chemometrics and Intelligent Laboratory Systems, 135,* 48–62.
19. Zhang, R. D., Cao, Z. X., Bo, C. M., Li, P., & Gao, F. R. (2014). New PID controller design using extended non-minimal state space model based predictive functional control structure. *Industrial & Engineering Chemistry Research, 53*(8), 3283–3292.
20. Wu, S. (2015). State space predictive functional control optimization based new PID design for multivariable processes. *Chemometrics and Intelligent Laboratory Systems, 143*(15), 16–27.
21. Rivera, D., Morari, M., & Skogestad, S. (1986). Internal model control: PID controller design. *Industrial & Engineering Chemistry Process Design and Development, 25,* 252–265.

Part II
System Performance Analysis, Optimization and Application

Chapter 8
Closed-Loop System Performance Analysis

8.1 Introduction

Compared with NMSS models, the tracking error dynamics are derived and included in ENMSS models, which provides more degrees of freedom for the design of the corresponding MPC strategies and improved control performance can be anticipated [1–3]. It is known that relevant theoretical proofs for the set-point tracking, disturbance rejection, etc., are necessary for the closed-loop system although the simulations in the foregoing chapters have indicated these facts. Meanwhile, the relationships between the ENMSS model based MPC and the NMSS model based MPC may need to be discussed to make it clear for readers.

Based on the above backgrounds, a transfer function interpretation of the ENMSS model based MPC is presented briefly in this chapter first, and the relevant proofs show that the set-point tracking and disturbance rejection are guaranteed for the closed-loop system. Then, the relationship between the ENMSS model based MPC and the NMSS model based MPC is discussed, and the conclusion that the NMSS model based MPC is a special case of ENMSS model based MPC is given finally.

8.2 Interpretations of ENMSS Model Predictive Control

In this section, a brief transfer function interpretation of ENMSS model based MPC and the relationship between ENMSS model based MPC and NMSS model based MPC are further described.

R. Zhang et al., *Model Predictive Control*,
https://doi.org/10.1007/978-981-13-0083-7_8

8.2.1 Transfer Function Interpretation [4]

Similar to the NMSS model based MPC in [5], the design of ENMSS model based MPC can also be cast in terms of transfer functions. In the following, a brief interpretation of ENMSS model based MPC is presented.

Suppose that the corresponding transfer function is $\frac{B_n(z)}{A_d(z)}$ and the order of the transfer function is n, then it is clear that the dimension of $z(k)$ is $2n$. Here, we denote the vectors k_F and k_s in Eq. (4.27) as

$$\begin{aligned} k_F &= [k_1 k_2 \dots k_n k_{n+1} k_{n+2} \dots k_{2n}] \\ k_s &= [k_{R1} k_{R2} \dots k_{RP}] \end{aligned} \tag{8.1}$$

Meanwhile, the following two polynomial functions are defined.

$$\begin{aligned} \underline{P}(z) &= k_1 + k_2 z^{-1} + k_3 z^{-2} + \dots + k_n z^{-(n-1)} \\ \underline{L}(z) &= 1 + 1_{n+1} z^{-1} + k_{n+2} z^{-2} + \dots + k_{2n-1} z^{-(n-1)} \end{aligned} \tag{8.2}$$

Select the relevant reference trajectory as follows.

$$\begin{aligned} r(k) &= y(k) \\ r(k+i) &= \alpha^i y(k) + (1-\alpha^i) y_s \\ i &= 1, 2, \dots, P \end{aligned} \tag{8.3}$$

where α is the smoothing factor of the reference trajectory, and y_s is the set-point.

Based on Eq. (8.3), we can obtain the following facts

$$\begin{aligned} r(k) &= y(k) \\ \Delta r(k+1) &= r(k+1) - r(k) \\ &= (1-\alpha)(y_s - y(k)) \\ \Delta r(k+2) &= r(k+2) - r(k+1) \\ &= \alpha(1-\alpha)(y_s - y(k)) \\ &\vdots \\ \Delta r(k+P) &= r(k+P) - r(k+P-1) \\ &= \alpha^{P-1}(1-\alpha)(y_s - y(k)) \end{aligned} \tag{8.4}$$

Further, the incremental reference trajectory in Eq. (4.22) can be rewritten as

$$\Delta R = \begin{bmatrix} (1-\alpha)(y_s - y(k)) \\ \alpha(1-\alpha)(y_s - y(k)) \\ \vdots \\ \alpha^{P-1}(1-\alpha)(y_s - y(k)) \end{bmatrix} \tag{8.5}$$

By synthesizing Eqs. (4.19), (4.27), (8.2), and (8.5), and denoting

$$k_R^{'} = k_{R1}(1-\alpha) + k_{R2}\alpha(1-\alpha) + \cdots + k_{RP}\alpha^{P-1}(1-\alpha) \tag{8.6}$$

the control law can be calculated as

$$(1-z^{-1})\underline{L}(z)U(z) = -(1-z^{-1})\underline{P}(z)Y(z) + k_R^{'}(Y_s(z) - Y(z)) \tag{8.7}$$

where $Y(z)$, $Y_s(z)$ are the z-transforms of $y(k)$ and y_s, respectively.

It is obvious that the transfer function from the set-point to the output is described as

$$\bar{T}(z) = \frac{k_R^{'} B_n(z)}{(1-z^{-1})(\underline{L}(z)A_d(z) + \underline{P}(z)B_n(z)) + k_R^{'} B_n(z)} \tag{8.8}$$

with

$$\lim_{z \to 1} \bar{T}(z) = 1 \tag{8.9}$$

indicating that the constant set-point tracking is ensured for the closed-loop system.

Meanwhile, the transfer function from the output disturbance to the output is expressed as

$$\bar{S}(z) = \frac{(1-z^{-1})\underline{L}(z)A_d(z)}{(1-z^{-1})(\underline{L}(z)A_d(z) + \underline{P}(z)B_n(z)) + k_R^{'} B_n(z)} \tag{8.10}$$

with

$$\lim_{z \to 1} \bar{S}(z) = 0 \tag{8.11}$$

and the transfer function from the input disturbance to the output is presented as

$$\bar{S}_i(z) = \frac{(1-z^{-1})\underline{L}(z)B_n(z)}{(1-z^{-1})(\underline{L}(z)A_d(z) + \underline{P}(z)B_n(z)) + k_R^{'} B_n(z)} \tag{8.12}$$

with

$$\lim_{z\to 1}\bar{S}_i(z)=0 \tag{8.13}$$

On the basis of Eqs. (8.10–8.13), it is clear that the closed-loop system can reject constant output disturbance and input disturbance completely without steady error.

From another viewpoint, Eq. (4.27) can be replaced by the following formulation

$$\begin{aligned}\Delta u(k)=&-\sum_{j=1}^{n}k_j\Delta y(k-j+1)-\sum_{j=n+1}^{2n-1}k_j\Delta u(k-j+n)-k_{2n}e(k)\\&-\sum_{j=1}^{P}k_{Rj}\Delta r(k+j)\end{aligned} \tag{8.14}$$

It can be easily seen that the integral action of the output tracking error, the state feedback, and the P-step set-points feed forward are included in the control law to enhance the dynamic performance of the closed-loop system.

8.2.2 *Relationship Between ENMSS Model Predictive Control and NMSS Model Predictive Control [6]*

The NMSS model based MPC is a special form of ENMSS model based MPC. The ENMSS model based MPC will be equal to the NMSS model based MPC if we choose $Q_j = \mathrm{diag}\{0,0,\ldots,0,0,0,\ldots 0,q_{je1},q_{je2},\ldots,q_{jeq}\}1\le j\le P$, that is, only the tracking errors are weighted in the corresponding performance index.

In the following, we will introduce some variable notations from [5] to finish the proof.

For the ENMSS model based MPC, the following objective function is adopted if we only consider the tracking errors in the controller design

$$J=\sum_{j=1}^{P}e^{\mathrm{T}}(k+j)\bar{Q}_j e(k+j)+\sum_{j=1}^{M}\Delta u^{\mathrm{T}}(k+j)L_j\Delta u(k+j) \tag{8.15}$$

where $\bar{Q}_j = \mathrm{diag}\{q_{je1},q_{je2},\ldots,q_{jeq}\}1\le j\le P, L_j(j=1,2,\ldots,M)$ are the weighting matrices for the tracking errors and the control input increments, respectively. P, M are the prediction horizon and control horizon, respectively.

By combining Eqs. (4.18–4.19), the following equation is obtained

$$e(k)=\begin{bmatrix}0_2 & I_q\end{bmatrix}\begin{bmatrix}\Delta x(k)\\ e(k)\end{bmatrix} \tag{8.16}$$

For simplicity, we define $\tilde{C}=\begin{bmatrix}0_2 & I_q\end{bmatrix}$ and the tracking error prediction as

$$E = [e(k+1), e(k+2), \cdots, e(k+P)]^{\mathrm{T}} \tag{8.17}$$

then the tracking error prediction can be presented as follows by synthesizing Eq. (4.22) with Eq. (8.16)

$$E = \widehat{C}Z = \widehat{C}Sz(k) + \widehat{C}F\Delta U + \widehat{C}\theta\Delta R \tag{8.18}$$

where

$$S = \begin{bmatrix} A \\ A^2 \\ \vdots \\ A^P \end{bmatrix}; \quad F = \begin{bmatrix} B & 0 & 0 & \cdots & 0 \\ AB & B & 0 & \cdots & 0 \\ A^2B & AB & B & \cdots & 0 \\ \vdots & \vdots & \vdots & \ddots & \vdots \\ A^{P-1}B & A^{P-2}B & A^{P-3}B & \cdots & A^{P-M}B \end{bmatrix}$$

$$\theta = \begin{bmatrix} C & 0 & 0 & 0 & 0 \\ AC & C & 0 & 0 & 0 \\ A^2C & AC & C & 0 & 0 \\ \vdots & \vdots & \vdots & \ddots & \vdots \\ A^{P-1}C & A^{P-2}C & A^{P-3}C & \cdots & C \end{bmatrix} \tag{8.19}$$

$\widehat{C}$ is the block diagonal matrix with matrix $\tilde{C}$ sitting on its diagonal.

At the same time, the performance index in Eq. (8.15) can be expressed as

$$J = E^{\mathrm{T}}\bar{Q}E + \Delta U^{\mathrm{T}}L\Delta U \tag{8.20}$$

where $\bar{Q}$ is the block diagonal matrix with matrix $\bar{Q}_j$ sitting on its diagonal, and L is the block diagonal matrix with L_j sitting on its diagonal.

By uniting Eq. (8.18) with Eq. (8.20), the optimal control law is derived as

$$\Delta U = -(F^T\widehat{C}^T\bar{Q}\widehat{C}F + L)^{-1}F^T\widehat{C}^T\bar{Q}(\widehat{C}Sz(k) + \widehat{C}\theta\Delta R) \tag{8.21}$$

From Eqs. (4.17) and (4.19), the following fact is obtained easily

$$\widehat{C}Sz(k) = \widehat{C}S\begin{bmatrix} \Delta x(k) \\ e(k) \end{bmatrix} = \widehat{C}S\begin{bmatrix} \Delta x(k) \\ y(k) - r(k) \end{bmatrix} = \widehat{C}S\begin{bmatrix} \Delta x(k) \\ y(k) \end{bmatrix} - \widehat{C}S\begin{bmatrix} 0 \\ r(k) \end{bmatrix} \tag{8.22}$$

Further, the detailed elements in $\widehat{C}S$ can be obtained by considering $\widehat{C}$ in Eq. (8.18) and S in Eq. (8.19).

$$\widehat{C}S = \begin{bmatrix} *_1 & I_q \\ *_2 & I_q \\ \vdots & \vdots \\ *_P & I_q \end{bmatrix} \tag{8.23}$$

where $*_i$, $(i = 1, 2, \ldots, P)$ are irrelevant elements for the proof.

Then, the following holds.

$$\widehat{C}S \begin{bmatrix} 0 \\ r(k) \end{bmatrix} = \begin{bmatrix} r(k) \\ r(k) \\ \vdots \\ r(k) \end{bmatrix} \tag{8.24}$$

Based on Eqs. (8.18–8.19), we can obtain

$$\widehat{C}\theta = \begin{bmatrix} -I_q & 0 & 0 & 0 \\ -I_q & -I_q & 0 & 0 \\ \vdots & \vdots & \ddots & \vdots \\ -I_q & -I_q & \cdots & -I_q \end{bmatrix} \tag{8.25}$$

and the following formulation can be obtained further

$$\widehat{C}\theta\Delta R = \begin{bmatrix} -\Delta r(k+1) \\ -\Delta r(k+1) - \Delta r(k+2) \\ \vdots \\ -\sum_{i=1}^{P} \Delta r(k+i) \end{bmatrix} \tag{8.26}$$

Meanwhile, it is obvious that

$$\begin{aligned} r(k+1) &= r(k) + \Delta r(k+1) \\ r(k+2) &= r(k+1) + \Delta r(k+2) = r(k) + \Delta r(k+1) + \Delta r(k+2) \\ &\vdots \\ r(k+P) &= r(k) + \sum_{i=1}^{P} \Delta r(k+i) \end{aligned} \tag{8.27}$$

On the basis of Eqs. (8.22), (8.24), (8.26), and (8.27), the following equation is obtained.

$$\widehat{C} S z(k) + \widehat{C} \theta \Delta R = \widehat{C} S x(k) - R \tag{8.28}$$

where

$$x(k) = \begin{bmatrix} \Delta x_m(k) \\ y(k) \end{bmatrix}; \quad R = \begin{bmatrix} r(k+1) \\ r(k+2) \\ \vdots \\ r(k+P) \end{bmatrix}$$

are the variable notations defined in [5].

At this stage, the optimal control law under the situation where only the tracking errors are considered can be calculated by substituting Eq. (8.28) into Eq. (8.21).

$$\Delta U = -(F^T \widehat{C}^T \bar{Q} \widehat{C} F + L)^{-1} F^T \widehat{C}^T \bar{Q} (\widehat{C} S x(k) - R) \tag{8.29}$$

which is just the optimal control law described in [5] by selecting the following performance index

$$J = \sum_{j=1}^{P} [y(k+j) - r(k+j)]^{\mathrm{T}} \vec{Q}_j [y(k+j) - r(k+j)] + \sum_{j=1}^{M} \Delta u^{\mathrm{T}}(k+j) L_j \Delta u(k+j) \tag{8.30}$$

This concludes the proof.

8.3 Summary

In this chapter, the transfer functional interpretation of ENMSS model based MPC is presented to analyze the corresponding closed-loop system performance first, then the relationship between the ENMSS model based MPC and NMSS model based

MPC is discussed. Furthermore, the conclusion that the NMSS model based MPC is a special case of ENMSS model based MPC is proved in detail.

References

1. Zhang, R. D., Zou, Q., Cao, Z. X., & Gao, F. R. (2017). Design of fractional order modeling based extended non-minimal state space MPC for temperature in an industrial electric heating furnace. *Journal of Process Control, 56,* 13–22.
2. Zhang, R. D., Xue, A. K., Wang, S. D., Zhang, J. M., & Gao, F. R. (2012). Partially decoupled approach of extended non-minimal state space predictive functional control for MIMO processes. *Journal of Process Control, 22*(5), 837–851.
3. Zhang, R. D., Xue, A. K., Wang, S. Q., & Zhang, J. M. (2012). An improved state-space model structure and a corresponding predictive functional control design with improved control performance. *International Journal of Control, 85*(8), 1146–1161.
4. Zhang, R. D., Xue, A. K., Wang, S. Q., & Ren, Z. Y. (2011). An improved model predictive control approach based on extended non-minimal state space formulation. *Journal of Process Control, 21*(8), 1183–1192.
5. Wang, L. P., & Young, P. C. (2006). An improved structure for model predictive control using non-minimal state space realisation. *Journal of Process Control, 16*(4), 355–371.
6. Zhang, R. D., Lu, J. Y., Qu, H. Y., & Gao, F. R. (2014). State space model predictive fault-tolerant control for batch processes with partial actuator failure. *Journal of Process Control, 24*(5), 613–620.

Chapter 9
Model Predictive Control Performance Optimized by Genetic Algorithm

9.1 Introduction

Driven by the rapid development of economy, there are challenges for MPC strategies to meet stricter and higher requirements in practice [1, 2]. In order to enhance the control performance of MPC schemes, many significant ideas are proposed, such as the introduction of novel models, the combination with other algorithms, etc. [3–8]. As to MPC approaches, the choices of the control parameters affect the corresponding control performance greatly [9–11]. However, these choices are usually based on experience and there are no specific instructions [12, 13].

For the extended state space model based MPC, the weighting matrix Q_j for the extended state vector contains more elements, meanwhile, the choices of the relevant weighting coefficients influence the dynamic performance of the system to a great extent [14, 15]. In order to obtain a better choice of Q_j, GA is employed in this chapter, and the details of the optimization of the Q_j for the extended state space PFC are presented as the example. The injection velocity control in the injection molding process under various uncertainty is introduced as the case study.

R. Zhang et al., *Model Predictive Control*,
https://doi.org/10.1007/978-981-13-0083-7_9

9.2 Extended State Space Predictive Functional Control

9.2.1 Extended State Space Model [16]

Consider a SISO process with the following state space model

$$\begin{cases} x(k+1) = \bar{A}x(k) + \bar{B}u(k-d) \\ y(k) = \bar{C}x(k) \end{cases} \tag{9.1}$$

where $x(k)$, $u(k)$, $y(k)$ are the state, control input and output at time instant k, respectively, d is the dead time. $\bar{A}$, $\bar{B}$, $\bar{C}$ are the relevant system matrices with appropriate dimensions.

By adding the difference operator Δ to Eq. (9.1), the following model is obtained.

$$\begin{cases} \Delta x(k+1) = \bar{A}\Delta x(k) + \bar{B}\Delta u(k-d) \\ \Delta y(k) = \bar{C}\Delta x(k) \end{cases} \tag{9.2}$$

Choose a new state vector as

$$\Delta x_m(k) = [\Delta x(k)\, \Delta u(k-1)\, \Delta u(k-2) \ldots \Delta u(k-d)]^T \tag{9.3}$$

then the state space model in Eq. (9.2) can be rewritten as

$$\begin{aligned} \Delta x_m(k+1) &= A_m \Delta x_m(k) + B_m \Delta u(k) \\ \Delta y(k) &= C_m \Delta x_m(k) \end{aligned} \tag{9.4}$$

where

$$A_m = \begin{bmatrix} \bar{A} & \bar{0} & \bar{0} & \cdots & \bar{0} & \bar{B} \\ \underline{0} & 0 & 0 & \cdots & 0 & 0 \\ \underline{0} & 1 & 0 & \cdots & \vdots & 0 \\ \underline{0} & 0 & 1 & 0 & 0 & \vdots \\ \vdots & \vdots & \ddots & \ddots & \ddots & \vdots \\ \underline{0} & 0 & \cdots & 0 & 1 & 0 \end{bmatrix}$$

$$B_m = [0 1 0 \ldots 0]^T$$

$$C_m = [\bar{C}\, 0\, 0 \ldots 0]$$

where $\bar{0}$, $\underline{0}$ in A_m are zero vectors with appropriate dimensions.

Here we denote the set-point as $r(k)$, then the output tracking error can be calculated as

$$e(k) = y(k) - r(k) \tag{9.5}$$

Based on Eq. (9.4), the output tracking error prediction at time instant $k + 1$ is derived as

$$e(k+1) = e(k) + C_m A_m \Delta x_m(k) + C_m B_m \Delta u(k) - \Delta r(k+1) \tag{9.6}$$

Further, the extended state vector is constructed as

$$z(k) = \begin{bmatrix} \Delta x_m(k) \\ e(k) \end{bmatrix} \tag{9.7}$$

then the corresponding extended state space model is obtained as follows

$$z(k+1) = Az(k) + B\Delta u(k) + C\Delta r(k+1) \tag{9.8}$$

where

$$A = \begin{bmatrix} A_m & 0 \\ C_m A_m & 1 \end{bmatrix};\ B = \begin{bmatrix} B_m \\ C_m B_m \end{bmatrix};\ C = \begin{bmatrix} 0 \\ -1 \end{bmatrix}$$

Here 0 in A, C are zero vectors with appropriate dimensions.

9.2.2 Controller Design

In order to achieve the set-point tracking, the following performance index is adopted

$$J = \sum_{j=1}^{P} z^T(k+j) Q_j z(k+j) \tag{9.9}$$

where P is the prediction horizon, and Q_j is the relevant weighting matrix defined as

$$Q_j = \text{diag}\{q_{jx1}, q_{jx2}, \ldots, q_{jxn}, q_{ju1}, q_{ju2}, \ldots, q_{jud}, q_{je}\}\ 1 \le j \le P \tag{9.10}$$

Note that the control law of the PFC can be presented as a linear combination of basis functions as follows

$$u(k+i) = \sum_{j=1}^{N} \mu_j f_j(i) \tag{9.11}$$

where N is the amount of the basis functions. $f_j(i)$ is the value of the basis function f_j at time instant $k+i$, and u_j is the corresponding weighting coefficient.

In order to simplify the derivation process, we define

$$\begin{aligned} T_i &= [f_1(i), f_2(i), \cdots, f_N(i)], (i = 0, 1, \cdots, P-1) \\ \Upsilon &= [\mu_1, \mu_2, \cdots, \mu_N]^T \end{aligned} \tag{9.12}$$

then the control law in Eq. (9.11) can be replaced by the following equation

$$u(k+i) = T_i \Upsilon \tag{9.13}$$

Denote

$$Z = \begin{bmatrix} z(k+1) \\ z(k+2) \\ \vdots \\ z(k+P) \end{bmatrix}, \quad \Delta R = \begin{bmatrix} \Delta r(k+1) \\ \Delta r(k+2) \\ \vdots \\ \Delta r(k+P) \end{bmatrix} \tag{9.14}$$

then the state prediction can be obtained on the basis of Eq. (9.8), and the details are

$$Z = Fz(k) - Gu(k-1) + \Phi\Upsilon + S\Delta R \tag{9.15}$$

where

$$F = \begin{bmatrix} A \\ A^2 \\ \vdots \\ A^P \end{bmatrix}, \quad G = \begin{bmatrix} B \\ AB \\ A^2B \\ \vdots \\ A^PB \end{bmatrix}, \quad S = \begin{bmatrix} C & 0 & 0 & 0 & 0 \\ AC & C & 0 & 0 & 0 \\ A^2C & AC & C & 0 & 0 \\ \vdots & \vdots & \vdots & \ddots & \vdots \\ A^{P-1}C & A^{P-2}C & A^{P-3}C & \cdots & C \end{bmatrix}$$

$$\Phi = \begin{bmatrix} BT_0 \\ (AB - B)T_0 + BT_1 \\ (A^2B - AB)T_0 + (AB - B)T_1 + BT_2 \\ \vdots \\ \sum_{k=1}^{P-1} (A^kB - A^{k-1}B)T_{P-1-k} + BT_{P-1} \end{bmatrix} \tag{9.16}$$

By combining Eq. (9.9) with Eq. (9.15), the optimal control law can be obtained by taking a derivative of the objective function J.

$$\Upsilon = -(\Phi^T Q \Phi)^{-1} \Phi^T Q(Fz(k) - Gu(k-1) + S\Delta R) \tag{9.17}$$

Further define

$$\begin{aligned} \mu_1 &= -(1, 0, \ldots, 0)(\Phi^T Q \Phi)^{-1}\ \Phi^T Q(Fz(k) - Gu(k-1) + S\Delta R) \\ &= -h_1 z(k) + h_{u1} u(k-1) - m_1 \Delta R \\ \mu_2 &= -(0, 1, \ldots, 0)(\Phi^T Q \Phi)^{-1} \Phi^T Q(Fz(k) - Gu(k-1) + S\Delta R) \\ &= -h_2 z(k) + h_{u2} u(k-1) - m_2 \Delta R \\ &\vdots \\ \mu_N &= -(0, 0, \ldots, 1)(\Phi^T Q \Phi)^{-1} \Phi^T Q(Fz(k) - Gu(k-1) + S\Delta R) \\ &= -h_N z(k) + h_{uN} u(k-1) - m_N \Delta R \end{aligned} \tag{9.18}$$

then the optimal control input is expressed as

$$u(k) = \sum_{j=1}^{N} \mu_j f_j(0) = -Hz(k) + H_u u(k-1) - M\Delta R \tag{9.19}$$

where

$$\begin{aligned} H &= \sum_{j=1}^{N} f_j(0) h_j \\ H_u &= \sum_{j=1}^{N} f_j(0) h_{uj} \\ M &= \sum_{j=1}^{N} f_j(0) m_j \end{aligned} \tag{9.20}$$

9.3 Optimization by Genetic Algorithm [17]

It is obvious that the elements in Q_j are important for the dynamic performance and a better selection of Q_j in the relevant performance index brings improved ensemble control performance. In order to obtain the good control performance for PFC, it is necessary to make a compromise between these elements. In this section, GA is introduced to optimize the choice of Q_j. Note that the weighting coefficient for the tracking error $q_{j\,e}$ can be chosen as a constant to simplify the optimization process. Here, $q_{j\,e}$ is selected as 1. At the same time, the weighting elements on the past control inputs $q_{j\,u1}, q_{j\,u2}, \ldots, q_{j\,ud}$ are not considered, due to the fact that the PFC approach generally requires a fast response, thus the optimization of the selection of $q_{j\,x1}, q_{j\,x2}, \ldots, q_{j\,xn}$ is the target that needs to be focused on.

9.3.1 Encoding Approach in Genetic Algorithm

It is known that all the elements can be obtained by the binary encoding approach in GA. Here, a ten-bit binary code is adopted as an example as follows.

$$|1\,|0\,|0\,|1\,|1\,|1\,|0\,|1\,|1\,|1| \tag{9.21}$$

Based on the following formulation, the elements $q_{j\,x1}, q_{j\,x2}, \ldots, q_{j\,xn}$ in Eq. (9.10) can be obtained.

$$q_{ji} = \max(q_{ji}) * b/2^{10}\ (i = 1, 2, \ldots, n) \tag{9.22}$$

9.3.2 Goal of $\mathbf{Q_j}$ *Optimization*

Overshoot and rise time are important indexes for the controlled system. In this section, the following objective is employed to anticipate both small overshoot and short rise time.

$$Min \quad o(t) + tr(t) \tag{9.23}$$

where $o(t)$, $tr(t)$are the overshoot and rise time, respectively.

For simplicity, the fitness function of GA is denoted as follows

$$Max \quad 1/[c + o(t) + tr(t)] \tag{9.24}$$

where c is a fixed value.

9.3.3 Operators in Genetic Algorithm

(1) Selection operators
Fitness value is the index for the selection of individuals in the current population for reproduction, and bigger fitness value brings bigger possibility for survival. Here, the Roulette wheel approach is introduced to obtain the possibility of an individual being chosen, and the details are

$$P(c_l) = \frac{f(c_l)}{\sum_{l=1}^{N} f(c_l)} \tag{9.25}$$

where $P(c_l)$ is the possibility for individual c_l being chosen, and $f(c_l)$ is the relevant fitness value. N is the amount of individuals.

(2) Crossover and mutation operators
When the crossover operation and mutation operation, p_c and p_m, are executed for individuals c_u and c_v, the offspring chromosomes c'_u, c'_v can be produced.

After the aforementioned steps, an appropriate selection of Q_j will be obtained.

9.4 Case Study

In this section, an injection molding process containing three stages, filling, packing, and cooling, is introduced [18]. Here, the injection velocity that is a key index for the quality of products in the filling stage is selected to be controlled at the given set-point.

The response of the injection velocity to the proportional value is modeled as

$$P(z) = \frac{1.69z + 1.419}{z^2 - 1.582z + 0.5916} \tag{9.26}$$

The set-point adopts the following forms

$$\begin{aligned} r(k) &= 15 \quad (\text{for} 1 \leq k < 40) \\ r(k) &= 30 \quad (\text{for} 51 \leq k < 80) \end{aligned} \tag{9.27}$$

Here, the state space predictive functional control (SSPFC) in [16] is employed as the comparison to test the control performance of GA optimization based SSPFC. For both methods, the general parameters are chosen as $P = 4$ and $q_{j\,e} = 1$. Note that the output changes $\Delta y(k)$ can be weighted additionally, and the weighting coefficient on $\Delta y(k)$, i.e., $q_{j\,x1}$ for SSPFC is determined based on experience, however, $q_{j\,x1}$ for the GA based SSPFC is selected through GA optimization. Refer to [16], $q_{j\,x1}$ is chosen as 2 for SSPFC method.

In order to verify the control performance of the GA optimization based SSPFC further, the partial actuator fault and unknown disturbance are considered in this section, and the details will be shown in the next subsection.

9.4.1 Constant Fault and Non-repetitive Unknown Disturbance

Here, three cases of constant faults are generated, and a random white noise of standard deviation 0.2 is added to the process output for both strategies.

Case 1. $\alpha = 0.65$
Case 2. $\alpha = 0.45$
Case 3. $\alpha = 0.25$

The parameters of GA are chosen as: the population size is 20, the crossover probability is 0.8, and the mutation probability is 0.05. Meanwhile, GA is optimized for 10 generations. Under such control parameters, the optimized results of $q_{j\,x1}$ are 2.52, 5.43, and 9.82 for the three cases, respectively.

Figures 9.1, 9.2, and 9.3 show the responses of both schemes under cases 1–3. In Fig. 9.1, we can easily see that the responses of the two approaches are very similar, due to the fact that the weighting coefficients $q_{j\,x1}$ are similar for the two methods, which are 2 and 2.52, respectively. Both methods achieve the set-point tracking successfully, but there are slight overshoots for SSPFC. From Figs. 9.2 and 9.3, it is obvious that the ensemble control performance of the GA optimization based SSPFC is better because there are bigger overshoots and more drastic oscillations in the responses of SSPFC. Meanwhile, the GA optimization based SSPFC shows smoother input signals in Figs. 9.1b and 9.3b, which verifies its improved control performance further.

9.4.2 Time-Varying Fault and Non-repetitive Unknown Disturbance

In this section, three cases of time-varying actuator fault are introduced as follows:

Case 4. $\alpha = 0.5 + 0.01\ \sin(k)$
Case 5. $\alpha = 0.5 + 0.1\ \sin(k)$
Case 6. $\alpha = 0.5 + 0.2\ \sin(k)$

Here, the white noise sequence and the control parameters of GA are the same as those in Sect. 9.4.1. Through GA optimization, the optimal values of $q_{j\,x1}$ for the three cases are 3.33, 4.30, and 4.46, respectively.

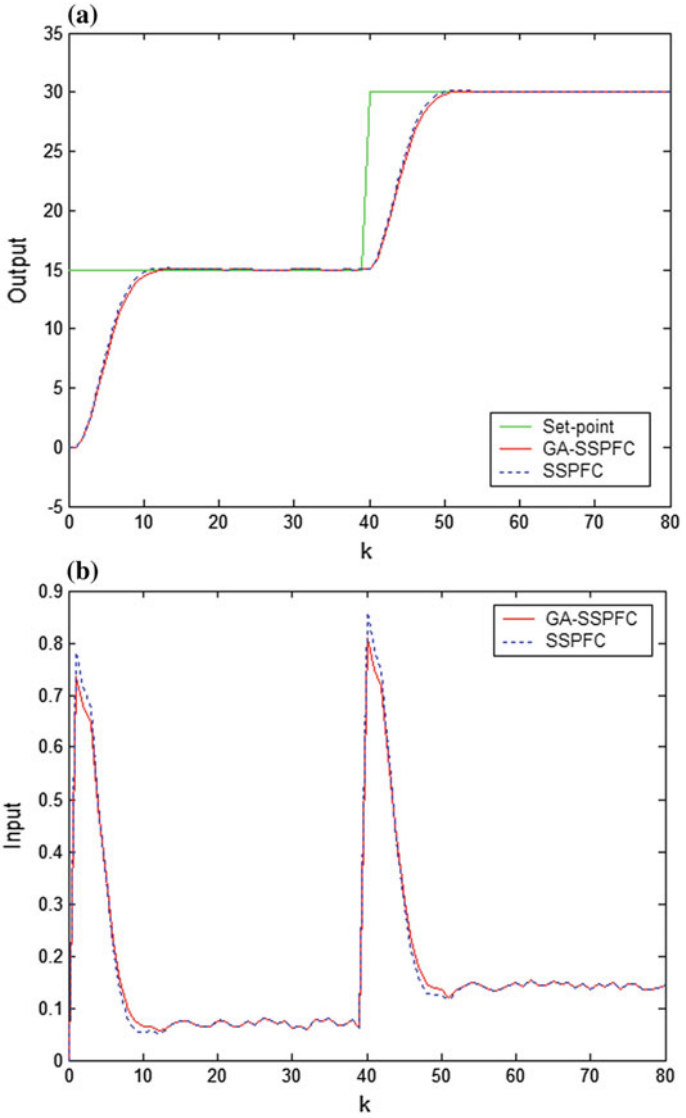

Fig. 9.1 **a** Output responses for both methods under case 1. **b** Input signals for both methods under case 1

Figures 9.4, 9.5, and 9.6 show the responses of both methods for cases 4–6. From an overall perspective, the GA optimization based SSPFC provides improved ensemble control performance. In Fig. 9.4a, it can be easily seen that the responses

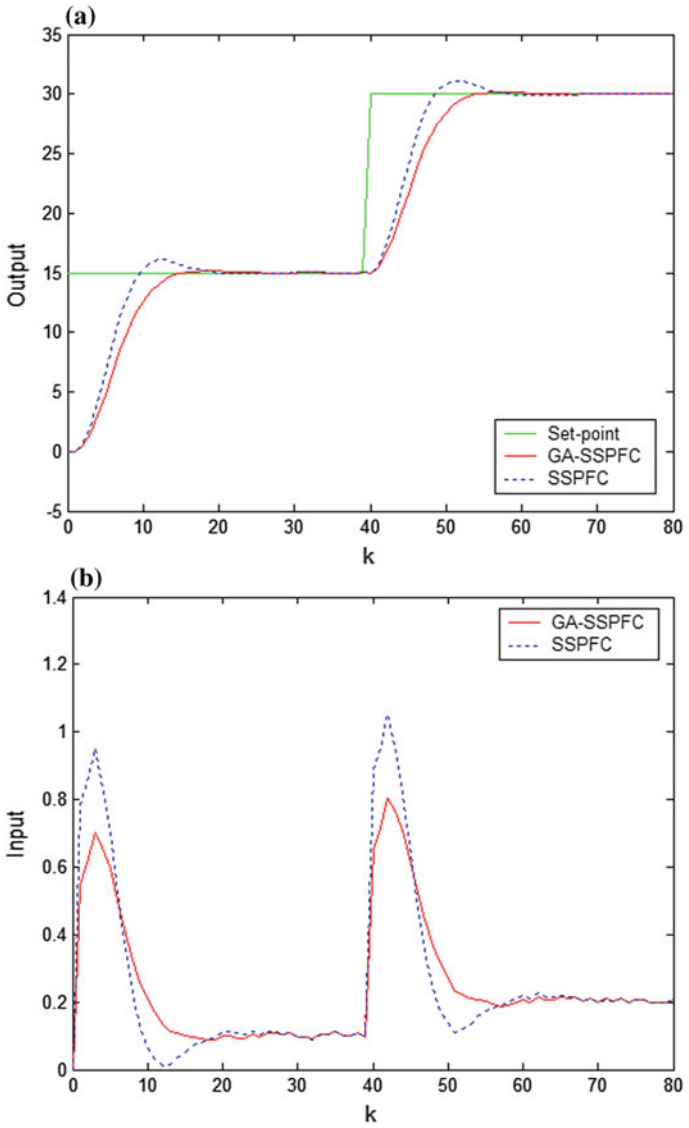

Fig. 9.2 **a** Output responses for both strategies under case 2. **b** Input signals for both strategies under case 2

of SSPFC show bigger overshoots. The situations in Figs. 9.5 and 9.6 are similar to those in Figs. 9.4, i.e., the GA optimization based SSPFC yields smoother responses with smaller overshoots in both output signals and input signals.

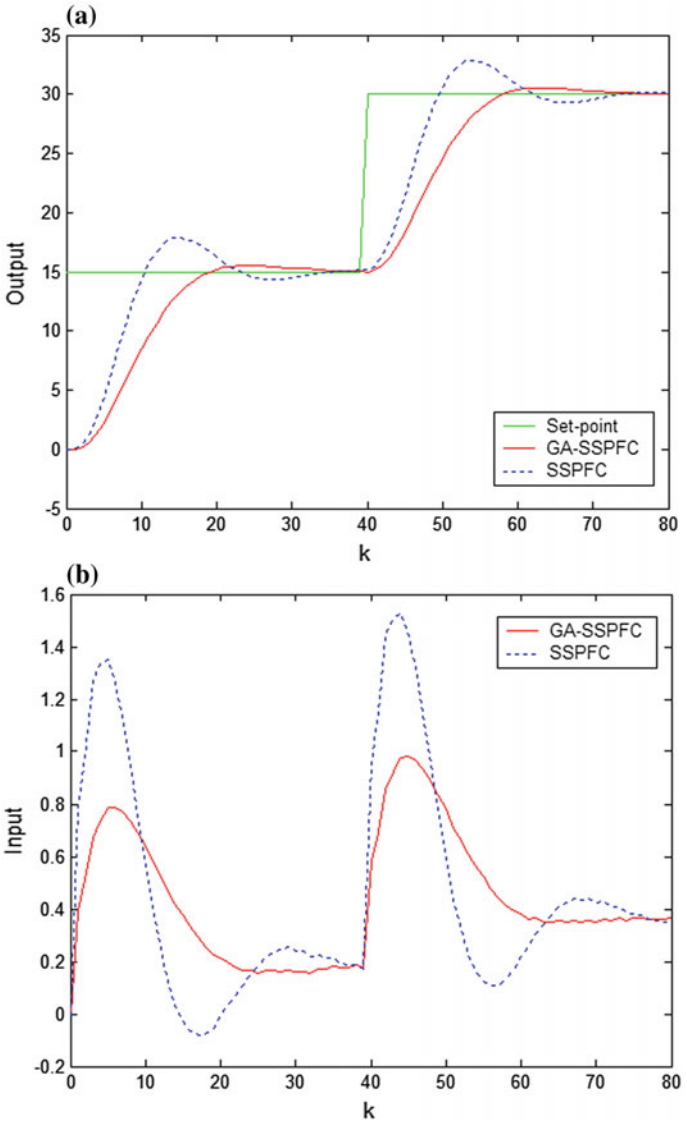

Fig. 9.3 **a** Output responses for both approaches under case 3. **b** Input signals for both approaches under case 3

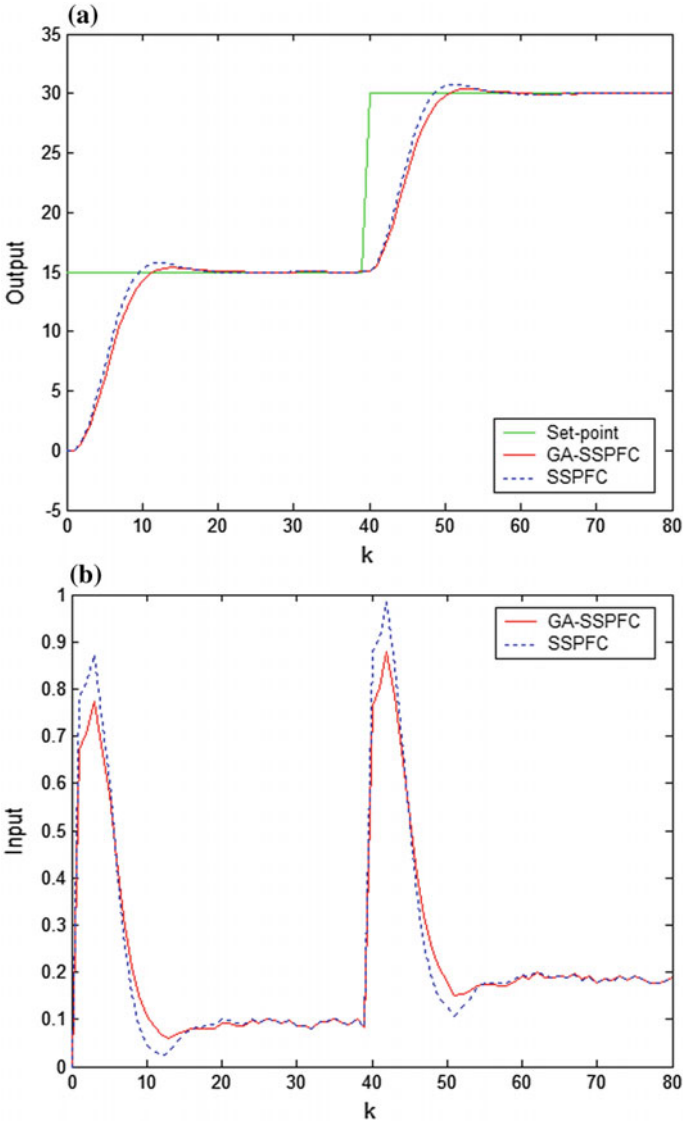

Fig. 9.4 **a** Output responses for two strategies under case 4. **b** Input signals for two strategies under case 4

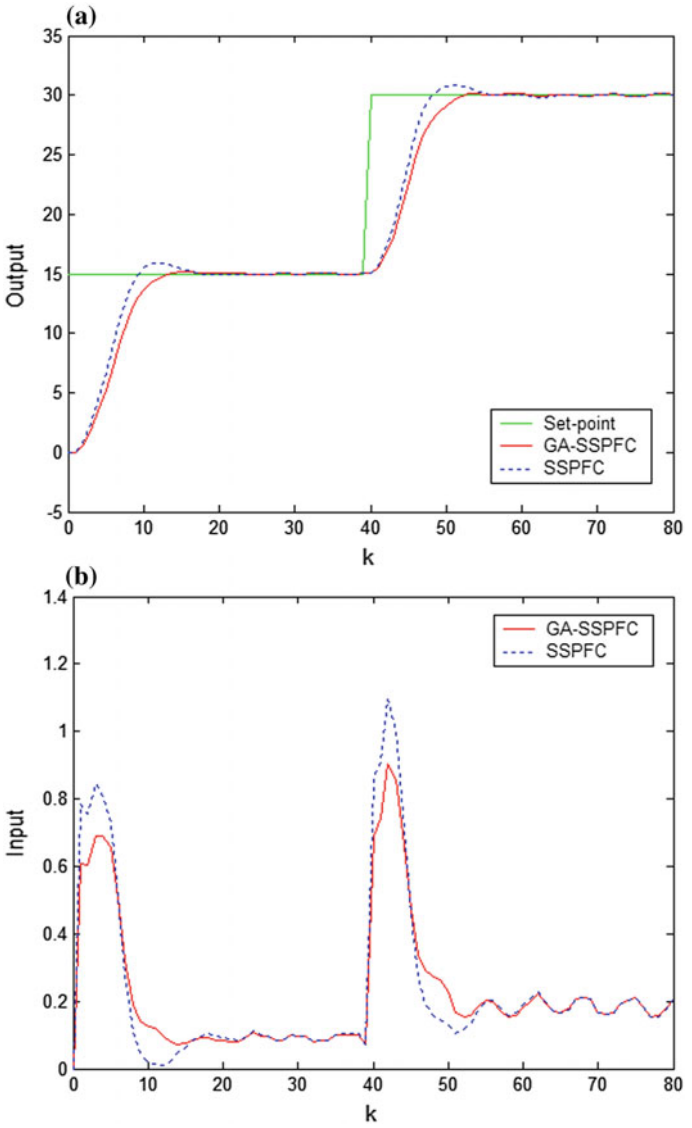

Fig. 9.5 **a** Output responses for two schemes under case 5. **b** Input signals for two schemes under case 5

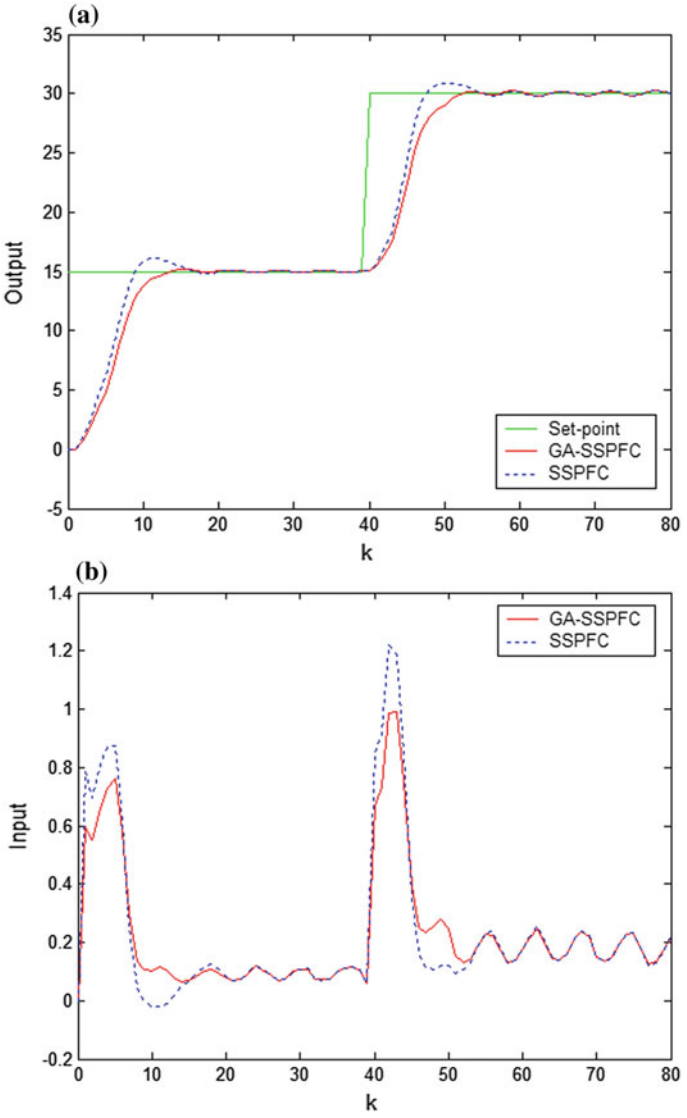

Fig. 9.6 **a** Output responses for two approaches under case 6. **b** Input signals for two approaches under case 6

9.5 Summary

In this chapter, GA is adopted to optimize the selection of the weighting matrix and tested on the extended state space based PFC. By employing the optimized weighting coefficients, improved ensemble control performance with small overshoot and short rise time is anticipated for the corresponding PFC. The case study on the injection velocity regulation in the injection molding process under partial actuator fault and unknown disturbances demonstrates the effectiveness.

References

1. Dragicevic, T. (2018). Model predictive control of power converters for robust and fast operation of AC microgrids. *IEEE Transactions on Power Electronics, 33*(7), 6304–6317.
2. Dias, L. S., Pattison, R. C., Tsay, C., Baldea, M., & Ierapetritou, M. G. (2018). A simulation-based optimization framework for integrating scheduling and model predictive control, and its application to air separation units. *Computers & Chemical Engineering, 113,* 139–151.
3. Morstyn, T., Hredzak, B., Aguilera, R. P., & Agelidis, V. G. (2018). Model predictive control for distributed microgrid battery energy storage systems. *IEEE Transactions on Control Systems Technology, 26*(3), 1107–1114.
4. Papangelis, L., Debry, M. S., Prevost, T., Panciatici, P., & Van Cutsem, T. (2018). Decentralized model predictive control of voltage source converters for AC frequency containment. *International Journal of Electrical Power & Energy Systems, 98,* 342–349.
5. Huang, J. J., Yang, B., Guo, F. H., Wang, Z. F., Tong, X. Q., Zhang, A. M., et al. (2018). Priority sorting approach for modular multilevel converter based on simplified model predictive control. *IEEE Transactions on Industrial Electronics, 65*(6), 4819–4830.
6. Wang, X. F., Yang, L. X., Sun, Y., & Deng, K. (2017). Adaptive model predictive control of nonlinear systems with state-dependent uncertainties. *International Journal of Robust and Nonlinear Control, 27*(17), 4138–4153.
7. Gholaminejad, T., Khaki-Sedigh, A., & Bagheri, P. (2017). Direct adaptive model predictive control tuning based on the first-order plus dead time models. *IET Control Theory and Applications, 11*(16), 2858–2869.
8. Geyer, T., & Quevedo, D. E. (2015). Performance of multistep finite control set model predictive control for power electronics. *IEEE Transactions on Power Electronics, 30*(3), 1633–1644.
9. Albalawi, F., Durand, H., & Christofides, P. D. (2017). Process operational safety using model predictive control based on a process Safeness Index. *Computers & Chemical Engineering, 104,* 76–88.
10. Wang, Z. M., & Ong, C. J. (2017). Distributed model predictive control of linear discrete-time systems with local and global constraints. *Automatica, 81,* 184–195.
11. Bo, T. I., & Johansen, T. A. (2017). Battery power smoothing control in a marine electric power plant using nonlinear model predictive control. *IEEE Transactions on Control Systems Technology, 25*(4), 1449–1456.
12. Xu, Q. Q., & Dubljevic, S. (2017). Linear model predictive control for transport-reaction processes. *AIChE Journal, 63*(7), 2644–2659.
13. Johansen, T. A. (2017). Toward dependable embedded model predictive control. *IEEE Systems Journal, 11*(2), 1208–1219.
14. Zhang, R. D., & Gao, F. R. (2015). An improved decoupling structure based state space MPC design with improved performance. *Systems & Control Letters, 75,* 77–83.
15. Zhang, R. D., Zou, Q., Cao, Z. X., & Gao, F. R. (2017). Design of fractional order modeling based extended non-minimal state space MPC for temperature in an industrial electric heating furnace. *Journal of Process Control, 56,* 13–22.

16. Zhang, R. D., Lu, R. Q., Xue, A. K., & Gao, F. R. (2014). Predictive functional control for linear systems under partial actuator faults and application on an injection molding batch process. *Industrial & Engineering Chemistry Research, 53*(2), 723–731.
17. Zhang, R. D., Zou, H. B., Xue, A. K., & Gao, F. R. (2014). GA based predictive functional control for batch processes under actuator faults. *Chemometrics and Intelligent Laboratory Systems, 137*(15), 67–73.
18. Zhang, R. D., Lu, J. Y., Qu, H. Y., & Gao, F. R. (2014). State space model predictive fault-tolerant control for batch processes with partial actuator failure. *Journal of Process Control, 24*(5), 613–620.

Chapter 10
Industrial Application

10.1 Introduction

Industrial products play a vital role in our daily life, such as various fuels, plastics, etc. [1, 2]. In order to maintain the normal production of these products, the effective control of corresponding industrial processes is necessary. It is known that MPC strategies have been applied to industrial processes for years and significant profits have been obtained [3–7]. To test the control performance of the ENMSS model based MPC, the outlet temperature control and the oxygen content control in the coke furnace are introduced as examples in this chapter.

As to the coke furnace, many petrochemical products can be obtained from the coking process in it. In the coking process, the quality of the final products and the coking rate are influenced by the outlet temperature and oxygen content of the coke furnace [8, 9]. Due to the fact that temperature regulation process and air supply system are complex, which are affected by various uncertainty, the ideal control performance may not be obtained by the application of conventional PID control [10–15]. In this chapter, the input–output process data of the outlet temperature process and air supply system are collected first, then the relevant ENMSS models are constructed. Finally, the corresponding MPC schemes are designed for these processes, and the experimental results demonstrate the effectiveness.

10.2 The Application of ENMSS Model Predictive Control

10.2.1 Process Flow of Coke Furnace [16, 17]

In Fig. 10.1, the flow of the coke furnace (F101/3) is presented in detail. First, the residual oil is separated into two flows (FRC8103/4) and preheated in the convection room, then the divided flows will join together and go into the fractionating tower (T102). In the fractionating tower, the preheated oil will exchange heat with the gas

R. Zhang et al., *Model Predictive Control*,
https://doi.org/10.1007/978-981-13-0083-7_10

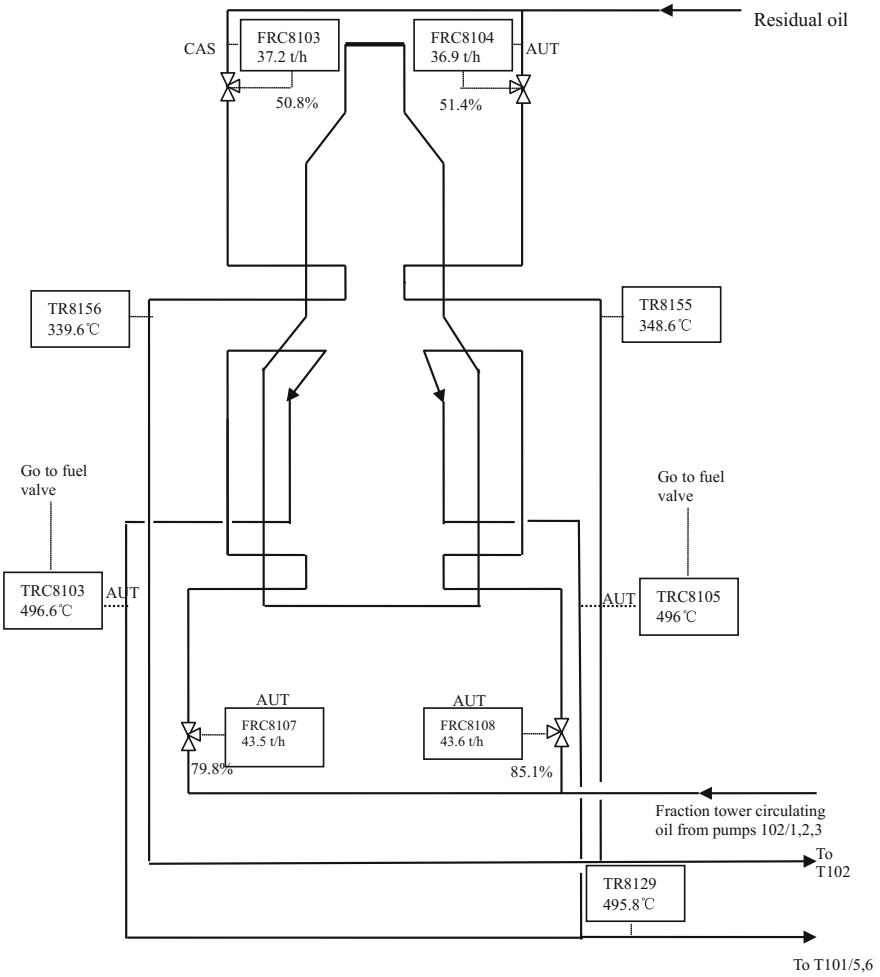

Fig. 10.1 Process flow of coking furnace (101/3)

oil. After that, the heavy part of them, which is called circulating oil, is pumped into two flows (FRC8107/8) and sent to the radiation room. Subsequently, they will be heated to about 495 °C and mixed again. Finally, they will be sent to the coke towers (T101/5, 6) for coke removal. Note that when one of the coke towers is full, it will be replaced by the other, which is known as the coke tower switches.

10.2.2 Control Targets

As to the outlet temperature process, the outlet temperature variables (TRC8103/5) of the radiation room are the controlled variables and the fuel volumes supplied to the furnace are the corresponding manipulated variables. Note that disturbance and various uncertainty exist inevitably such that the accurate relationship between them is hard to be obtained. For example, due to the significant change of the volume of the circulating oil, the temperature is affected by the corresponding heat exchange in the fractionating tower (T102) to some extent. Meanwhile, the temperature is also influenced by the changes of the volume of gas oil and circulating oil, which are caused by the coking of residues in the coke towers and the coke tower switches, respectively.

For the air supply system, the accurate relationship between the air flow and the oxygen content is also difficult to be obtained due to the nonlinearity in the process caused by inevitable uncertainty and disturbances, such as variations in the circulating oil temperature, the residual oil flow changes, the switch of coke towers, the coke removal in the coke towers, and so on. The switch of the coke tower is the most difficult stage during operation because the volume of gas oil going into the fractionating tower drops drastically and the variations of oxygen content are significant, such that the action of PID controller for the fuel volumes is also drastic.

For these complex systems, the employment of traditional methods to achieve accurate and steady control is difficult. It is known that abrupt disturbance can be handled by PID control, hence the master–slave architecture can be adopted in these processes. Under such architecture, MPC provides the set-point for the PID controller, and the target is to let the controlled variable (the outlet temperature and oxygen content for the aforementioned processes, respectively) track the given value as close as possible. Here, the original PID controllers are implemented through the modules in the CENTUM CS3000 control system.

10.2.3 Modeling

It is a fact that the relevant model will be complex if we consider all the influences. For simplicity of the controller design, constructing a simple model that contains the main process dynamics is common practice. In this section, the first-order plus dead time (FOPDT) model is introduced using the experimental test, and the details are as follows.

$$G(s) = \frac{K\mathrm{e}^{-\tau s}}{T_s + 1} \tag{10.1}$$

where K, T, τ are the steady state gain, the time constant, and the dead time of the process, respectively.

As to the three model parameters, the relevant identification method can be referred to in many textbooks [18, 19]. Through the division of the steady value of the process output with the control input change, K is obtained. Based on several approaches, such as "Time for 63.2% Approach to New Steady State", "Two-point Method", and "Maximum Slope Method", T and τ can be derived. Here, the "Two-point Method" is chosen to calculate T and τ. Meanwhile, the two time points are selected on the basis of the process output values, which is different from the method in [19]. Under such situations, the derivations of the model parameters are simpler, and the corresponding derivation process is described as follows.

Denote $y(t)$as the outlet temperature variable whose steady-state value is $y(\infty)$ and U_0 as the step input, then the steady-state gain of the process is calculated as $K = y(\infty)/U_0$.

Based on the FOPDT model in Eq. (10.1), $y(t)$ can be obtained.

$$y(t) = \begin{cases} 0 & t < \tau \\ K - K\mathrm{e}^{-\frac{t-\tau}{T}} & t \geq \tau \end{cases} \tag{10.2}$$

Select two sampling time points $t_2 > t_1 > \tau$, then the following holds.

$$\begin{aligned} y(t_1) &= K - Ke^{-\frac{t_1-\tau}{T}} \quad t \geq \tau \\ y(t_2) &= K - Ke^{-\frac{t_2-\tau}{T}} \quad t \geq \tau \end{aligned} \tag{10.3}$$

Further, we can obtain the following equations

$$\begin{aligned} T &= \frac{t_2 - t_1}{\ln[1 - y(t_1)/K] - \ln[1 - y(t_2)/K]} \\ \tau &= \frac{t_2 \ln[1 - y(t_1)/K] - t_1 \ln[1 - y(t_2)/K]}{\ln[1 - y(t_1)/K] - \ln[1 - y(t_2)/K]} \end{aligned} \tag{10.4}$$

Finally, T and τ can be obtained by choosing $y(t_1) = 0.39\ K$ and $y(t_2) = 0.63\ K$.

$$\begin{aligned} T &= 2(t_2 - t_1) \\ \tau &= 2t_1 - t_2 \end{aligned} \tag{10.5}$$

10.2.4 Controller Design

For the FOPDT model in Eq. (10.1), its discrete form under sampling time T_s is

$$y(k+1) + Fy(k) = Hu(k - L) \tag{10.6}$$

where $y(k)$, $u(k - L)$ are the output variable and input variable at corresponding time instants, respectively. F, H, L are the relevant coefficients calculated as follows.

$$\begin{aligned} F &= -\exp(-T_s/T) \\ H &= K(1+F) \\ L &= \tau/T_s \end{aligned} \tag{10.7}$$

By adding the difference operator $\Delta = 1 - z^{-1}$ to Eq. (10.6), the following equation is obtained.

$$\Delta y(k+1) + F\Delta y(k) = H\Delta u(k-L) \tag{10.8}$$

Construct a state vector as

$$\Delta x_m(k)^{\mathbf{T}} = [\Delta y(k), \Delta u(k-1), \Delta u(k-2), \ldots, \Delta u(k-L)] \tag{10.9}$$

then the corresponding state space model is obtained.

$$\begin{aligned} \Delta x_m(k+1) &= A_m \Delta x_m(k) + B_m \Delta u(k) \\ \Delta y(k+1) &= C_m \Delta x_m(k+1) \end{aligned} \tag{10.10}$$

where

$$A_m = \begin{bmatrix} -F & 0 & \cdots & 0 & H \\ 0 & \cdots & \cdots & \cdots & 0 \\ 0 & 1 & 0 & \cdots & 0 \\ \vdots & \vdots & \ddots & \ddots & \vdots \\ 0 & \cdots & 0 & 1 & 0 \end{bmatrix}, B_m = \begin{bmatrix} 0 \\ 1 \\ 0 \\ \vdots \\ 0 \end{bmatrix}, C_m = [1\ 0\ 0 \cdots 0] \tag{10.11}$$

Define the set-point as $r(k)$, then the output tracking error can be described as

$$e(k) = y(k) - r(k) \tag{10.12}$$

By combining Eq. (10.10) and Eq. (10.12), the output tracking error prediction $e(k+1)$ is derived as

$$e(k+1) = e(k) + C_m A_m \Delta x_m(k) + C_m B_m \Delta u(k) - \Delta r(k+1) \tag{10.13}$$

Further, we define an extended state vector as

$$z(k) = \begin{bmatrix} \Delta x_m(k) \\ e(k) \end{bmatrix} \tag{10.14}$$

then the relevant ENMSS model is

$$z(k+1) = Az(k) + B\Delta u(k) + C\Delta r(k+1) \tag{10.15}$$

where

$$A = \begin{bmatrix} A_m & 0 \\ C_m A_m & 1 \end{bmatrix}, \quad B = \begin{bmatrix} B_m \\ C_m B_m \end{bmatrix}, \quad C = \begin{bmatrix} 0 \\ -1 \end{bmatrix} \tag{10.16}$$

Here 0 in A, C are zero vectors with appropriate dimensions.

In order to achieve set-point tracking for the ENMSS model based MPC, the following objective function is adopted.

$$\begin{aligned} J = &\sum_{j=1}^{N_y} z^{\mathrm{T}}(k+j) Q_j z(k+j) + \sum_{j=1}^{N_u} \Delta u^{\mathrm{T}}(k+j-1) L_j \Delta u(k+j-1) \\ &\text{s.t.} \quad \Delta u(k+j) = 0 \quad j \geq N_u \end{aligned} \tag{10.17}$$

where N_y, N_u are the prediction horizon and control horizon, respectively. $z(k+j)$ is the relevant state prediction. Q_j is the weighting matrix for the state variables, and L_j is the weighting coefficient for the control input increment. Note that Q_j takes the following form

$$Q_j = \mathrm{diag}\{q_{jy}, q_{ju1}, \cdots, q_{juL}, q_{je}\}, 1 \leq j \leq N_y \tag{10.18}$$

Denote

$$Z = \begin{bmatrix} z(k+1) \\ z(k+2) \\ \vdots \\ z(k+N_y) \end{bmatrix}, \quad \Delta U = \begin{bmatrix} \Delta u(k) \\ \Delta u(k+1) \\ \vdots \\ \Delta u(k+N_u-1) \end{bmatrix}, \Delta R = \begin{bmatrix} \Delta r(k+1) \\ \Delta r(k+2) \\ \vdots \\ \Delta r(k+N_y) \end{bmatrix} \tag{10.19}$$

then the state prediction based on Eq. (10.15) is

$$Z = Fz(k) + \Phi \Delta U + S \Delta R \tag{10.20}$$

where

$$\Phi = \begin{bmatrix} B & 0 & 0 & \cdots & 0 \\ AB & B & 0 & \cdots & 0 \\ A^2 B & AB & B & \cdots & 0 \\ \vdots & \vdots & \vdots & \ddots & \vdots \\ A^{N_y-1} B & A^{N_y-2} B & A^{N_y-3} B & \cdots & A^{N_y-N_u} B \end{bmatrix}; \quad F = \begin{bmatrix} A \\ A^2 \\ \vdots \\ A^{N_y} \end{bmatrix}$$

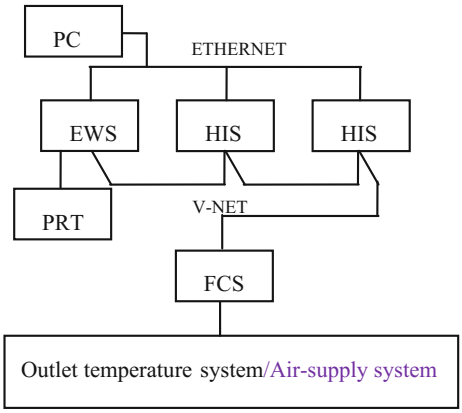

Fig. 10.2 Automation system of the outlet temperature system/air supply system

$$S = \begin{bmatrix} C & 0 & 0 & 0 & 0 \\ AC & C & 0 & 0 & 0 \\ A^2C & AC & C & 0 & 0 \\ \vdots & \vdots & \vdots & \ddots & \vdots \\ A^{N_y-1}C & A^{N_y-2}C & A^{N_y-3}C & \dots & C \end{bmatrix}$$

By synthesizing Eqs. (10.17) and (10.20) and taking a derivative of the cost function J, the optimal control law is derived as

$$\Delta U = -(\Phi^{\mathbf{T}} Q \Phi + L)^{-1} \Phi^{\mathbf{T}} Q (Fz(k) + S\Delta R) \tag{10.21}$$

where

$$Q = \text{block diag}\{Q_1, Q_2, \dots, Q_{N_y}\}$$
$$L = \text{block diag}\{L_1, L_2, \dots, L_{N_u}\}$$

10.2.5 Experiment Results [20, 21]

The experiments are completed using CENTUM CS3000 Distributed Control System (DCS) shown in Fig. 10.2. Here, the DCS consists of industrial field control stations (FCS), two human interface stations (HIS), an engineering station (EWS), a monitor computer (PC), a printer (PRT), and many I/O modules.

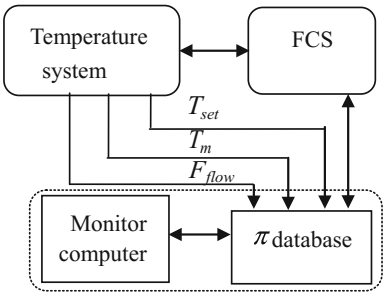

Fig. 10.3 Data acquisition configuration for outlet temperature system

Table 10.1 Transfer function models

Group 1	Group 2
A: $G_1(s) = \frac{1.15e^{-120s}}{400s+1}$	C: $G_3(s) = \frac{0.96e^{-140s}}{500s+1}$
B: $G_2(s) = \frac{0.85e^{-150s}}{600s+1}$	D: $G_4(s) = \frac{1.1e^{-150s}}{300s+1}$

10.2.5.1 Control of Outlet Temperature System

Select the outlet temperature set-point of the PID as the input and the measured outlet temperature as the output, the generalized process is modeled as a SISO model that can be obtained by testing the step response of the process around an operation point. For the SISO model, the PID controller with parameters $K_c = 70$, $T_I = 120$, $T_D = 20$ is adopted.

From Fig. 10.3, it can be easily seen that the output temperature T_{set}, the measured outlet temperature T_m, and the input fuel flow F_{flow} are stored in a database (π database) in DCS.

Here, the sampling time is 10 s. The process response is obtained by both increasing and decreasing the set-point of the PID controller, and the change cycle of the set-point is 495 °C → 497 °C → 495 °C → 493 °C → 495 °C. In order to decrease the influence of noise, the low-pass filter with the following form is introduced

$$G_f(z) = \frac{0.15}{z - 0.85} \tag{10.22}$$

In Fig. 10.4, the real-time responses, filtered responses, and the modeling results are shown. It is clear that the corresponding dynamic responses of the process are complex and it is hard to obtain an accurate process model.

The identified transfer functions are listed in Table 10.1, and it is obvious that these models are quite different. Even for the two forward step-response tests "A" and "D" or the two reverse step-response tests "B" and "C", the results also differ a lot.

Note that the time delays of $G_2(s)$ and $G_4(s)$ are the largest, thus the process model can be selected from one of them to include the delays. At the same time, due to the

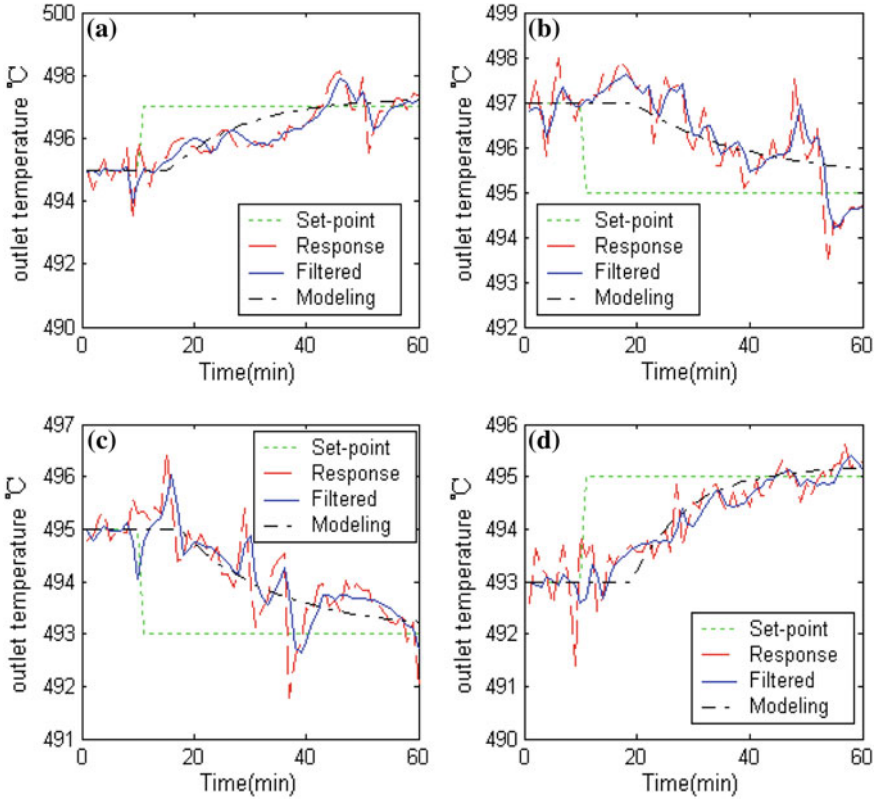

Fig. 10.4 Real-time forward and reverse step-response tests

fact that the constants of $G_1(s)$, $G_3(s)$, and $G_4(s)$ are close to each other, therefore, $G_4(s)$ is chosen as the process model.

The discrete form of $G_4(s)$ under sampling time $T_s = 30$ s is

$$G_{T_s}(z) = \frac{0.1047}{z^6 - 0.9048z^5} \tag{10.23}$$

which can be easily converted into the input–output model in Eq. (10.6).

For the model shown in Eq. (10.23), the ENMSS model based MPC is designed.

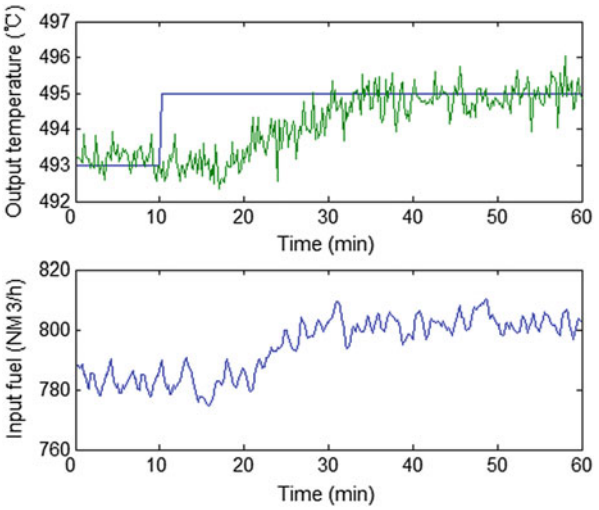

Fig. 10.5 Performance of the closed-loop system for tracking

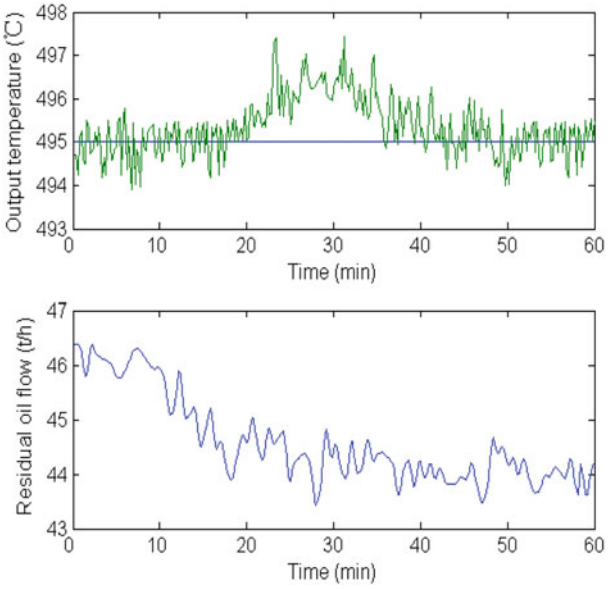

Fig. 10.6 Residual oil flow load change test

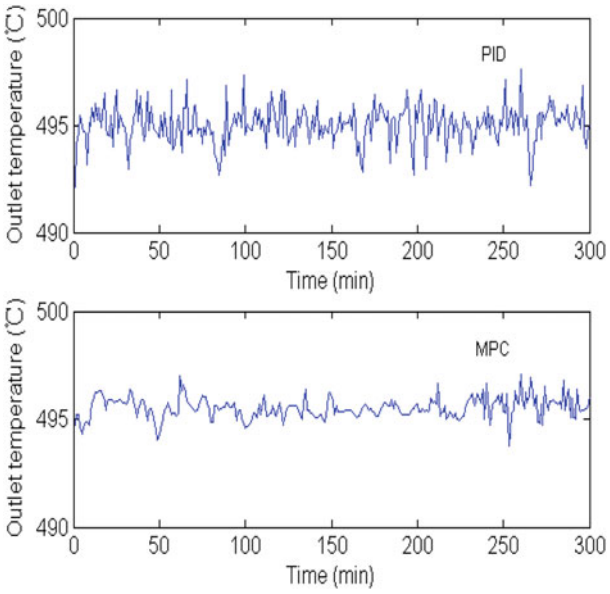

Fig. 10.7 Experimental results of PID and MPC: Group 1

The responses of the set-point tracking from 493 to 495 °C are shown in Fig. 10.5. It can be easily seen that the MPC controller shows a fast response, which is approximately 25 min. However, the response of the original PID controller is more than 33 min, which can be seen in Fig. 10.4.

In order to test the load disturbance rejection of the MPC controller, we change the residual oil flow that goes into the coke furnace from 46 t/h to about 44 t/h at $t =$ 10 min. The corresponding responses are shown in Fig. 10.6, and the results show that the required set-point is maintained successfully by the ENMSS model based MPC controller.

In Figs. 10.7–10.8, two groups of regulatory control results are shown. We can easily see that the temperature is more stable compared with before. Meanwhile, the statistical results concerning the average value, the maximum value, the minimum value, the standard deviation, and the extreme deviation of the outlet temperature are listed in Table 10.2, which prove that the ENMSS model based MPC controller provides more steady control.

10.2.5.2 Control of Air Supply System

Choose the oxygen content set-point O_{set} of the PID as the input and the measured oxygen content value O_m as the output, the generalized process is modeled as a SISO model that can be obtained by testing the step response of the air supply

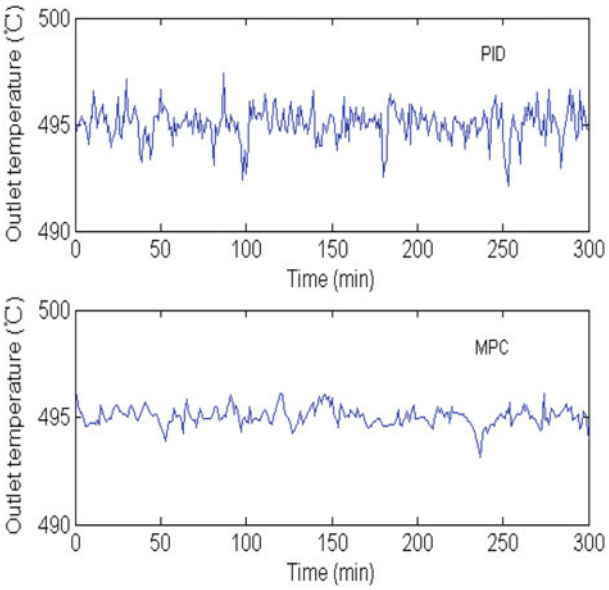

Fig. 10.8 Experimental results of PID and MPC: Group 2

Table 10.2 Statistical results

Group	Item	Average	Max	Min	Standard deviation	Extreme deviation
1	PID	495.6	497.6	492.1	0.8474	5.5
1	MPC	495.2	497.1	493.7	0.4806	3.4
2	PID	495.5	497.4	492.1	0.7661	5.3
2	MPC	495.2	496.1	493.1	0.4176	3.0

system around an operation point. Here, the PID with the proportional, integral, and derivative constants $K_c = 110$, $T_I = 70$, $T_D = 0$ is employed to control the blower.

As can be seen in Fig. 10.9, the required process data, i.e., the measured oxygen content values O_m, the oxygen content set-point O_{set}, and the inlet air flow A_{flow} are collected from relevant sensors and stored in a data storage database (π database).

The step-response modeling method in [22] can be adopted after these data are obtained. As to the oxygen content system, it is roughly modeled as a typical FOPDT model. Consider the high level of noise component, these data are processed by the following filter

$$G_f(z) = \frac{0.25}{z - 0.75} \tag{10.24}$$

In Fig. 10.10, two groups of modeling results are shown. Here, the operation point is 4.5%, the step change is ±0.5%, and the sampling time is 5 s. Table 10.3 lists the

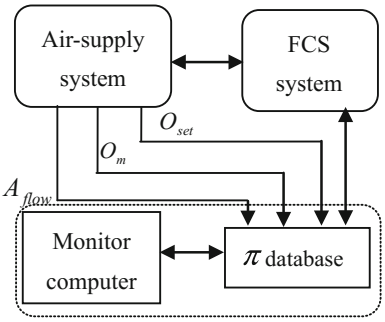

Fig. 10.9 Data–acquisition configuration for air supply system

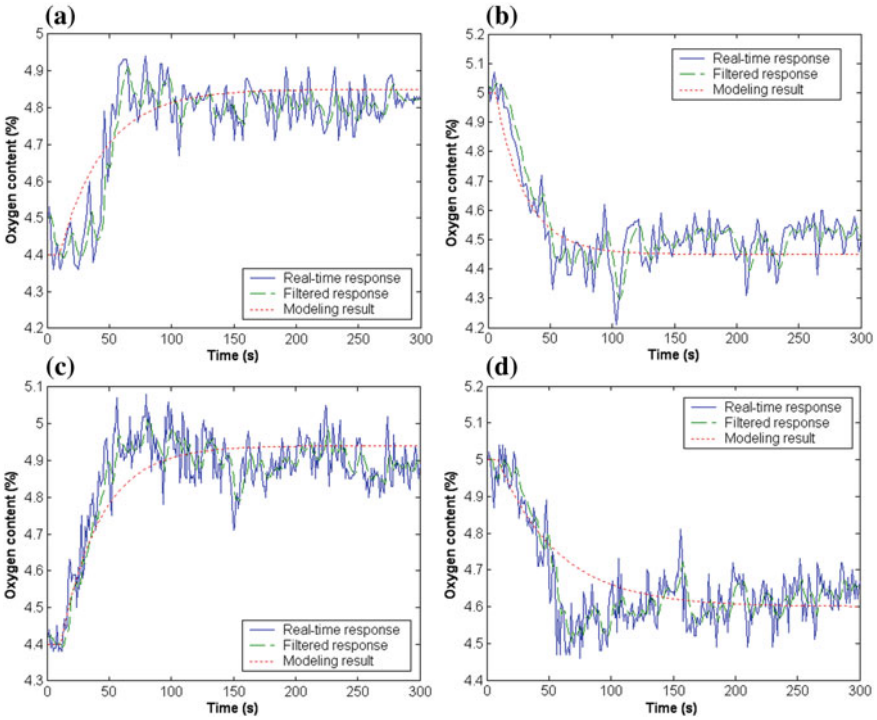

Fig. 10.10 **a** Forward step-response modeling (Group 1). **b** Reverse step-response modeling (Group 1). **c** Forward step-response modeling (Group 2).**d** Reverse step-response modeling (Group 2)

corresponding rough transfer function models, and it is obvious that the relevant dynamics differ a lot.

The MPC is designed based on the model in $G_3(s)$ because its time delay is the largest. Under the sampling time of 5 s, the corresponding discrete transfer function model is

Table 10.3 Step-response models

Group	Forward model	Reverse model
1	$G_1(s) = \frac{0.72e^{-8s}}{240s+1}$	$G_2(s) = \frac{0.95e^{-5s}}{120s+1}$
2	$G_3(s) = \frac{0.94e^{-10s}}{160s+1}$	$G_4(s) = \frac{0.8e^{-8s}}{240s+1}$

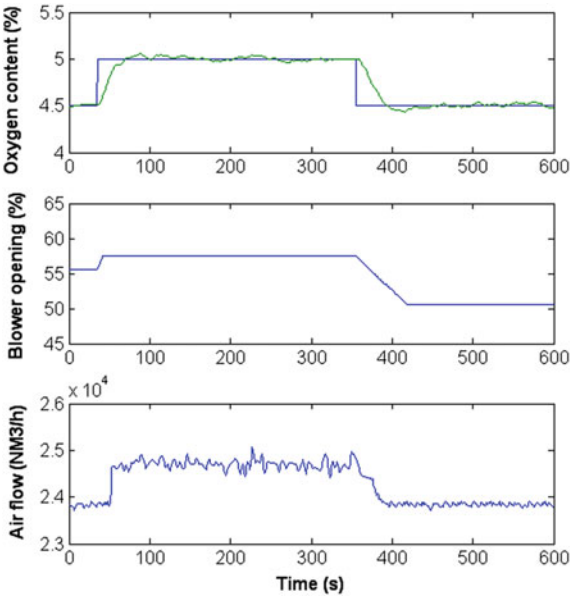

Fig. 10.11 Performance of the closed-loop system for set-point tracking

$$G_{O_m}(z) = \frac{0.029}{z^3 - 0.9692z^2} \tag{10.25}$$

In this section, various experiments are done to test the validation of the ENMSS model based MPC, and the experimental results are shown in Fig. 10.11. The set-point of the oxygen content is changed from 4.5 to 5%, and the relevant blower opening is displayed in the middle graph.

In order to avoid the fast damage and aging of the blower due to the frequent blower movements, the blower opening is restricted to remain constant if the absolute error value between the actual oxygen content and the desired set-point is smaller than 0.05%. The lower graph shows the air flow, and we can see that the blower opening cannot return to its original position after a cycle of set-point change because its forward and reverse dynamics are different. Nevertheless, the required set-point is maintained successfully by the controller.

The change of the fuel flow into the coke furnace is introduced as the load disturbance to test the disturbance rejection ability of the MPC. Here, the fuel flow going into the coke furnace is changed from 785 NM^3/h to about 805 NM^3/h at $t = 100$ s,

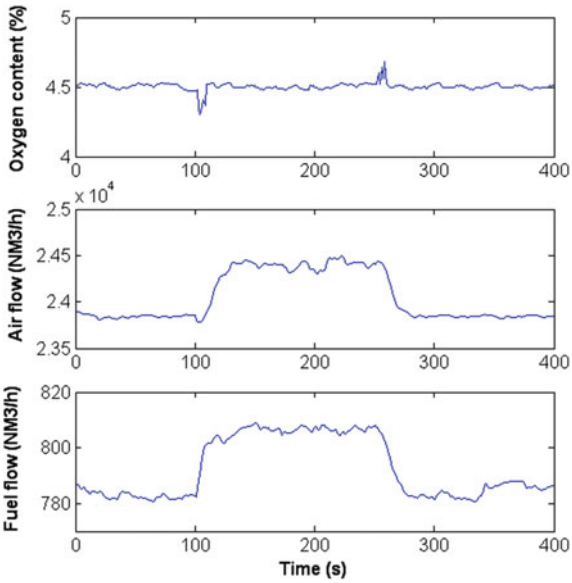

Fig. 10.12 Fuel flow load change test

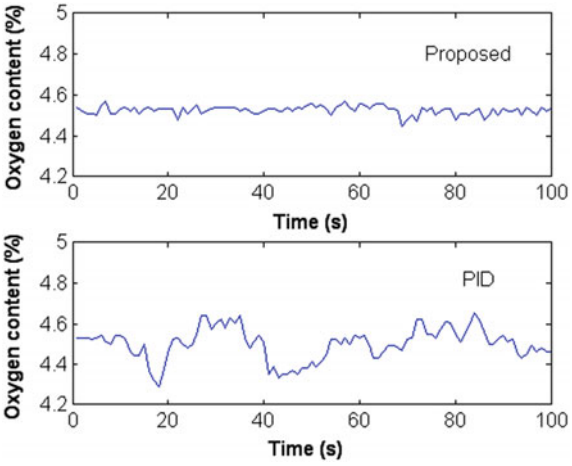

Fig. 10.13 Steady state comparison: Group 1

and then back to its original value at $t = 250$ s. As is shown in Fig. 10.12, the oxygen content set-point is successfully kept by the MPC.

For further evaluation of the control performance, results of the existing PID method are shown in Figs. 10.13 and 10.14. The standard deviation values are calculated as 0.21 and 0.0795 for PID and MPC, respectively in the first group, and 0.206 and 0.067 for PID and MPC, respectively in the second group. It is obvious that a more satisfactory range is obtained for these items under the ENMSS model based MPC.

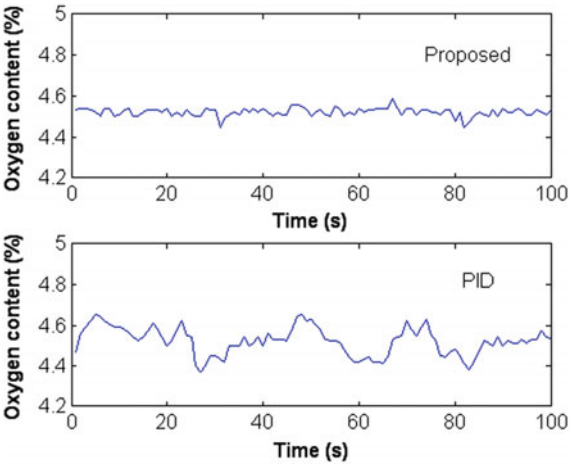

Fig. 10.14 Steady state comparison: Group 2

10.3 Summary

In this chapter, the outlet temperature process and the air supply system in the coke furnace are introduced as industrial applications to test the control performance of the ENMSS model based MPC. By collecting the input–output process data, the corresponding FOPDT models are established, then the corresponding ENMSS models are derived. Finally, the relevant MPC schemes are designed for the temperature control system and air supply system. The experimental results show the effectiveness of the ENMSS model based MPC.

References

1. Yang, B., & Li, H. G. (2018). A novel dynamic timed fuzzy Petri nets modeling method with applications to industrial processes. *Expert Systems with Applications, 97,* 276–289.
2. Yuan, X. F., Wang, Y. L., Yang, C. H., Gui, W. H., & Ye, L. J. (2017). Probabilistic density-based regression model for soft sensing of nonlinear industrial processes. *Journal of Process Control, 57,* 15–25.
3. Lu, X. L., Kiumarsi, B., Chai, T. Y., & Lewis, F. L. (2016). Data-driven optimal control of operational indices for a class of industrial processes. *IET Control Theory and Applications, 10*(12), 1348–1356.
4. Wang, T., Gao, H. J., & Qiu, J. B. (2016). A combined fault-tolerant and predictive control for network-based industrial processes. *IEEE Transactions on Industrial Electronics, 63*(4), 2529–2536.
5. Bindlish, R. (2015). Nonlinear model predictive control of an industrial polymerization process. *Computers & Chemical Engineering, 73,* 43–48.
6. Huyck, B., Brabanter, J., Moor, B., Van Impe, J. F., & Logist, F. (2014). Online model predictive control of industrial processes using low level control hardware: A pilot-scale distillation column case study. *Control Engineering Practice, 28,* 34–48.

7. Han, H. G., & Qiao, J. F. (2014). Nonlinear model-predictive control for industrial processes: An application to wastewater treatment process. *IEEE Transactions on Industrial Electronics, 61*(4), 1970–1982.
8. Zhang, R. D., Tao, J. L., & Gao, F. R. (2016). A new approach of Takagi-Sugeno fuzzy modeling using an improved genetic algorithm optimization for oxygen content in a coke furnace. *Industrial & Engineering Chemistry Research, 55*(22), 6465–6474.
9. Su, C. L., Shi, H. Y., Li, P., & Cao, J. T. (2015). Advanced control in a delayed coking furnace. *Measurement & Control, 48*(2), 54–59.
10. Taysom, B. S., Sorensen, C. D., & Hedengren, J. D. (2017). A comparison of model predictive control and PID temperature control in friction stir welding. *Journal of Manufacturing Processes, 29,* 232–241.
11. Zhang, R. D., Cao, Z. X., Bo, C. M., Li, P., & Gao, F. R. (2014). New PID controller design using extended nonminimal state space model based predictive functional control structure. *Industrial & Engineering Chemistry Research, 53*(8), 3283–3292.
12. Na, M. G. (2001). Auto-tuned PID controller using a model predictive control method for the steam generator water level. *IEEE Transactions on Nuclear Science, 48*(5), 1664–1671.
13. Lepetic, M., Skrjanc, I., Chiacchiarini, H. G., & Matko, D. (2003). Predictive functional control based on fuzzy model: Comparison with linear predictive functional control and PID control. *Journal of Intelligent and Robotic Systems, 36*(4), 467–480.
14. Abdelrauf, A. A., Abdel-Geliel, M., & Zakzouk, E. (2016). Adaptive PID controller based on model predictive control. *European Control Conference, 2016,* 746–751.
15. Wu, S. (2015). Multivariable PID control using improved state space model predictive control optimization. *Industrial & Engineering Chemistry Research, 54*(20), 5505–5513.
16. Zhang, J. M. (2017). Design of a new PID controller using predictive functional control optimization for chamber pressure in a coke furnace. *ISA Transactions, 67,* 208–214.
17. Zhang, R. D., & Gao, F. R. (2013). Multivariable decoupling predictive functional control with non-zero-pole cancellation and state weighting: Application on chamber pressure in a coke furnace. *Chemical Engineering Science, 94,* 30–43.
18. Zhang, R. D., Li, P., Xue, A. K., Jiang, A. P., & Wang, S. Q. (2010). A simplified linear iterative predictive functional control approach for chamber pressure of industrial coke furnace. *Journal of Process Control, 20*(4), 464–471.
19. Bequette, B. W. (2003). *Process Control: Modeling*. Prentice Hall, Upper Saddle River, NJ: Design and Simulation.
20. Zhang, R. D., Wu, S., & Gao, F. R. (2017). State space model predictive control for advanced process operation: A review of recent developments, new results, and insight. *Industrial & Engineering Chemistry Research, 56*(18), 5360–5394.
21. Zhang, R. D., Xue, A. K., Lu, R. Q., Li, P., & Gao, F. R. (2014). Real-time implementation of improved state-space MPC for air supply in a coke furnace. *IEEE Transactions on Industrial Electronics, 61*(7), 3532–3539.
22. Zhang, R. D., Xue, A. K., & Wang, S. Q. (2011). Modeling and nonlinear predictive functional control of liquid level in a coke fraction tower. *Chemical Engineering Science, 66*(23), 6002–6013.

Chapter 11
Further Ideas on MPC and PFC Using Relaxed Constrained Optimization

11.1 Introduction

Constraints are necessary for safe operation and profits in industrial processes [1, 2]. In order to handle constraints effectively, many approaches have been developed, such as linear programming (LP) methods [3–5], quadratic programming (QP) methods [6–8], linear matrix inequality (LMI) based methods[9–11], etc. As for constrained MPC, the employment of QP method is common because the relevant performance index with various constraints can be transformed into the QP problem easily, and there are many significant results [12–16].

Note that the working conditions are changing in practice and the preset parameters may be too rigorous for the constrained optimization problem such that there may be no feasible solutions under such situations. To cope with this problem, an improved constraint handling approach in which relaxations are introduced and combined in the corresponding objective function is adopted and the control law is obtained by solving a relaxed QP problem in this chapter. Based on such enhanced constraint dealing method, the relaxations will work when the controlled system is over-constrained, and the probability of finding the suitable solution of the relevant constrained optimization problem is increased.

In the following contents, this relaxed constrained optimization strategy is employed for the ENMSS model based MPC and PFC approaches, respectively.

R. Zhang et al., *Model Predictive Control*,
https://doi.org/10.1007/978-981-13-0083-7_11

11.2 The Relaxed Constrained Optimization Method

11.2.1 The Relaxed Constrained ENMSS Model Predictive Control

For simplicity, we consider the following SISO industrial process whose input–output model is as follows

$$\begin{aligned} &y(k+1)+H_1y(k)+H_2y(k-1)+\cdots+H_my(k-m+1)\\ &\quad=L_1u(k)+L_2u(k-1)+\cdots+L_nu(k-n+1) \end{aligned} \tag{11.1}$$

where $y(k)$ is the process output at time instant k, and $u(k)$ is the control input at time instant k. $H_1,\ldots,H_m$ and $L_1,\cdots,L_n$ are the relevant coefficients.

As for Eq. (11.1), the following equation can be obtained by adding the difference operator Δ

$$\begin{aligned} &\Delta y(k+1)+H_1\Delta y(k)+H_2\Delta y(k-1)+\cdots+H_m\Delta y(k-m+1)\\ &\quad=L_1\Delta u(k)+L_2\Delta u(k-1)+\cdots+L_n\Delta u(k-n+1) \end{aligned} \tag{11.2}$$

First, we choose the NMSS vector as

$$\begin{aligned} \Delta x(k)^{\mathrm{T}}=&[\Delta y(k),\Delta y(k-1),\ldots,\Delta y(k-m+1),\\ &\Delta u(k-1),\Delta u(k-2),\ldots,\Delta u(k-n+1)] \end{aligned} \tag{11.3}$$

then the corresponding NMSS model is

$$\begin{aligned} \Delta x(k+1)&=A\Delta x(k)+B\Delta u(k)\\ \Delta y(k+1)&=C\Delta x(k+1) \end{aligned} \tag{11.4}$$

where

$$A=\begin{bmatrix} -H_1 & -H_2 & \cdots & -H_{m-1} & -H_m & L_2 & \cdots & L_{n-1} & L_n\\ 1 & 0 & \cdots & 0 & 0 & 0 & \cdots & 0 & 0\\ 0 & 1 & \cdots & 0 & 0 & 0 & \cdots & 0 & 0\\ \vdots & \vdots & \cdots & \vdots & \vdots & \vdots & \cdots & \vdots & \vdots\\ 0 & 0 & \cdots & 1 & 0 & 0 & \cdots & 0 & 0\\ 0 & 0 & \cdots & 0 & 0 & 0 & \cdots & 0 & 0\\ 0 & 0 & \cdots & 0 & 0 & 1 & \cdots & 0 & 0\\ \vdots & \vdots & \cdots & \vdots & \vdots & \vdots & \cdots & \vdots & \vdots\\ 0 & 0 & \cdots & 0 & 0 & 0 & \cdots & 1 & 0 \end{bmatrix}$$

$$B = \left[L_1 \, 0 \, 0 \cdots 1 \, 0 \cdots 0 \right]^{\mathrm{T}}$$
$$C = \left[1 \, 0 \, 0 \cdots 0 \, 0 \, 0 \, 0 \right]$$

Define the set-point as y_s and the reference trajectory as

$$\begin{aligned} r(k) &= y(k) \\ r(k+i) &= \alpha^i y(k) + (1-\alpha^i) y_s \quad i = 1, 2, \ldots, P \end{aligned} \tag{11.5}$$

where α is the smoothing factor of the reference trajectory and P is the prediction horizon.

The tracking error at time instant k can be calculated as

$$e(k) = y(k) - r(k) \tag{11.6}$$

By combining Eqs. (11.4) and (11.6), the output tracking error prediction at time instant $k+1$ can be presented as

$$e(k+1) = e(k) + CA\Delta x(k) + CB\Delta u(k) - \Delta r(k+1) \tag{11.7}$$

Further, we construct the extended state vector as

$$z(k) = \begin{bmatrix} \Delta x(k) \\ e(k) \end{bmatrix} \tag{11.8}$$

then the relevant ENMSS model is described as

$$z(k+1) = A_m z(k) + B_m \Delta u(k) + C_m \Delta r(k+1) \tag{11.9}$$

where

$$A_m = \begin{bmatrix} A & 0 \\ CA & 1 \end{bmatrix}; \quad B_m = \begin{bmatrix} B \\ CB \end{bmatrix}; \quad C_m = \begin{bmatrix} 0 \\ -1 \end{bmatrix}$$

Here 0 in A_m and C_m are zero vectors with appropriate dimensions.

It is obvious that the state prediction can be obtained based on Eq. (11.9). Define M as the control horizon and

$$Z = \begin{bmatrix} z(k+1) \\ z(k+2) \\ \vdots \\ z(k+P) \end{bmatrix}; \quad \Delta U = \begin{bmatrix} \Delta u(k) \\ \Delta u(k+1) \\ \vdots \\ \Delta u(k+M-1) \end{bmatrix}; \quad \Delta R = \begin{bmatrix} \Delta r(k+1) \\ \Delta r(k+2) \\ \vdots \\ \Delta r(k+P) \end{bmatrix} \tag{11.10}$$

then the relevant state prediction is derived as

$$Z = Sz(k) + F\Delta U + \theta\Delta R \tag{11.11}$$

where

$$S = \begin{bmatrix} A_m \\ A_m^2 \\ \vdots \\ A_m^P \end{bmatrix}; \quad F = \begin{bmatrix} B_m & 0 & 0 & \cdots & 0 \\ A_m B_m & B_m & 0 & \cdots & 0 \\ A_m^2 B_m & A_m B_m & B_m & \cdots & 0 \\ \vdots & \vdots & \vdots & \ddots & \vdots \\ A_m^{P-1} B_m & A_m^{P-2} B_m & A_m^{P-3} B_m & \cdots & A_m^{P-M} B_m \end{bmatrix}$$

$$\theta = \begin{bmatrix} C_m & 0 & 0 & 0 & 0 \\ A_m C_m & C_m & 0 & 0 & 0 \\ A_m^2 C_m & A_m C_m & C_m & 0 & 0 \\ \vdots & \vdots & \vdots & \ddots & \vdots \\ A_m^{P-1} C_m & A_m^{P-2} C_m & A_m^{P-3} C_m & \cdots & C_m \end{bmatrix}$$

In order to achieve the set-point tracking, the performance index for the ENMSS model based constrained MPC is selected as

$$J(k) = Z^{\mathrm{T}} Q Z + \Delta U^{\mathrm{T}} L \Delta U \tag{11.12}$$

subject to

$$\begin{aligned} \Delta u_{\min} \le \Delta u(k+i) \le \Delta u_{\max} \\ u_{\min} \le u(k+i) \le u_{\max}, i = 0, 1, \ldots, M-1 \\ y_{\min} \le y(k+j) \le y_{\max}, j = 1, 2, \ldots, P \end{aligned} \tag{11.13}$$

where Q and L are the corresponding weighting matrices for the state variables and the control input increments, respectively. $\Delta u_{\min}$, $\Delta u_{\max}$ are the lower bound and upper bound of the incremental control input. $u_{\min}$, $u_{\max}$ are the lower bound and upper bound of the control input, and $y_{\min}$, $y_{\max}$ are the lower bound and upper bound of the output.

As for the constraints in Eq. (11.13), it is clear that the constraints on the control input and the incremental control input may not be changed due to the fact that the relevant ranges of devices are limited. In order to increase the probability of successfully solving the corresponding QP problem, the relaxations are introduced for the constraints on the output, and the details are as follows.

$$\begin{aligned} y(k+j) &\le y_{\max} + S_{\max}(j) \\ y_{\min} &\le y(k+j) + S_{\min}(j) \\ S_{\max}(j) \ge 0; &\quad S_{\min}(j) \ge 0 \\ j &= 1, 2, \ldots, P \end{aligned} \tag{11.14}$$

where $S_{\max}(j)$, $S_{\min}(j)$ are the introduced relaxations.

Then, the relaxed performance index is described as

$$J(k) = Z^{\mathrm{T}} Q Z + \Delta U^{\mathrm{T}} L \Delta U + S_{\max}^{\mathrm{T}} Q_{\max} S_{\max} + S_{\min}^{\mathrm{T}} Q_{\min} S_{\min} \tag{11.15}$$

subject to

$$\begin{aligned} \Delta u_{\min} &\le \Delta u(k+i) \le \Delta u_{\max} \\ u_{\min} &\le u(k+i) \le u_{\max}, i = 0, 1, \ldots, M-1 \\ y(k+j) &\le y_{\max} + S_{\max}(j) \\ y_{\min} &\le y(k+j) + S_{\min}(j) \\ S_{\max}(j) \ge 0; &\quad S_{\min}(j) \ge 0 \\ j &= 1, 2, \ldots, P \end{aligned} \tag{11.16}$$

where $Q_{\max}$, $Q_{\min}$ are the relevant weighting matrices.

Remark 11.1 Note that the cost function and constraints in Eqs. (11.15) and (11.16) will be the same as those in Eqs. (11.12) and (11.13) if $S_{\max}$, $S_{\min}$ are zero vectors; that is, the solutions for the two objective functions will be the same when the constraints on the outputs are loose.

Remark 11.2 When the constraints on the outputs are too rigorous, there may be no feasible solutions to the optimization problem in Eq. (11.12). However, the solutions with the smallest constraint violation will still be provided by minimizing the performance index in Eq. (11.15).

It is obvious that the following QP problem can be obtained by expanding the objective function in Eq. (11.15)

$$\min_{x(k)} q(x(k)) = \frac{1}{2} x(k)^{\mathrm{T}} H_x x(k) + f_x^{\mathrm{T}} x(k) \tag{11.17}$$

subject to

$$A_x x(k) \le b_x$$

where

$$x(k) = \begin{bmatrix} \Delta U \\ S_{\max} \\ S_{\min} \end{bmatrix}; H_x = \begin{bmatrix} 2(F^{\mathrm{T}}QF + L) & 0 & 0 \\ 0 & 2Q_{\max} & 0 \\ 0 & 0 & 2Q_{\min} \end{bmatrix}; f_x = \begin{bmatrix} 2(F^{\mathrm{T}}Q(Sz(k) + \theta\Delta R))^{\mathrm{T}} \\ 0 \\ 0 \end{bmatrix}$$

$$A_x = \begin{bmatrix} A_{x1} & 0 & 0 \\ -A_{x1} & 0 & 0 \\ A_{x2} & 0 & 0 \\ -A_{x2} & 0 & 0 \\ C_xF & -1 & 0 \\ -C_xF & 0 & -1 \\ 0 & -1 & 0 \\ 0 & 0 & -1 \end{bmatrix}; b_x = \begin{bmatrix} b_{x1} \\ b_{x2} \\ b_{x3} \\ b_{x4} \\ b_{x5} \\ b_{x6} \\ 0 \\ 0 \end{bmatrix}; A_{x1} = \begin{bmatrix} 1 & 0 & \cdots & 0 \\ 0 & 1 & \cdots & 0 \\ \vdots & \vdots & \ddots & \vdots \\ 0 & 0 & \cdots & 1 \end{bmatrix}; A_{x2} = \begin{bmatrix} 1 & 0 & 0 & \cdots & 0 \\ 1 & 1 & 0 & \cdots & 0 \\ \vdots & \vdots & \vdots & \ddots & \vdots \\ 1 & \cdots & 1 & 1 & 0 \\ 1 & 1 & \cdots & 1 & 1 \end{bmatrix}$$

$$C_x = \begin{bmatrix} 0 & 1 & 0 & 0 & 0 & \cdots & 0 & 0 \\ 0 & 0 & 0 & 1 & 0 & \cdots & 0 & 0 \\ \vdots & \vdots & \vdots & \cdots & \ddots & \vdots & \vdots & \vdots \\ 0 & 0 & 0 & \cdots & 0 & 1 & 0 & 0 \\ 0 & 0 & 0 & \cdots & 0 & 0 & 0 & 1 \end{bmatrix}; \begin{aligned} b_{x1} &= \Delta u_{\max}; b_{x2} = -\Delta u_{\min} \\ b_{x3} &= u_{\max} - u(k-1) \\ b_{x4} &= -u_{\min} + u(k-1) \\ b_{x5} &= y_{\max} - C_xSz(k) - C_x\theta\Delta R - R \\ b_{x6} &= -y_{\min} + C_xSz(k) + C_x\theta\Delta R + R \end{aligned}; R = \begin{bmatrix} r(k+1) \\ r(k+2) \\ \vdots \\ r(k+P) \end{bmatrix}$$

Here, 0 in H_x, f_x, A_x, b_x, C_x are zero matrices with appropriate dimensions. 1 in A_x are unit matrices with appropriate dimensions.

Finally, the optimal control law can be obtained by solving the QP problem in Eq. (11.17).

11.2.2 The Relaxed Constrained ENMSS Predictive Functional Control

Consider the same SISO process in Eq. (11.1), we can obtain the ENMSS model in Eq. (11.9) first. Here, the same derivation processes are omitted to make this chapter concise.

As for the PFC strategy, its general control law is a linear combination of basis functions [17, 18] and the details are

$$u(k+i) = \sum_{j=1}^{N} \mu_j f_j(i) \tag{11.18}$$

where $u(k+i)$ is the control law of PFC at time instant $k+i$. $f_j(i)$ is the value of the basis function f_j at time instant $k+i$, and μ_j is the corresponding weighting coefficient. N is the number of the basis functions.

Without loss of generality, the prediction and control horizons are both chosen as P and denote

$$\begin{aligned} T_i &= [f_1(i), f_2(i), \ldots, f_N(i)], (i = 0, 1, \ldots, P-1) \\ \eta &= [\mu_1, \mu_2, \ldots, \mu_N]^{\mathrm{T}} \end{aligned} \tag{11.19}$$

then the control law in Eq. (11.18) can be rewritten as

$$u(k+i) = T_i \eta \tag{11.20}$$

Further, define

$$Z = \begin{bmatrix} z(k+1) \\ z(k+2) \\ \vdots \\ z(k+P) \end{bmatrix}; \quad \Delta R = \begin{bmatrix} \Delta r(k+1) \\ \Delta r(k+2) \\ \vdots \\ \Delta r(k+P) \end{bmatrix} \tag{11.21}$$

then the relevant state prediction can be derived by combining Eqs. (11.9) and (11.20) as

$$Z = Sz(k) + \varphi\eta - Fu(k-1) + \theta\Delta R \tag{11.22}$$

where

$$S = \begin{bmatrix} A_m \\ A_m^2 \\ \vdots \\ A_m^P \end{bmatrix}; \quad F = \begin{bmatrix} B_m \\ A_m B_m \\ \vdots \\ A_m^{P-1} B_m \end{bmatrix};$$

$$\varphi = \begin{bmatrix} B_m T_0 \\ (A_m B_m - B_m) T_0 + B_m T_1 \\ (A_m^2 B_m - A_m B_m) T_0 + (A_m B_m - B_m) T_1 + B_m T_2 \\ \vdots \\ \sum_{k=1}^{P-1} (A_m^k B_m - A_m^{k-1} B_m) T_{P-1-k} + B_m T_{P-1} \end{bmatrix}$$

$$\theta = \begin{bmatrix} C_m & 0 & 0 & 0 & 0 \\ A_m C_m & C_m & 0 & 0 & 0 \\ A_m^2 C_m & A_m C_m & C_m & 0 & 0 \\ \vdots & \vdots & \vdots & \ddots & \vdots \\ A_m^{P-1} C_m & A_m^{P-2} C_m & A_m^{P-3} C_m & \cdots & C_m \end{bmatrix}$$

The objective function for the ENMSS model based constrained PFC is chosen as

$$J(k) = Z^{\mathrm{T}} Q Z \tag{11.23}$$

subject to

$$\begin{aligned} \Delta u_{\min} \le \Delta u(k+i) \le \Delta u_{\max} \\ u_{\min} \le u(k+i) \le u_{\max}, i = 0, 1, \ldots, P-1 \\ y_{\min} \le y(k+j) \le y_{\max}, j = 1, 2, \ldots, P \end{aligned} \tag{11.24}$$

where Q is the weighting matrix for the state variables. $\Delta u_{\min}$, $\Delta u_{\max}$ are the lower limit and upper limit of the incremental control input, and $u_{\min}$, $u_{\max}$ are the lower limit and upper limit of the control input. $y_{\min}$, $y_{\max}$ are the lower limit and upper limit of the output.

Similar to Sect. 11.2.1, the constraints on the control input and the incremental control input cannot be relaxed. Here, relaxations are adopted for the constraints on the output to increase the probability of successfully solving the corresponding optimization problem, and the details are as follows.

$$\begin{aligned} y(k+j) \le y_{\max} + S_{\max}(j) \\ y_{\min} \le y(k+j) + S_{\min}(j) \\ S_{\max}(j) \ge 0; \quad S_{\min}(j) \ge 0 \\ j = 1, 2, \ldots, P \end{aligned} \tag{11.25}$$

where $S_{\max}(j)$, $S_{\min}(j)$ are the relevant relaxations.

Then, the following relaxed cost function is considered.

$$J(k) = Z^{\mathrm{T}} Q Z + S_{\max}^{\mathrm{T}} Q_{\max} S_{\max} + S_{\min}^{\mathrm{T}} Q_{\min} S_{\min} \tag{11.26}$$

subject to

$$\begin{aligned}
\Delta u_{\min} &\le \Delta u(k+i) \le \Delta u_{\max} \\
u_{\min} &\le u(k+i) \le u_{\max}, i = 0, 1, \ldots, P-1 \\
y(k+j) &\le y_{\max} + S_{\max}(j) \\
y_{\min} &\le y(k+j) + S_{\min}(j) \\
S_{\max}(j) &\ge 0; \quad S_{\min}(j) \ge 0 \\
j &= 1, 2, \ldots, P
\end{aligned} \tag{11.27}$$

where $Q_{\max}$, $Q_{\min}$ are the weighting matrices for $S_{\max}$ and $S_{\min}$, respectively.

By decomposing the cost function in Eq. (11.26), we can obtain the following QP problem

$$\min_{x(k)} q(x(k)) = \frac{1}{2} x(k)^{\mathrm{T}} H_x x(k) + f_x^{\mathrm{T}} x(k) \tag{11.28}$$

subject to

$$A_x x(k) \le b_x$$

where

$$x(k) = \begin{bmatrix} \eta \\ S_{\max} \\ S_{\min} \end{bmatrix}; \; H_x = \begin{bmatrix} 2\varphi^{\mathrm{T}} Q \varphi & 0 & 0 \\ 0 & 2Q_{\max} & 0 \\ 0 & 0 & 2Q_{\min} \end{bmatrix}$$

$$f_x = \begin{bmatrix} 2(\varphi^{\mathrm{T}} Q(Sz(k) - Fu(k-1) + \theta \Delta R))^{\mathrm{T}} \\ 0 \\ 0 \end{bmatrix}; \; A_x = \begin{bmatrix} A_{x1} & 0 & 0 \\ -A_{x1} & 0 & 0 \\ A_{x2} & 0 & 0 \\ -A_{x2} & 0 & 0 \\ C_x \varphi & -1 & 0 \\ -C_x \varphi & 0 & -1 \\ 0 & -1 & 0 \\ 0 & 0 & -1 \end{bmatrix}; \; b_x = \begin{bmatrix} b_{x1} \\ b_{x2} \\ b_{x3} \\ b_{x4} \\ b_{x5} \\ b_{x6} \\ 0 \\ 0 \end{bmatrix}$$

$$A_{x1} = \begin{bmatrix} T_0 & 0 & \cdots & 0 \\ 0 & T_1 - T_0 & \cdots & 0 \\ \vdots & \vdots & \ddots & \vdots \\ 0 & 0 & \cdots & T_{P-1} - T_{P-2} \end{bmatrix}; \; A_{x2} = \begin{bmatrix} T_0 & 0 & \cdots & 0 \\ 0 & T_1 & \cdots & 0 \\ \vdots & \vdots & \ddots & 0 \\ 0 & 0 & \cdots & T_{P-1} \end{bmatrix}$$

$$b_{x1} = \begin{bmatrix} \Delta u_{\max} + u(k-1) \\ \Delta u_{\max} \\ \vdots \\ \Delta u_{\max} \end{bmatrix}; \; b_{x2} = \begin{bmatrix} -\Delta u_{\min} - u(k-1) \\ -\Delta u_{\min} \\ \vdots \\ -\Delta u_{\min} \end{bmatrix}; \; R = \begin{bmatrix} r(k+1) \\ r(k+2) \\ \vdots \\ r(k+P) \end{bmatrix}$$

$$b_{x3} = u_{\max}; b_{x4} = -u_{\min}$$
$$b_{x5} = y_{\max} - C_x Sz(k) + C_x Fu(k-1) - C_x \theta \Delta R - R \; ; C_x = \begin{bmatrix} 0\,1\,0\,0\,0\cdots 0\,0 \\ 0\,0\,0\,1\,0\cdots 0\,0 \\ \vdots\;\vdots\;\vdots\cdots\ddots\;\vdots\;\vdots\;\vdots \\ 0\,0\,0\cdots 0\,1\,0\,0 \\ 0\,0\,0\cdots 0\,0\,0\,1 \end{bmatrix}$$
$$b_{x6} = -y_{\min} + C_x Sz(k) - C_x Fu(k-1) + C_x \theta \Delta R + R$$

0 in H_x, f_x, A_x, b_x, C_x are zero matrices with appropriate dimensions, and 1 in A_x are unit matrices with appropriate dimensions.

By solving the QP problem in Eq. (11.28), the control law η can be obtained, and the control input of ENMSS model based constrained PFC in Eq. (11.20) can be calculated finally.

11.3 Summary

In this chapter, a relaxed constrained optimization method is presented. By introducing the relaxations into the performance index and output constraints, the probability of successfully solving the relevant QP problem is increased and this improved constraint handling method is employed in the ENMSS model based constrained MPC and PFC strategies finally.

References

1. Adetol, V., Dehaan, D., & Guay, M. (2009). Adaptive model predictive control for constrained nonlinear systems. *Systems & Control Letters, 58*(5), 320–326.
2. Li, H. P., & Shi, Y. (2014). Robust distributed model predictive control of constrained continuous-time nonlinear systems: A robustness constraint approach. *IEEE Transactions on Automatic Control, 59*(6), 1673–1678.
3. Deng, K., Sun, Y., Li, S. S., Lu, Y., Brouwer, J., Mehta, P. G., et al. (2015). Model predictive control of central chiller plant with thermal energy storage via dynamic programming and mixed-integer linear programming. *IEEE Transactions on Automation Science and Engineering, 12*(2), 565–579.
4. Vichik, S., & Borrelli, F. (2014). Solving linear and quadratic programs with an analog circuit. *Computers & Chemical Engineering, 70,* 160–171.
5. Jones, C. N., Grieder, P., & Rakovic, S. V. (2006). A logarithmic-time solution to the point location problem for parametric linear programming. *Automatica, 42*(12), 2215–2218.
6. Ke, F., Li, Z. J., Xiao, H. Z., & Zhang, X. B. (2017). Visual servoing of constrained mobile robots based on model predictive control. *IEEE Transactions on Systems Man Cybernetics: Systems, 47*(7), 1428–1438.
7. Harrison, C. A., & Qin, S. J. (2009). Minimum variance performance map for constrained model predictive control. *Journal of Process Control, 19*(7), 1199–1204.
8. Baker, R., & Swartz, C. L. E. (2008). Interior point solution of multilevel quadratic programming problems in constrained model predictive control applications. *Industrial & Engineering Chemistry Research, 47*(1), 81–91.
9. Bernardini, D., & Bemporad, A. (2012). Stabilizing model predictive control of stochastic constrained linear systems. *IEEE Transactions on Automatic Control, 57*(6), 1468–1480.

10. Lee, S. M., & Won, S. C. (2007). Robust constrained predictive control using a sector bounded nonlinear model. *IET Control Theory and Applications, 1*(4), 999–1007.
11. Bououden, S., Chadli, M., Zhang, L. X., & Yang, T. (2016). Constrained model predictive control for time-varying delay systems: Application to an active car suspension. *International Journal of Control, Automation and Systems, 14*(1), 51–58.
12. Gawthrop, P. J., & Wang, L. P. (2009). Constrained intermittent model predictive control. *International of Journal of Control, 82*(6), 1138–1147.
13. Fukushima, H., & Bitmead, R. R. (2005). Robust constrained predictive control using comparison model. *Automatica, 41*(1), 97–106.
14. Abdullah, M., & Idres, M. (2014). Constrained model predictive control of proton exchange membrane fuel cell. *Journal of Mechanical Science and Technology, 28*(9), 3855–3862.
15. Patrinos, P., Sopasakis, P., Sarimveis, H., & Bemporad, A. (2014). Stochastic model predictive control for constrained discrete-time Markovian switching systems. *Automatica, 50*(10), 2504–2514.
16. Khouaja, A., Garna, T., Ragot, J., & Messaoud, H. (2017). Constrained predictive control of a SISO nonlinear system based on third-order S-PARAFAC Volterra models. *Transactions of the Institute of Measurement and Control, 39*(6), 907–920.
17. Kassem, A. M. (2012). Robust voltage control of a stand alone wind energy conversion system based on functional model predictive approach. *International Journal of Electrical Power & Energy Systems, 41*(1), 124–132.
18. Rossiter, J. A., Haber, R., & Zabet, K. (2016). Pole-placement predictive functional control for over-damped systems with real poles. *ISA Transactions, 61,* 229–239.